DEVELOPMENT OF LIQUID SEQUENCING VALVES BY CONTROLLING AIR-FLOW TO PERFORM BIOMEDICAL PROCESSES ON CENTRIFUGAL MICROFLUIDIC PLATFORMS

WISAM SALAH HUSSEIN AL FAQHERI

THESIS SUBMITTED IN FULFILMENT OF THE REQUIREMENT FOR THE DEGREE OF DOCTOR OF PHILOSOPHY

FACULTY OF ENGINEERING
UNIVERSITY OF MALAYA
KUALA LUMPUR

2015

ORIGINAL LITERARY WORK DECLARATION

Name of Candidate: WISAM SALAH HUSSEIN AL FAQHERI

(Passport No. A8665302)

Registration/Matric No.: KHA110024

Name of Degree: Doctor of Philosophy (Ph.D.)

Title of Thesis: Development of Liquid Sequencing Valves by Controlling Air-Flow to Perform Biomedical Processes on Centrifugal Microfluidic Platforms.

Field of Study: BIOMEMS

I do solemnly and sincerely declare that:

(1) I am the sole author/writer of this Work;
(2) This Work is original;
(3) Any use of any work in which copyright exists was done by way of fair dealing and for permitted purposes and any excerpt or extract from, or reference to or reproduction of any copyright work has been disclosed expressly and sufficiently and the title of the work and its authorship have been acknowledged in this Work;
(4) I do not have any actual knowledge or ought I reasonably to know that the making of this Work constitutes an infringement of any copyright work;
(5) I hereby assign all and every rights in the copyright to this Work to the University of Malaya ("UM"), who henceforth shall be owner of the copyright in this Work and that any reproduction or use in any form or by any means whatsoever is prohibited without the written consent of UM having been the first had and obtained;
(6) I am fully aware that if in the course of making this Work I have infringed any copyright whether intentionally or otherwise, I may be subject to legal action or any other action as may be determined by UM.

Candidate's Signature   Date:

Subscribed and solemnly declared before,

Witness's signature   Date:

Name:

Designation:

ABSTRACT

This thesis presents three different liquid valving methods for the centrifugal microfluidic platform, namely vacuum/compression wax valve, passive liquid valve (PLV), and check valve. The mechanism of the proposed valves is simply based on sequencing the liquid flow by controlling air-flow inside the microfluidic network. Specifically, the wax valve and passive liquid valve utilize a volume of trapped air in the source chamber or the destination chamber to control the burst frequency of the liquid. In contrast, the check valve controls the direction of the air to control the flow direction of the pumped liquid. Compared with the previously proposed valves, this mechanism prevents any direct contact between the valving materials and the sample/reagents. This will reduce the chance of sample/reagents contamination, and allow the use of wider range of valving materials. As a proof of concept, liquid metering, liquid switching, and liquid swapping are conducted using the proposed valving methods. Furthermore, Bradford assay for protein concentration detection, and enzyme linked-immunosorbent assays (ELISAs) for dengue are demonstrated to show the capability of the developed valves to perform biomedical applications.

The results illustrate that the valves reduce the required spinning frequency to perform the microfluidic processes on the centrifugal platforms. In addition, the presence of physical barriers improves the ability of the developed valves to reduce vapour and contamination effect. Furthermore, the proposed valves show additional advantages such as the simplicity of fabrication and implementation, reversibility and multi-actuation, and compatibility with biomedical applications. Finally, the demonstration of the ELISA and the Bradford assays illustrate the ability of the presented valves to be integrated in any multistep biomedical and chemical application on the centrifugal microfluidic platform.

ABSTRAK

Dalam tesis ini, tiga kaedah cecair injap yang berbeza dibangunkan untuk platform microfluidic empar. Tiga injap adalah: injap lilin vakum/mampatan, injap cecair pasif (PLV), dan injap periksa. Mekanisme ketiga-tiga injap untuk penjujukan aliran cecair adalah dengan mengawal aliran udara di dalam rangkaian microfluidic. Secara khusus, injap lilin dan PLV menggunakan isipadu udara terperangkap di dalam kebuk sumber/destinasi untuk mengawal frekuensi pecah cecair. Sebaliknya, injap sehala mengawal arah udara untuk mengawal arah aliran cecair yang dipamkan. Berbanding dengan injap yang dicadangkan sebelum ini, mekanisme ini menghalang sebarang hubungan langsung antara bahan injap dan sampel/reagen. Ini mengurangkan peluang pencemaran sampel/reagen dan membolehkan pengunaan pelbagai bahan injap. Sebagai bukti konsep, pemeteran, pensuisan, dan penukaran cecair telah dijalankan menggunakan injap yang dicadangkan. Tambahan pula, untuk menunjukkan sesesuaian injap untuk melaksanakan aplikasi bioperubatan, asai imunoserapan berkaitan enzim (ELISA) untuk mengesan denggi, dan asai Bradford telah ditunjukkan.

Keputusan yang diperolehi menunjukkan bahawa injap yang dibangunkan mengurangkan frekuensi putaran yang diperlukan untuk melaksanakan proses microfluidic pada platform empar. Di samping itu, kehadiran halangan fizikal meningkatkan keupayaan injap untuk mengurangkan kesan wap dan pencemaran. Injap yang dibangunkan juga menunjukkan kelebihan seperti kemudahan process fabrikasi dan pelaksanaan, kebolehbalikan, kebolehulangan, dan kesesuaian untuk aplikasi bioperubatan. Akhirnya, demonstrasi asai ELISA dan asai Bradford membuktikan keupayaan injap yang dibangunkan untuk diintegrasikan dalam apa-apa applikasi bioperubatan dan kimia kepelbagaian langkah pada platform microfluidic empar.

ACKNOWLEDGMENT

DEDICATIONS

To those who offered me unconditional love and support,

To those who waited so long for this,

I dedicate this work to my parents, brother, sisters, and to my wife and daughter.

TABLE OF CONTENTS

TABLE OF FIGURES

LIST OF TABLES

LIST OF ABBREVIATIONS

μTAS	Micro total analysis systems
BCV	Bridge check valve
BSA	Bovine serum albumin
CAD	Computer-aided design
CD	Compact disc
CNC	Computer numerical control
DF	Dissolvable film
DI	Deionised
D-PLV	Passive liquid valve for the destination chamber
ELISA	Enzyme linked-immunosorbent assays
IR	Infrared
LOC	Lab on Chip
PC	Polycarbonate
PCR	Polymerase chain reaction
PDMS	Poly(dimethylsiloxame)
PMMA	Poly(methylmethacrylate)
PSA	Pressure-sensitive adhesive
RPM	Revolutions per minute
S-PLV	Passive liquid valve for the source chamber
TCV	Terminal check valve
TMB	Tetramethylbenzidine
TPP	Thermo-pneumatic pump
VCV	Vacuum/compression valve

LIST OF APPENDICES

CHAPTER 1: INTRODUCTION

1.1 Background

Since the invention of the miniaturized total analysis system by Manz *et al.* (1990), the miniaturization of commercial conventional diagnostic system has become the focus of researchers in this field. As a result, several biomedical and chemical processes were successfully demonstrated on two main types of microfluidic platforms: Lab-on-Chip (LOC) and centrifugal microfluidic platforms (Haeberle *et al.*, 2012; Madou *et al.*, 2006; Manz *et al.*, 1990). Although both platforms aim to reduce the amount of liquid and time consumption, LOC is a stationary platform that mostly dependent on external forces for liquid pumping. In contrast, centrifugal microfluidic platforms rely on the centrifugal force (which is derived from spinning the platform) to pump liquid on the platform. In addition, the centrifugal microfluidic platforms can also utilize capillary pressure as passive valves for fluid flow sequencing (Madou *et al.*, 2006). The final goal of researchers working in the centrifugal microfluidic field is to miniaturize the platform so that it can be tested on conventional computer CD ROM drive for quick analysis and better portability.

Several successful biomedical process were reported on the centrifugal microfluidic platforms and some examples include: ELISA (Lai *et al.*, 2004; Yusoff *et al.*, 2009), plasma and particles separation (Burger *et al.*, 2012; Imaad *et al.*, 2011; Morijiri *et al.*, 2010), and real time polymerase chain reaction (PCR) (Amasia *et al.*, 2012; Focke *et al.*, 2010; Strohmeier *et al.*, 2014). However, liquid flow control in complex multistep processes (processes with more than three microfluidic steps) still presents a serious challenge for the researchers in this field. During the last few decades, the field of microvalves has been heavily investigated and various types of valves have been reported in various literatures. Most of the proposed valving methods can be classified under two main categories: active valves or passive valves (Madou *et al.*,

2006; Oh & Ahn, 2006). An active valve can be defined as a valve that requires an external force to be actuated (open or close). In contrast, a passive valve utilizes centrifugal and capillary forces to control liquid flow without the need for external force for actuation. Although, the use of external force or trigger to operate an active valve is considered as its main disadvantage, it makes flow control more accurate and robust.

In general, the main criteria of a practical microvalve that can be successfully commercialized for biomedical applications include simplicity, prevention of evaporation or sample leakage, reduction of the dead volume, short actuation time, and reduced power consumption (Oh *et al.*, 2006). Failure to adhere to most of these requirements will reduce the chances of implementation in real biomedical applications. Despite this fact, most of the proposed microvalves for the centrifugal microfluidic platforms are either complex and require lengthy fabrication process, or lack of physical barriers that reduce sample evaporation and contamination. Therefore, the aim of this study is to develop an easy-to-implement liquid sequencing valves that can be utilized to perform biomedical applications on centrifugal microfluidic platforms. Three active and passive valves are designed and developed in this study. The three valves are: vacuum/compression wax valve, passive liquid valve (PLV), and check valve. The development valves have three main advantages; (first) it is easy to fabricate and implement; (second) it contains physical barriers to reduce vapor effect and isolate sample from surrounding environment; (third) it has better compatibility with biomedical applications as there is no direct contact between the sample and valving material.

Vacuum/compression wax valve presents a novel valving technique for the centrifugal microfluidic platform where the liquid burst frequency is controlled by controlling the air flow of the source and destination chambers. This liquid sequencing mechanism prevents any direct contact between the sample and the valving material (the

paraffin wax). The second valving technique (i.e., PLV) is an improvement of the vacuum/compression wax valve where the wax plug is replaced by liquid venting chamber. The venting chamber is introduced to control the air flow of the source and destination chambers via two different configurations (i.e., passive liquid valve for the source chamber (S-PLV) and passive liquid valve for the destination chamber (D-PLV)). This improvement eliminates the need for external convection heating source to activate the wax valve (convert an active valve to a passive valve). The third valving method (i.e., check valve) presents an easy-to-fabricate and implement passive check valves that control the flow direction of liquid and air on the centrifugal microfluidic platforms. Two types of check valves are developed in this stage which are: terminal check valve (TCV) and bridge check valve (BCV). The check valves is utilized to improve the ability of thermo-pneumatic pumping (TPP) in controlling the pumping direction of liquid on the centrifugal microfluidic platform.

Three basic microfluidic processes, liquid switching, liquid metering, and liquid swapping, are performed utilizing the developed valves. Moreover, to demonstrate the ability of the developed valves to perform biomedical applications, Bradford assay to detect protein concentration, and ELISA assay for dengue detection are demonstrated using the PLV and check valve, respectively.

1.2 Research Objectives

The main objective of this study is to develop active and passive liquid sequencing methods for centrifugal microfluidic platform by controlling the air-flow on the centrifugal microfluidic platforms. In order to meet the main objective, the following specific sub objectives should be achieved:

- Development of active wax vacuum/compression valving method to control liquid burst frequency.

- Development of passive liquid valving mechanism by introducing venting chamber to control the air flow of the source and/or destination chambers.

- Development of passive check valve technique to control liquid and air flow direction.

- Performance of Bradford assay for protein concentration detection utilizing the developed liquid valve.

- Demonstration of the ELISA assay for dengue detection utilizing the developed check valving method.

1.3   Scope of Work

This research focuses on the development of passive and active microvalves for the centrifugal microfluidic platform that can be implemented in biomedical applications. Therefore, this thesis will extensively cover liquid sequencing methods of the centrifugal microfluidic platforms, while briefly presents other aspects of the platform such as pumping methods. The conducted Bradford assay and ELISA assay do not comprise the use of real human biological samples (e.g., blood or serum) during experimental tests. Instead, bovine serum albumin (BSA) is utilized in the Bradford assay and colored deionised water is implemented in the ELISA experiment.

1.4   Thesis Outlines

This thesis is structured as follows:

Chapter 1 presents a brief introduction about the background of this research and the motivation for the defined objectives is given.

Chapter 2 presents a literature review on lab on chip and centrifugal microfluidic platform. A brief introduction to the structure of centrifugal microfluidic platform and

its pumping and valving mechanisms is give. This is followed by a short discussion of their biomedical applications.

Chapter 3 explains the research methodology and procedures to execute the defined objectives in three sections. The first section deals with the methodology of the vacuum/compress paraffin wax valves. This is followed by the methodology of the developed passive liquid valve in the second section. The last section deals with the check valve introduced for the centrifugal microfluidic platforms.

Chapter 4 discusses the experimental results of each of the developed valve. In addition, the results of two biomedical applications demonstrated utilizing the developed valving methods are also presented in a separate subsection.

In Chapter 5, the work is summarized and a conclusion is drawn. A number of suggestions for possible future work are also offered.

CHAPTER 2: LITERATURE REIVEW

2.1 Introduction

Over the last few decades, microfluidic-based platforms have become the focus of research as an attempt to solve various problems related to conventional diagnostic methods such as the high consumption of sample and expensive reagents, long processing time, complex and expensive setup. Moreover, the overwhelming desire to decentralize healthcare process from hospitals and clinics has motivated researchers in academia and industry to invent point-of-care (POC) diagnostic methods. Therefore, microfluidic platforms attract the attention as POC, low requirements, and disposable solution for the benchtop diagnostic procedures. As mentioned earlier in the Introduction chapter, most of the reported microfluidic platforms can be classified under two main categories: LOC and centrifugal microfluidic platform (Madou *et al.*, 2006; Oh *et al.*, 2006).

2.2 Centrifugal Microfluidic Platform VS. Lab-on-a-chip (LOC)

The LOC or as it might known as micro total analysis systems (µTAS) is a research field that aims to invent micro-scale, fast, disposable, and portable diagnostic platform to perform biochemical applications (Auroux *et al.*, 2002; Reyes *et al.*, 2002). In general, LOC is a platform that contains micro-scale chambers and channels where external pumping force is used to pump liquid. Different pumping techniques are employed for various LOC platforms such as pressure pumping, acoustic pumping, and electrokinetic pumping. Pressure pumping is the standard pumping method most widely used but difficult to miniaturize and multiplex (due to the fact that it requires external air/liquid pump and physical connections) (Abi-Samra, 2012).

LOC platform has been utilized for many applications especially for clinical diagnostic. LOC for clinical applications is targeted to be *sample-to-answer*, where the

process starts with a droplet of patient sample (e.g., blood, urine), and rapidly end with important information about the sample. This is due to its ability to rapidly perform biomedical test procedure with fraction of reagents and sample volume. It is also portable, consume low power, and has high reproducibility (Abi-Samra, 2012). Moreover, these devices can be operated without the need for trained individuals and can be performed at any place. Glucose strips and pregnancy home tests are two examples of commercially available LOC device. However, there is no commercially available LOC platform that can replicate a multistep biomedical assay.

On the other hand, centrifugal microfluidic platform (also known microfluidic CD) is more recent field-of-research where its first basic design was reported by N. G Anderson in 1969 (Anderson, 1969; Burtis *et al.*, 1972). In term of pumping mechanism, centrifugal microfluidic platforms obviate the need for external pumps by utilizing centrifugal force to move liquids outward to the outer edge of the platform (Madou *et al.*, 2006). This configuration eliminates the need for tubing and external air-connections with the platform (better portability). In term of pumping strength, both LOC and centrifugal platforms can generate a wide range of fluid flows from few nanoliter per second up to microliter or even liter per second (Madou *et al.*, 2006; Soroori, 2013). Moreover, centrifugal platform can passively perform different micro-processes such as liquid mixing, liquid metering, and liquid switching (Madou *et al.*, 2006). This makes the centrifugal microfluidic platform an attractive field for researchers looking for inexpensive, portable, and integrated diagnostic tool. Various chemical and biomedical applications have been developed on the centrifugal microfluidic platform and they will be briefly discussed in subsection "*2.4 Biomedical Applications on the Centrifugal Microfluidic Platforms*".

From a fabrication perspective, different materials and methods are utilized to build both the LOC and the centrifugal microfluidic platforms. The most common

fabrication materials are poly(dimethylsiloxame) (PDMS), polycarbonate (PC), and poly(methylmethacrylate) (PMMA) due to their transparency, ease to fabricate, low cost, surface stability, and high impermeability to gas (Abi-Samra *et al.*, 2011; Burger *et al.*, 2012; Focke *et al.*, 2010; Garcia-Cordero *et al.*, 2010; Kim *et al.*, 2007; Kirby *et al.*, 2012; Lee *et al.*, 2009; Soroori, 2013). While PDMS is widely used to fabricate microfluidic platforms, using rigid plastic like PC and PMMA is more practical for mass production as it is cheaper and easy to be inject molded (Abi-Samra, 2012). To fabricate the microfluidic platform out of PDMS, photolithography is usually utilized where micro-features are introduced by processing a photoresist (usually SU-8) on a silicon wafer that will be the plastic mold. In contrast, computer numerical control (CNC) machine is a popular and easy way to introduce the microfeatures in the PC and PMMA materials.

Some examples of commercially available centrifugal microfluidic platform for biomedical applications are: Piccolo ® by Abaxis, Inc (USA), and Bioaffy ® by Gryos AB (Sweden). Piccolo ® was developed in 1995 as a blood analyzer tool to detect electrolyte level, urea nitrogen, and alanin aminotransferase activity. On the other hand, Bioaffy ® produced in 2000 to automate and miniaturize immunoassay with a fraction of patient sample (nano-liter range).

The key feature differences between the centrifugal microfluidic platform and the LOC are shown in Table 2.1 published by Madou *et al.* (2006). It can be seen that the centrifugal microfluidic platform is inexpensive, easily utilized for mixing, compatible with most samples including cells, and better for diagnostic applications. Moreover, the centrifugal microfluidic platform has a range of valving methods that can handle both liquid and vapor.

Table 2.1: Comparison between the centrifugal microfluidic platform and the LOC
The table is adopted from Madou *et al.* (2006)

	Fluid propulsion mechanism			
Comparison	Centrifuge	Pressure	Acoustic	Electrokinetic
Valving solved?	Yes for liquids, and for vapor	Yes for liquids, and for vapor	No solution shown yet for liquid or vapor	Yes for liquids, no for vapor
Maturity	Products available	Products available	Research	Products available
Propulsion force influenced by	Density	Generic	Generic	pH, ionic strength
Power source	Rotary motor	Pump, mechanical roller	5 to 40 V (AC)	10 KV (DC)
Scaling of forces	L^3	L^3	L^2	L^2
Flow rate	From less than 1 nl s^{-1} to greater than 100 µl s^{-1}	Very wide range (less than nl s^{-1} to liter s^{-1})	20 µl s^{-1}	0.001 – 1 µl s^{-1}
General remarks	Inexpensive CD drive, mixing is easy, most samples possible (including cells). Better for diagnostics	Standard techniques. Difficult to miniaturize and multiplex	Least mature of the four techniques. Might be too expensive. Better for smallest samples	Mixing difficult. High voltage source is dangerous and m parameters influence propulsion, better for smallest samples (HTS)

2.3   Centrifugal Microfluidic Platform Fundamentals

In this subsection, the fundamental elements of the centrifugal microfluidic platform are discussed (i.e., micro pumping and micro valving). For each element, the previously developed methods are presented with highlights on their pros and cons. Note that for the reviewed micro valving methods, some LOC valving techniques will be presented as well since they are related to the scope of this work and can be implemented on the centrifugal microfluidic platforms.

2.3.1   Micro Pumping

Pumping the liquid on the centrifugal microfluidic platform is the main key factor to perform multi-step applications. Different methods are utilized to perform liquid pumping. These methods can be classified under two main categories: passive pumping (no external force is utilized) and active pumping (external force is utilized).

2.3.1.1   Passive Micropumps

As mentioned earlier, passive pumping can be defined as propelling the liquid through the microfluidic network without the need for external force or trigger. On the centrifugal microfluidic platform, the centrifugal force ($P_{centrifugal}$) which is generated from the spinning process is widely utilized to passively pump the liquid towards the outer edge of the platform. This force can be calculated by the following equation (Madou *et al.*, 2006; Thio *et al.*, 2013):

$$P_{centrifugd} = \rho\omega^2 \Delta r \bar{r} \tag{2.1}$$

where ρ is the liquid density, ω is the centrifugal platform spin speed in radians per second (rad/s), Δr is the difference between the top and bottom liquid levels at rest with respect to the rotation center, and $\bar{r}$ is the average distance of the liquid from the rotation center (see Figure 2.1). It is clear from equation (2.1) that the $P_{centrifugal}$

(pumping force) depends on the density of the pumped liquid, spinning speed, and the position of the pumped liquid in respect to the center of rotation. However, this is not the only parameters that should be considered when calculating the $P_{centrifugal}$ because, when the liquid flowing in a capillary channel reaches a sudden expansion (such as an opening into a destination chamber), the capillary pressure (P_{cap}) holds the fluid in the channel and prevents it from bursting into the destination chamber. This pressure is calculated by the flowing equation (Madou *et al.*, 2006; Thio *et al.*, 2013):

$$P_{cap} = \frac{4\cos\theta_c\gamma_{la}}{D_h} \tag{2.2}$$

where θ_c is the liquid contact angle, γ_{la} is the liquid-air surface energy and D_h is the channel hydraulic diameter. When the spinning speed increases, the liquid will burst into the destination chamber as the centrifugal pressure overcomes the capillary pressure. The spinning speed when the liquid enters the destination chamber is referred to as the "burst frequency", and it can be calculated by equating the centrifugal pressure to the capillary pressure (Thio *et al.*, 2013):

$$rpm = \omega \times \frac{30}{\pi} = \sqrt{\frac{P_{centrifugd}}{\rho\Delta r\bar{r}}}\left(\frac{30}{\pi}\right) \tag{2.3}$$

The centrifugal pressure is widely employed to passively pump liquid on the centrifugal microfluidic platform (Kazemzadeh *et al.*, 2014; Lai *et al.*, 2004; Madou *et al.*, 2001; Mark *et al.*, 2011; Thio *et al.*, 2013). However, the unidirectional pumping of the centrifugal force (always towards the outer edge of the platform) limits the available microfluidic space to area between the center of rotation and the outer edge of the platform (a distance equal to the radius of the platform). Therefore, the development of

an alternative multidirectional passive pumping on the centrifugal platform has became the focal point of research in this field.
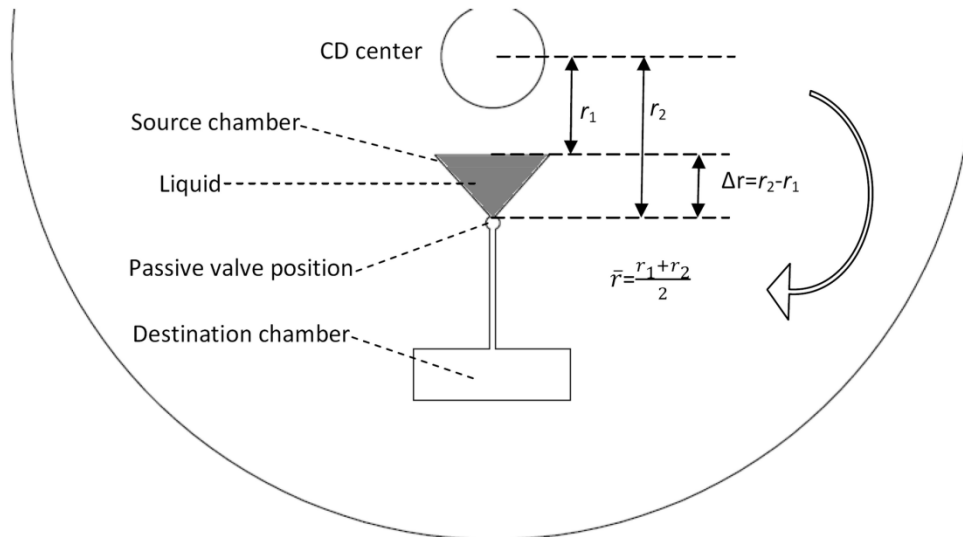
Figure 2.1: Centrifugal microfluidic platform main parameters
top of the liquid distance from platform center (r_1), bottom of the liquid distance from the platform center (r_2), difference between the top and bottom of the liquid levels (Δr), average of r_1 and r_2 ($\bar{r}$) and the position of passive valve from the source chamber

Gorkin *et al.* (2010) proposed a passive pneumatic pumping towards the center of the centrifugal platform by employing a combination of the centrifugal force and pneumatic air compression (see Figure 2.2). As shown in Figure 2.2, a compression compartment is introduced to trap and compress air at high spinning speed (store energy), then pump the liquid back towards the spinning center when the spinning speed reduces. As a proof of concept, Gorkin *et al.* employed this concept to actuate liquid siphoning process in a design shown in Figure 2.2(b1 – b6).

Using the same concept, Aeinehvand *et al.* (2013) proposed an improvement of Gorkin pumping method by introducing a circular latex layer on top of the compression compartment. This integration improves the ability and the flexibility of the air

compartment to store more energy. This innovation reduces the required spinning speed to perform liquid pumping, and increases the amount of liquid that can be pumped. In a relevant mechanism, Zehnle *et al.* (2012) proposed a passive pumping method to propel liquid towards the center of the platform. The proposed method is based on trapping and compressing air in a cavity and then release the stored pneumatic energy be reducing the spinning speed. Liquid pumping direction is controlled by have inlet channel with high hydraulic resistance and outlet channel with low hydraulic resistance. Therefore, the dominant amount of liquid will be pushed through the outlet channel towards the collection chamber. The author reported more than 75% pump efficiency per pumping cycle for water, ethanol, and whole blood.
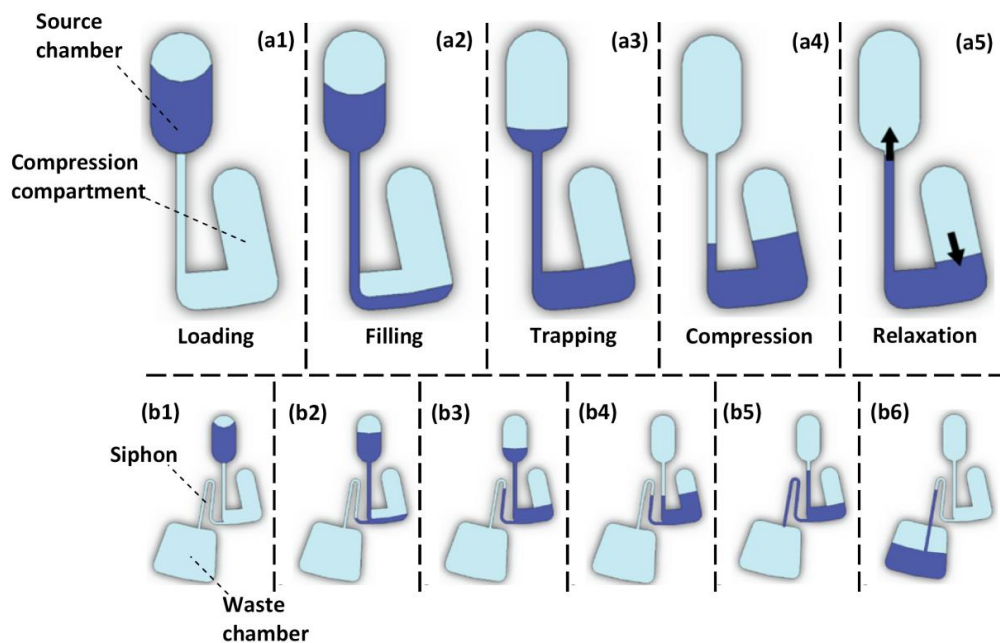
Figure 2.2 Pneumatic pumping towards the center of the centrifugal platform (a1) liquids loaded in the source chamber (initial state in low spinning speed) (a2) liquid bursts to fill in the compression compartment (a3) liquid traps air in the compression compartment (a4) increase the spinning speed to compress the trapped air (a5) decrease the spinning speed to relax the compressed air and pump the liquid back (b1) implementing the developed pneumatic pumping to activate liquid siphoning, in this stage, liquid injected in the source chamber (b2) liquid bursts towards compression compartment (b3) liquid traps air (b4) air compression (b5) and (b6) air relaxation and siphon activation (Gorkin *et al.*, 2010)

Kong *et al.* (2011) and Soroori *et al.* (2013) developed two passive pumping methods based on the same idea of pumping liquid with the effect of another liquid flowing on the platform. However, Kong *et al.* utilized a push-like state (compression) to pump the liquid while Soroori *et al.* utilizes pull-like state (vacuum) for liquid pumping. In Kong *et al.* work, two designs (i.e., immiscible and arbitrary) were developed to pump the liquid radially inward. The author reported 55% and 60% pumping effectiveness for immiscible and arbitrary, respectively, with a low spinning speed (less than 700 rpm).

In Soroori's work, a simple passive pumping method (namely micro-pulleys pump) is developed for the centrifugal microfluidic platform. The micro-pulleys mechanism is based on pumping a sample liquid that is injected in ventless microfluidic network towards the spinning center by a column of working liquid. As the working fluid bursts towards the outer edge of the platform, the sample liquid is pulled up in an analogy similar to the work of mechanical pulley. Note that both liquids (sample liquid and working liquid) are connected by the trapped air inside the ventless network. This work presents a simple-to-implement passive pumping on the microfluidic platform. However, the air that acts as a rope connecting the two liquid can withstand only specific amount of pressure on both sides. When the pressure exceeds the defined limits, the air connection breaks and the pumping method will not function properly.

Passive pumping methods increase the ability of the centrifugal microfluidic platform to pump liquid passively towards the spinning center. However, the limited liquid volume that can be pumped, and the dependence on the spinning speed, motivate researchers in this field to look for a more powerful and rotational-independent active pumping for the centrifugal microfluidic platform.

2.3.1.2 Active Micropumps

Active pumping can be defined as the utilization of external force to pump liquid towards the rotational center with less dependency on the centrifugal force. In 2007, Haeberle *et al.* developed an active pumping method on the centrifugal microfluidic platform by employing an external permanent magnet. As can be seen in Figure 2.3, a layer of PDMS membrane with two embedded steel plates is covering two chambers: pump chamber and valve chamber. Each steel plate is vertically positioned on top of one of the two chambers. To actuate the pumping process, a stationary magnet is positioned under the centrifugal platform on the radial track of the two steel plates. When the platform starts rotating, the two steel plates start fluctuating up and down by the effect of the magnetic field and according to a specific sequence (see Figure 2.3 (a – d)). This movement actuates the active pumping and valving processes to drive the liquid through the microfluidic network.
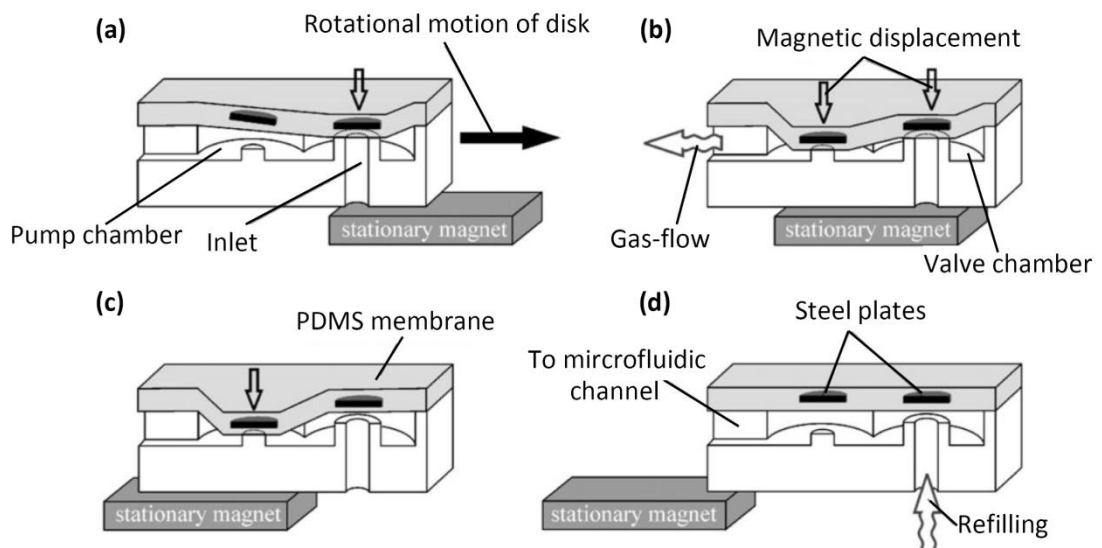
Figure 2.3 Magnet pumping and valving on the centrifugal microfluidic platform (a) Valve chamber passes on top of the stationary magnet causing the inlet to be closed (b) the steel plate of the pump chamber dragged down cause the air to flow from the outlet hole (c) the valve steel plate released (d) the pump steel plate release causing the air to be pulled in from the inlet hole (Haeberle *et al.*, 2007)

It is clear that Haeberle *et al*. developed a robust pumping method that can pump any volume of liquid in any direction. However, it still mainly depends on the spinning speed to control the pumping flow rate. Moreover, this method requires high-end fabrication techniques to accurately build the micropump.

Abi-Samra *et al.* (2011) proposed a relatively easier and simple-to-fabricate active pumping technique for the centrifugal microfluidic platform called thermo-pneumatic pump (TPP). Figure 2.4 shows the basic design of the TPP mechanism which consists of a ventless main microfluidic reservoir where the liquid initially injected, and a collection reservoir as a destination chamber where the liquid will be pumped for. Moreover, a ventless air chamber is connected to the main microfluidic reservoir as a pumping chamber. The system also requires external infrared (IR) source to actuate the pump. Simply, when the centrifugal platform is loaded and the platform is spun, the IR light heats the air chamber. This heating process causes the air in the chamber to expand thereby increasing the air pressure. The air pressure exerts pumping effect on the liquid in the microfluidic reservoir, forcing it to flow towards the collection reservoir (see Figure 2.4). This method can be considered as a simple solution to reverse the flow of liquid on a centrifugal microfluidic platform.

Along the same line with Abi-samra, Thio *et al*. (2013) proposed a two directional TPP pumping as an improvement to the pumping method developed by Abi-Samra *et al.* (2011). The idea is based on introducing a U-bent channel (like a siphon) to the connecting channel between the liquid reservoir and the collection chamber. This configuration allows for pushing the liquid from the microfluidic reservoir to the collection reservoir in the heating process; then pulls it back to the microfluidic reservoir during the cooling process of the air chamber. Thio *et al*. employed this idea to demonstrate two microfluidic processes which are switch pumping and serial washing. In spite of the many advantages TPP brings to the table, the volume of liquid to be

pumped is significantly limited by the volume of the implemented air chamber. Moreover, the use of external actuator (heating source) can partially eliminates the portability of the developed platform.
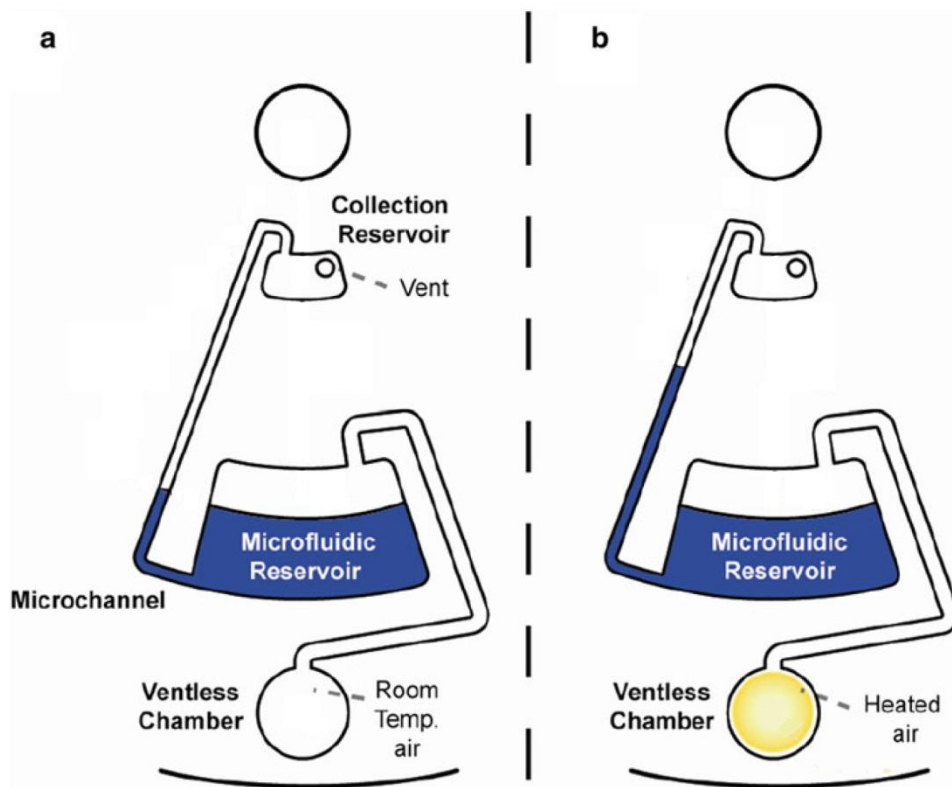
Figure 2.4 TPP pneumatic pumping method on the centrifugal microfluidic platform
(a) liquid injected in the microfluidicreservoir and all venting holes are sealed (b) heating the air chamber by IR lamp causing the air to expand and the liquid to flow towards the collection chamber (Abi-Samra *et al.*, 2011)

From the same research group of Abi-samra, Noroozi *et al.* (2011) utilized electrolysis method to generate pressure for liquid pumping instead of an external heating source. The design is similar to the one in Figure 2.4, but the air chamber is replaced with an electrolysis chamber. Still, electrolysis pumping method requires complex physical electrical connections to provide DC current to the electrolysis chamber while the platform is spinning.

To simplify the active pumping process and develop contactless pumping technique, M C R Kong and E Salin (2011) proposed the use of an external beam of compressed air to pump the liquid on the centrifugal microfluidic platform. The external air flow is focused into the venting holes of the chambers where the liquid to be pumped is located. The liquid pumping rate is controlled by the spinning speed of the platform and the air flow from the external valve. Although the method is easy to utilize, it can causes enormous amount of contamination for the samples and reagents inside the platform if it implemented outside clean rooms. Moreover, the use of external compressed air source can reduce the portability of the developed platform.

2.3.2 Micro Valving

During the last few decades, the micro valving field has been intensely investigated and various types of microvalves have been reported. A valve can be defined as a component that stops fluid flow (normally-open valve), starts fluid flow (normally-closed valve) or controls fluid flow (proportional valve) through a specialized passage or channel (Madou *et al.*, 2006). As mentioned earlier, most of the developed microfluidic valves fall under one of the main two categories: passive valve (dependent on centrifugal forces) and active valve (independent of centrifugal forces). Two kinds of valving methods are classified under each category and they are mechanical, and non-mechanical valves. In the following two subsections, the previous developed active and passive valving methods are discussed and some examples of applications preformed using the two methods are presented.

2.3.2.1 Passive Microvalves

In general, passive valve can be defined as the valving method that does not require external force or trigger to be actuated. Various mechanical and non-mechanical passive valves have been reported for the LOC and the centrifugal microfluidic platforms. The mechanical passive valves are actuated by moving mechanical parts to

control fluid flow. In contrast, non-mechanical passive valves do not contain any moving mechanical parts.

For LOC, passive check valve is the most popular valving method adopted. Two main categories of check valves are widely reported which are: flap valve (Feng & Kim, 2004; Nguyen & Truong, 2004; Ni *et al.*, 2010; Voigt *et al.*, 1998; Voldman *et al.*, 2000), and spherical ball valve (Accoto *et al.*, 2000). Figure 2.5 (a) and (b) present a simple valving configuration of the flap valve where the liquid flow is controlled by bendable gate at the connecting point between the upper and lower channel. The flap valve is actuated (opened) when the liquid pressure is high enough to bend the valving gate (see Figure 2.5(a)). At the same time, the flap valve does not allow for the liquid to flow back as the valving gate can only be bended in one direction. Figure 2.5(c) and (d) demonstrate the spherical ball valving mechanism. It is clear that the spherical ball valves let the liquid to flow in one direction while stop the flow when the it is reversed backwards. In many literature, the flap and spherical ball valves are integrated with active or passive pumping methods to build a microscale pump (Accoto *et al.*, 2000; Carrozza *et al.*, 1995; B Li *et al.*, 2005; Ni *et al.*, 2010; Pan *et al.*, 2005; Yamahata *et al.*, 2005). Flap and spherical valves present an easy way to control liquid flow direction. However, the efficiency of these valves to prevent reverse flow is relatively poor as it depends on input pressure and that can cause leakage in low pressure.

On the other hand, a number of passive valving methods were proposed for the centrifugal microfluidic platform. Examples include hydrophobic and capillary valves (Ducr´ee *et al.*, 2007; Madou *et al.*, 2001), pneumatic valve (Mark *et al.*, 2009; Mark *et al.*, 2011; Strohmeier *et al.*, 2014), siphon valves (Kitsara *et al.*, 2012; Siegrist *et al.*, 2010), flap valves (Thio *et al.*, 2011) and dissolvable films valve (Gorkin *et al.*, 2012). Figure 2.5(e), (f), (g), (h), (i), and (j) show an illustration of hydrophobic, capillary, pneumatic, and siphon valve, respectively.

Hydrophobic and capillary valves control the flow of the liquid by integrating hydrophobic region (for hydrophobic valve), or by introducing sudden expansion (for capillary valve) on the way of liquid flow (see Figure 2.5(e) and (f)). For these two valves, hydrophobic and capillary forces are utilized to stop liquid flow until the liquid has enough pressure to overcome these forces. These two valving method is considered the easiest way to control liquid flow passively on the centrifugal microfluidic platform. However, the lack of physical barrier could cause for liquid evaporation in long term storage. Moreover, these valves can be actuated once as wetting their structure can reduce their ability to control liquid flow.

Figure 2.5(g) and (h) present the passive pneumatic valving method proposed by Mark *et al.* (2009). Mark and his team proposed a ventless destination chamber where the air is trapped and compressed to stop the liquid at the source chamber. This liquid stoppage continues until the pressure of the source chamber liquid overcomes the pressure of the trapped air in the destination chamber. To illustrate the capability of the proposed valve, Mark *et al*. integrated the developed valve in the centrifugal platform to perform liquid metering process (Mark *et al.*, 2011). In spite of the simplicity of the proposed valve to control liquid flow, the user required to adjust the destination chamber volume in order to adjust the burst frequency of the liquid. Moreover, proposed valve limits the implementable microfluidic process to two steps only.

Figure 2.5(i) and (j) present a popular valving technique in the centrifugal microfluidic field where a siphon shaped channel is utilized to control the fluid flow (Kitsara *et al.*, 2012; Siegrist *et al.*, 2010). This configuration is usually utilized to empty/flush out a specific chamber (usually the detection chamber) at a specific rotational speed. The siphon valve is actuated by increasing the spinning speed to a level where the liquid reaches the crust of the siphon channel and then burst. Passive siphon valve has been utilized in many researches to control liquid flow; however, it

requires a special hydrophobicity surface treatment in prior to implement the valve in any process. Moreover, the lack of physical barrier can cause vapor problem when this valve is implemented.
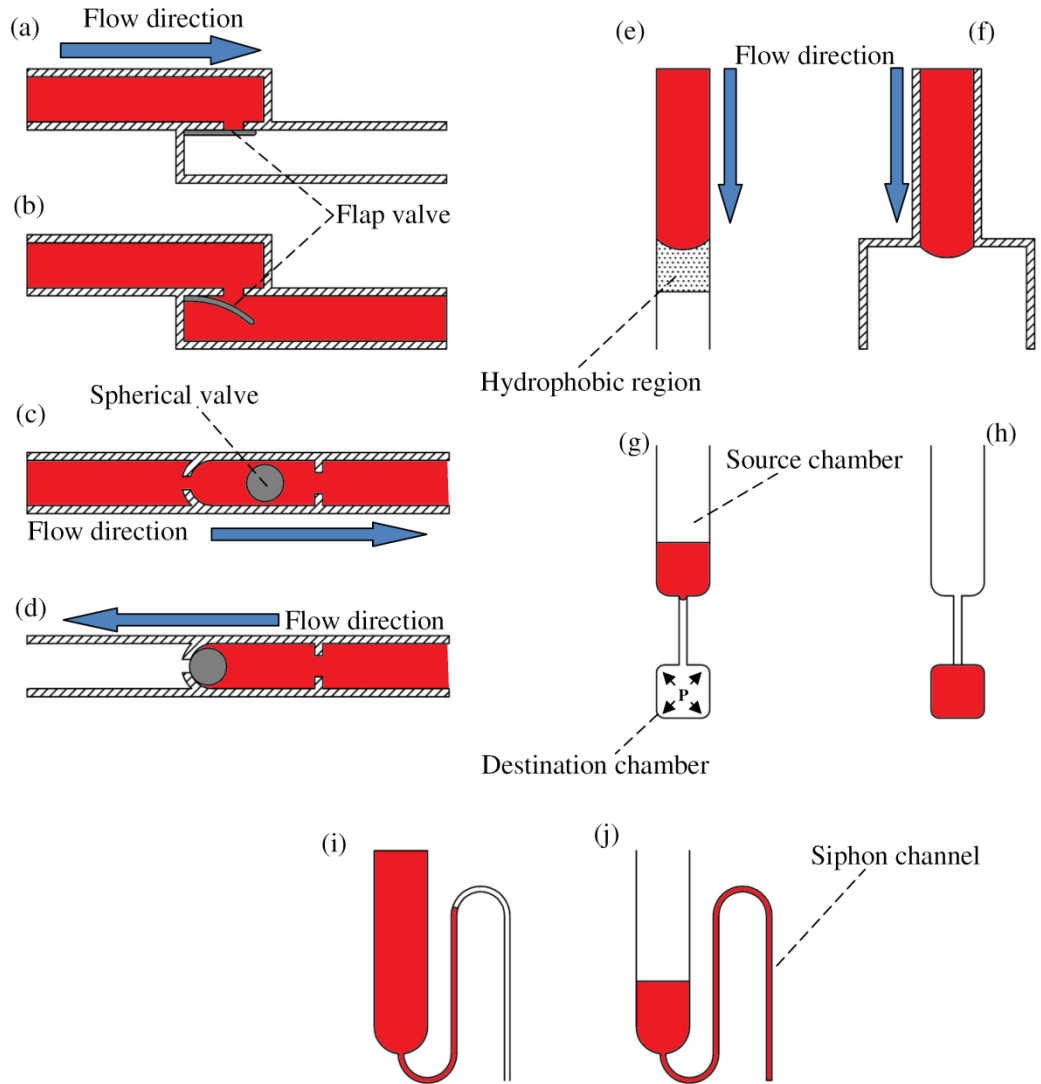
Figure 2.5: Examples of passive valving methods for the microfluidic platforms (a) and (b) flap valve mechanism, (c) and (d) spherical ball valve, (e) hydrophobic valve, (f) capillary valve, (g) and (h) pneumatic valve, (i) and (j) siphon valve

To solve the vapor seal limitation in the previous presented passive valves and to present a solution for long term storate, Gorkin *et al.* (2012) proposed a passive dissolvable film (DF) valve to control liquid flow on the centrifugal microfluidic platform. As can be seen from Figure 2.6, the DF valve is installed in the channel

connecting between two chambers (loading chamber, and waste chamber). When the load chamber is filled with liquid, there will be trapped air between the loading chamber liquid and the DF valve. In a high rotational speed, the trapped air will be overcompressed and the loading chamber liquid will wet the DF valve. When the valve is wetted, the DF will breakdown and the liquid will burst towards the waste chamber. As a proof of concept, Gorkin *et al*. proposed a microfluidic design with multi DF valve to perform advance biomedical process starting from a whole blood sample. This valve has solved the lack of physical barrier in most of the passive valving method. However, complex procedures need be followed in order to fabricate and install the valve to eliminate any possible air/liquid leakage.
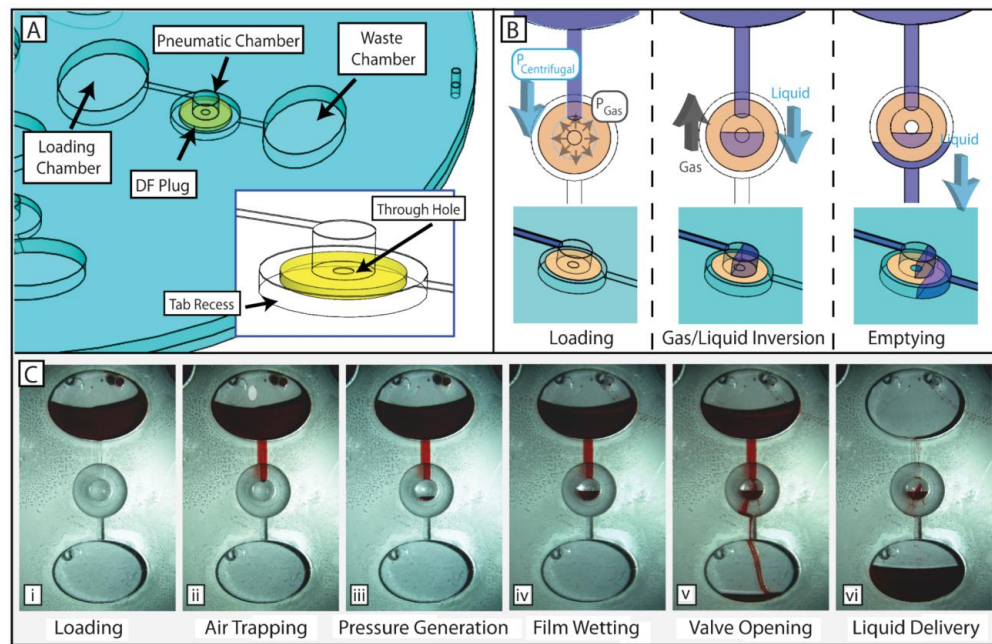
Figure 2.6: Passive dissolvable valve for the centrifugal microfluidic platform (a) DF valve plug installation, (b) DF valving actuation steps, and (c) pictures from the various step of DF valving process (Gorkin *et al.*, 2012)

To improve the commercialization potentials of centrifugal microfluidic platforms, van Oordt *et al.* (2013) proposed the use of stick-packaging method to store and release dry and wet reagents with a volume range of 80-500 µl. The author integrated frangible seal that allow for controlling the burst frequency of the reagents in

a range from 20 to 140 kPa. Van Oordt *et al.* reported 99% successful recovery rate with less than 0.5% of reagent loss in long term storage (two simulated years).

For the most of the reviewed passive valving techniques, the lack of physical barrier to prevent evaporation of liquids during test storage and operation is considered the main disadvantage (Thio *et al.*, 2011). This drawback presents an obstacle in the way of the integration of these valving methods in microfluidic platforms that need to be stored for a long time. Furthermore, there are serious challenges involved in making passive valves repeatable (multi-time usage) and manufacturable (easy to be fabricated) (Madou *et al.*, 2006). Finally, each proposed passive valve needs to be biocompatible (material-wise) for easer integration in biological and biomedical processes (Gorkin *et al.*, 2010). In conclusion, even though passive valve is considered easy method to control fluid flow without the need for external power, many parameters needs to be considered for successful integration of these valving methods in multi-step complex application.

2.3.2.2 Active Microvalves

Active microvalves can be defined as the valving method that requires external force to be actuated. According to the valve structure and the operation mechanism, active valves can be classified under two main categories: mechanical and non-mechanical valves (Au *et al.*, 2011; Oh *et al.*, 2006; Zhang C., 2007). Various microvalves that fall under these two categories were developed for the LOC platforms. These valve are classified according to their actuation methods to: magnetic actuation (Bae *et al.*, 2002; Fu *et al.*, 2003; Meckes *et al.*, 1999; Terry *et al.*, 1979), electric actuation (Teymoori & Abbaspour-Sani, 2005; van der Wijngaart *et al.*, 2002; Yobas *et al.*, 2003; Yobas *et al.*, 2001), piezoelectric actuation (H Li *et al.*, 2004; Shao *et al.*, 2004; E-H Yang *et al.*, 2004), thermal actuation (Rich & Wise, 2003; Takao *et al.*, 2005), electrochemical actuation (Neagu *et al.*, 1997; Suzuki & Yoneyama, 2003),

phase change actuation (Liu *et al.*, 2004; B Yang & Lin, 2007; Yoo *et al.*, 2007), and pneumatic actuation (Pandolfi & Ortiz, 2007; Studer *et al.*, 2004).

For the centrifugal microfluidic platforms, few active valves were reported and some example include; magnetic valve (Haeberle *et al.*, 2007), pneumatic valve (Kong & Salin, 2011), ice valves (Amasia *et al.*, 2012), and wax valves (Abi-Samra *et al.*, 2011).

Haeberle *et al.* (2007) proposed an externally actuated magnetic valve with a piece of steel plate is installed on a PDMS layer covering the valving chamber (see Figure 2.3). A permanent magnet is positioned in a specific place under the rotating platform so that while the platform rotates, the valve starts switches OFF and ON according to a predefined sequence. The developed method is well integrated with magnetically-actuated pumping mechanism to actively pump the liquid on the centrifugal microfluidic platform. However, magnetic actuation can affect the platform rotation stability due to the strong steel attraction to the magnetic field.

External compressed air-flow was utilized as an active valve to liquid flow in centrifugal microfluidic platform by Kong and Salin (2011). A beam of compressed air is positioned ON and OFF the venting holes of the destination chambers to control the liquid flow to those chambers. To demonstrate the capability of the valving method, the author performed flow switching process on the centrifugal microfluidic platform. Although the valve is simple to implement, the use of external air source is considered an obstacle on the way of platform miniaturization and a source of contamination of the samples inside the platform.

Amasia *et al.* (2012) utilized ice valve as a vapor sealed active valve to perform PCR on the centrifugal microfluidic platform as shown in Figure 2.7. The presented design contains two detection chambers with two sample inlets (A and B). When both samples are injected, the two chambers and channels are positioned on top of

thermocycling TE and ice valve TE (direct contact between the platform surface and the thermocycling should be established). The thermocycling TE is utilized to heat up the sample chambers, while ice-valve TE is utilized to freeze the liquid in the inlet channels to prevent any liquid evaporation.
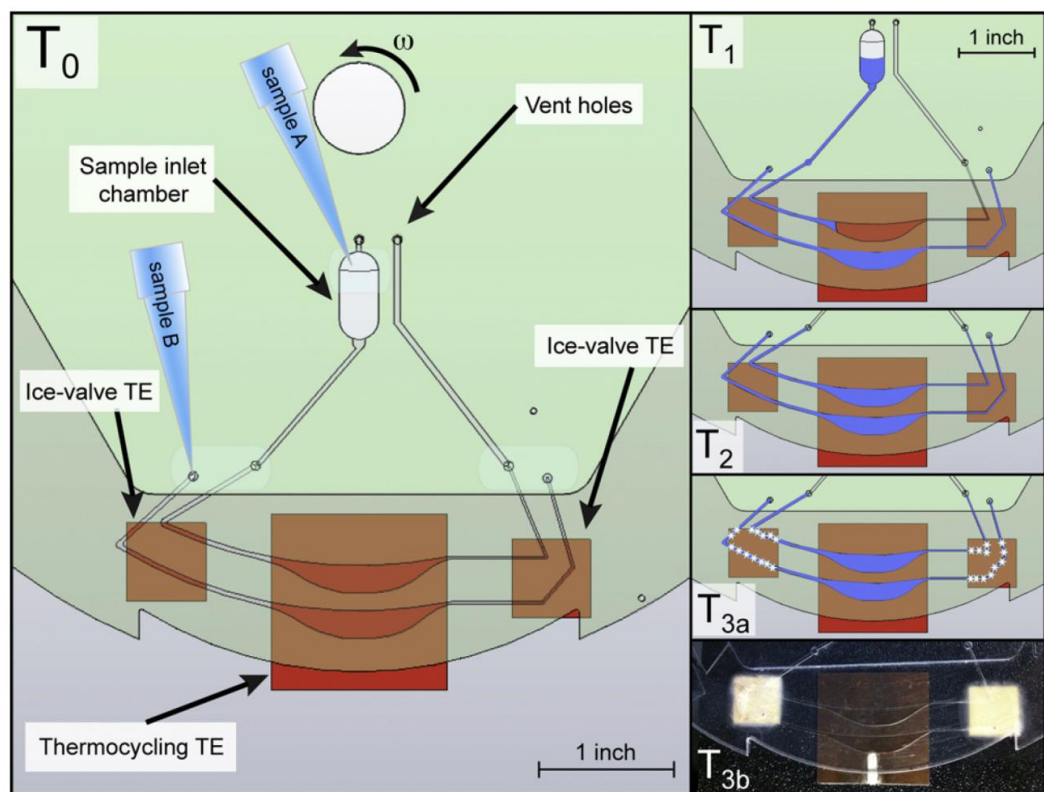
Figure 2.7: Centrifugal microfluidic platform design for PCR using ice valving PCR microfluidic design which contains two main reaction chambers for main and negative samples. The thermocycling TE is located under the two chambers while the two ice-valve TEs (square modules) placed under the inlet and outlet channels. The PCR samples are injected into the two chamber from the inlet holes (T0) and (T1). When the two chambers are fully filled (T2), the ice-valve thermoelectrics are actuated to seal off the microchannels by freezing the liquid there (T3a). When the PCR process is over (chambers are heated then cooled down), the ice-valve thermoelectric are deactivated and the sample liquid is released for further analysis. (T3b) (Amasia _et al._, 2012)

The proposed ice valving method is a good way to prevent liquid from evaporating during any process that requires heating process. However, the process requires complex set up that contains thermocycling terminals and an accurate control

system. Moreover, the centrifugal platform needs to be stopped in order to establish a surface contact between the thermocycling and the platform.

Recently, paraffin wax was utilized as an active valve on the centrifugal microfluidic platform proposed by Abi-Samra *et al.* (2011) and Kong *et al.* (2014). Figure 2.8 illustrates the microfluidic design where the process starts with blocking the micro-channels with two wax plugs with two different melting temperatures. To release the first liquid, the centrifugal microfluidic platform is heated with an IR source to reach the melting temperature of the first wax plug (see Figure 2.8(a)). Then, the temperature is increased to melting temperature of the second wax plug to release the second liquid (see Figure 2.8(c)). Kong *et al.* proposed a method encapsulating the liquid sample with two layers of paraffin wax (on top and bottom of the sample). This method combines a liquid valving method (same as Abi-Samra *et al*. valve), and a vapor-tight sealing mechanism for long term storage.

Among the proposed active valves, wax valves are the simplest, cheapest to introduce, and it also eliminates liquid evaporation. Moreover, by implementing wax with different melting temperature, different valves can be actuated at different instances in the same process. However, two obvious disadvantages associated with wax valve are the unnecessary heating of sample and reagents that are in close proximity to the valve, and the mixing between the sample/reagent and the wax after valve actuation that can affect the biomedical reactions and output signal (such as colorimetric reading in ELISA assay).

Table 2.2 summarizes the characteristics of various valving methods discussed in this chapter. It summarizes each valve in term of valve category, valving method, the presence of physical barrier, compatibility with biomedical applications, isolation, actuation time, reusability, and fabrication complexity. This table gives the reader a better understanding for the strength and weakness points for each valve, and where it

can be suitable to implement. For example, for applications that require long term storage, the developer should avoid the valves that do not contain physical barrier, and valves that are poor in term of isolation. Therefore, more vapor tight valve, such as ice valve and wax valve, are suitable for this kind of applications. However, Ice valve and wax valve suffer from average to slow actuation response, and both valves require complex system setup.
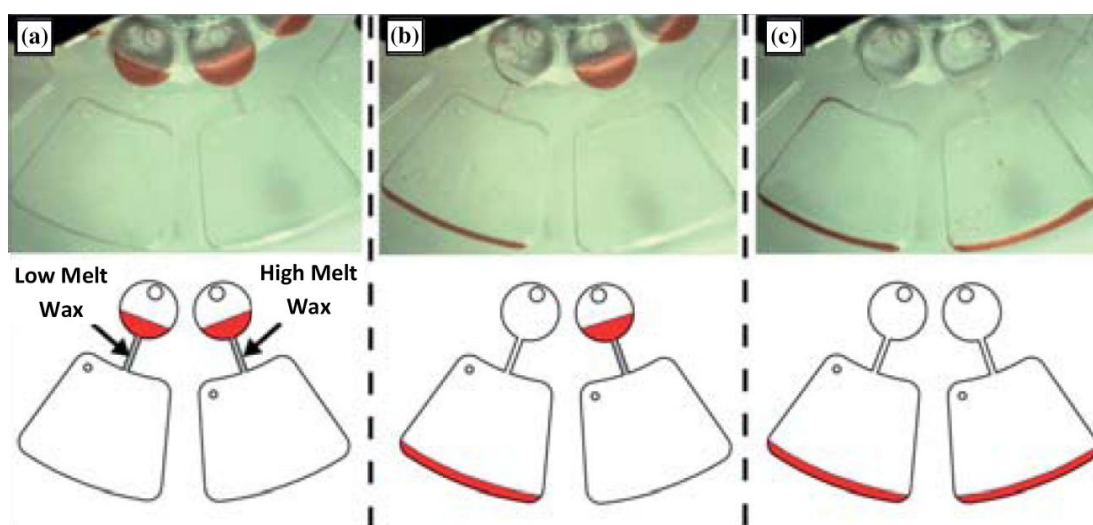
Figure 2.8: Wax-valve for the centrifugal microfluidic platform
(A) two different melting temperature wax installed in the micro-channels, (A) heat the centrifugal microfluidic platform to reach the melting temperature of the low melt wax, (C) increase the temperature to melt the high melting temperature wax (Abi-Samra *et al.*, 2011)

2.4   Biomedical Applications on the Centrifugal Microfluidic Platfrom

Recently centrifugal microfluidic platforms have been featured in a wide variety of applications. ELISA has been performed successfully on the centrifugal microfluidic platform (Ibrahim *et al.*, 2010; Ishizawa *et al.*, 2012; Lai *et al.*, 2004; Madou *et al.*, 2001; Noroozi *et al.*, 2011; Park *et al.*, 2012; Yusoff *et al.*, 2009). Lai *et al.* (2004) performed rat Immunoglobulin type G (IgG) antigen detection on the centrifugal platform starting from a hybridoma cell culture. Yusoff *et al.* (2009) and Ibrahim *et al.* (2010) proposed simple designs of centrifugal microfluidic platforms for Dengue fever

detection constructing a centrifugal microfluidic platform by CNC machining features into a PMMA layer and sealing this machined layer with Adhesive Sealing Film (ASF).

Amasia *et al.* (2012) and Focke *et al.* (2010) proposed LOD platforms for real-time polymerase chain reaction (PCR) amplification. These authors reported that PCR amplification of B. anthracis/cereus was successfully completed in 57 minutes with high specificity and efficiency. In 2014, Strohmeier *et al.* developed a real time PCR detection for 6 different food pathogens on the centrifugal microfluidic platform. The author proved that his presented "LabDisk" platform can be used in both qualitative and quantitative modes depends on the reagent prestorage scheme.

Particles capturing, distribution, and perform multiplexed assays on the centrifugal microfluidic platform were reported by Burger *et al.* (2012). The detection chamber in this case is designed with V-cup barriers to trap particles using a stopped-flow sedimentation method. The authors reported nearly 100% capturing efficiency and presented bead-based immunoassays for IgG detection. Other ideas such as cell counting were successfully performed by Imaad *et al.* (2011). Imaad and his team were able to modify a commercial CD drive to count the blood cells in preloaded centrifugal microfluidic platform. Moreover, cell or micro-particles separation performed on centrifugal microfluidic platform by Morijiri *et al.* (2010) and Kirby *et al.* (2012). Other applications were reported on the centrifugal microfluidic platform such as cell cultivation (Kim *et al.*, 2007), DNA purification (Strohmeier *et al.*, 2013), and water quality analysis (Czugala *et al.*, 2012).

Table 2.2: Microfluidic valving methods.

Microfluidic valving methods characteristics in term of valving mechanism, containing physical barriers, sample isolation from surrounding environment, actuation response, the ability to reuse the valve, and fabrication complexity and system setup

Valve	Category	Mechanism	Physical barrier	Compatible with biomedical applications/ contamination	Isolation / vapor	Actuation time	Multi-actuation	Fabrication complexity / system setup
Flap valve	Passive	Implementing flappable gate to control liquid flow between two channels	YES	Depends on the flap valve material	Average[1]	Fast	YES	Average
Spherical ball valve	Passive	Implementing spherical ball as a check valve to control liquid flow direction	YES	Depends on the spherical material	Average[1]	Fast	YES	Average
Hydrophobic valve	Passive	Integration a hydrophobic region inside liquid channel to control liquid flow	NO	Good	Poor	Fast	NO[2]	Average
Capillary valve	Passive	Implementing sudden expansion or contraction in the liquid channel to control liquid flow	NO	Good	Poor	Fast	NO[2]	Easy

[1] Not tight seal.
[2] Not multi-actuatable as the valve loses its ability to control liquid flow when it wet.

Table 2.2: 'Continued'

Valve	Category	Mechanism	Physical barrier	Compatible with biomedical applications/ contamination	Isolation / vapor	Actuation time	Multi-actuation?	Fabrication complexity / system setup
Passive pneumatic valve	Passive	Implementing ventless destination chamber and trapped air to control liquid flow	NO	Good	Poor	Average	NO	Easy
Dissolvable film valve	Passive	Implementing dissolvable layer to control liquid flow between two chambers	YES	Good	Good	Average	NO	Average
Siphon valve	Passive	Implementing siphon shaped channel to control liquid flow	NO	Good	Poor	Fast	YES	Average
Active pneumatic valve	Active	Implementing external air flow pressure to control liquid flow direction	NO	Good	Poor	Fast	YES	Average
Ice valve	Active	Freezing ice plugs in the micro-channel to control liquid flow	YES	Good	Good	Average	YES	Hard
Wax valve	Active	Injecting paraffin wax in the micro-channel to control liquid flow	YES	Good	Good	Slow	NO	Average

2.5 Summary

In this chapter, literatures related to the field of this study were reviewed. A brief comparison between the two main microfluidic platforms (LOC and centrifugal microfluidic platform) was presented. Then, the fundamental components of the centrifugal microfluidic platform were discussed (i.e., micro pumping and micro valving).

The literature reported different passive pumping method for the centrifugal microfluidic platform such as centrifugal pumping, pneumatic pumping, and micro-pulleys pumping. In contrast, several active pumping where developed such as magnetic pumping, TPP pumping, electrolysis pumping, and active pneumatic pumping. Similar to the pumping methods, different passive and active valving method were reported. Check valve, hydrophobic/hydrophilic valve, pneumatic valve, and DF valve are examples of the reported passive valving methods for the centrifugal microfluidic platform. In contrast, many active valving methods were proposed such as magnetic valves, pneumatic valves, ice valves and wax valves.

In spite of the big amount of research that explored the valving field of the centrifugal platform, the current available valving mechanism still need further improvement to be: reliable mechanism with physical barrier, vapor-tight for long term storage, reduce contact between sample and valving material, re-actuatable in multistep assay, and easy to fabricate and implement. Without the fulfilment of all or most of these conditions, the valve will not be practical to perform biomedical applications. Therefore, the centrifugal microfluidic platform field still need continues research to deliver more complete passive and active valving methods.

In this work, three different liquid valving mechanisms are presented in this work to solve some of the current valving drawbacks mentioned above. The three valves are: vacuum/compression wax valve, passive liquid valve (PLV), and check valve. The

three valves combine the implementation of physical barriers to control liquid flow with the simplicity of fabrication and implementation. To improve the compatibility of the developed valves with biomedical applications, the three valves control the liquid flow in a contactless fashion (control the air flow to control liquid flow). As a proof of concepts, the PLV and check valve were integrated on the centrifugal microfluidic platform to demonstrate the Bradford assay for protein concentration detection, and ELISA assay for dengue detection.

CHAPTER 3: METHODOLOGY

3.1 Introduction

The methods followed to achieve the objectives of this work are reported in this chapter. Together with the resources and equipment needed, a complete description of the fabrication procedures is presented. Three main sections are introduced in this chapter. Section 1 deals with the methodology of the vacuum/compression paraffin wax valves while section 2 describes the methodology of the developed passive liquid valve (PLV). The last section presents the methodology of the introduced check valve for the centrifugal microfluidic platforms. In addition, biomedical applications conducted utilizing the developed valving methods will be presented in a separate subsection. Figure 3.1 shows the methodology flow chart of this study.

3.2 Materials and Fabrication Methods

Different centrifugal microfluidic platforms were developed for this work. However, the basic fabrication materials and procedures are the same for all. Therefore, in this section, the general fabrication materials and methods of the centrifugal microfluidic platform for the three developed valve are discussed.

For all the developed valves, the fabricated microfluidic platforms for the experimental tests are either three layers, or five layers platform. For the three layers platform, the top and bottom layers are made of Polymethyl methacrylate (PMMA) plastic (by Asia Ply Industrial Sdn. Bhd., Selangor, Malaysia), while the middle layer is a pressure-sensitive adhesive (PSA) material (by FLEXcon, Spencer, MA USA). On the other hand, some implementations require the fabrication of five layers platform. Five layers platforms contain three PMMA layers (top, middle, and bottom layers), and two PSA layers (in between each two PMMA layers). The thickness of the PMMA layers is either 2 mm or 4 mm thick according to the platform designed features. Figure 3.2 illustrates the different layers of the three and five layers platforms.
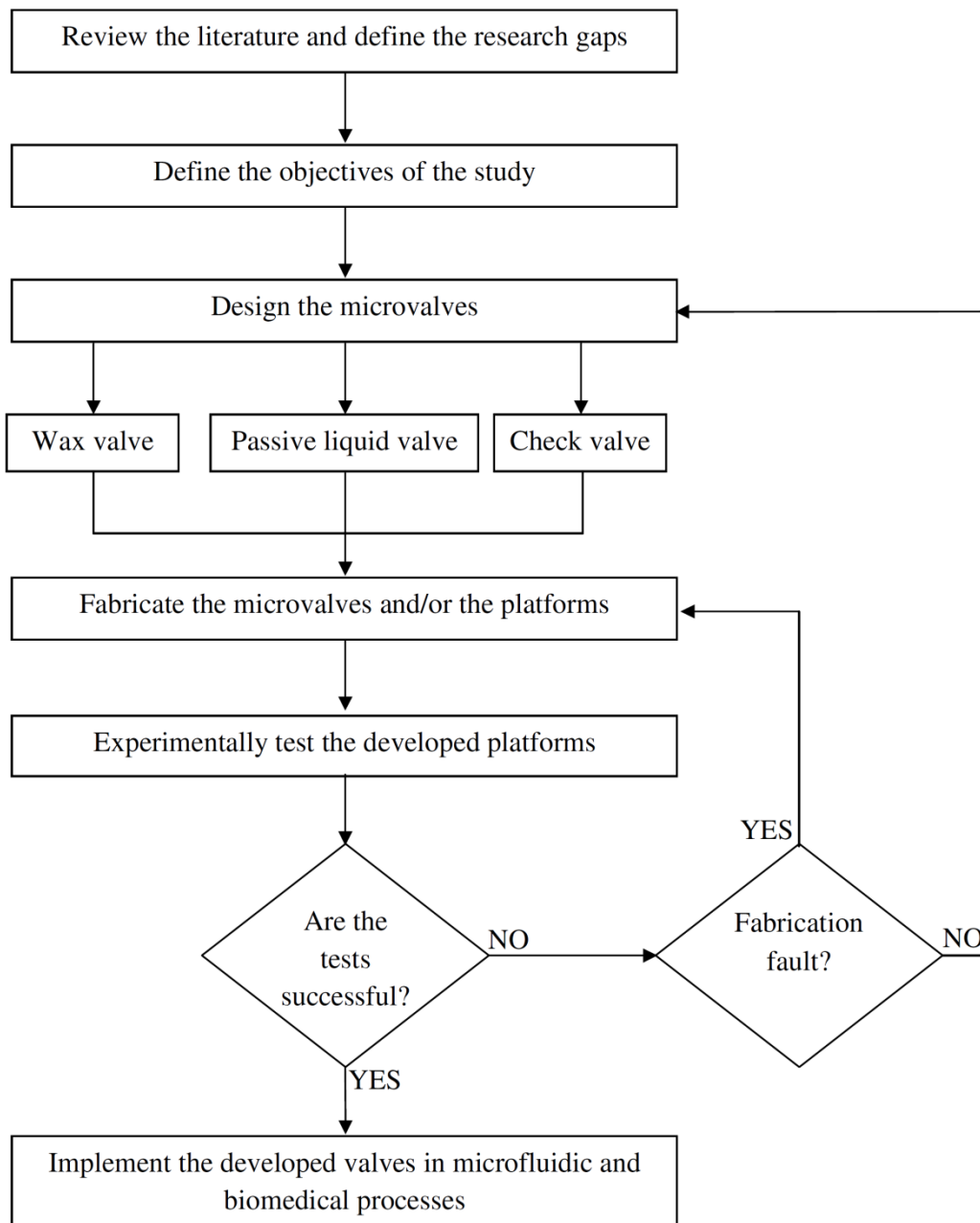
Figure 3.1: Flowchart of the research methodology
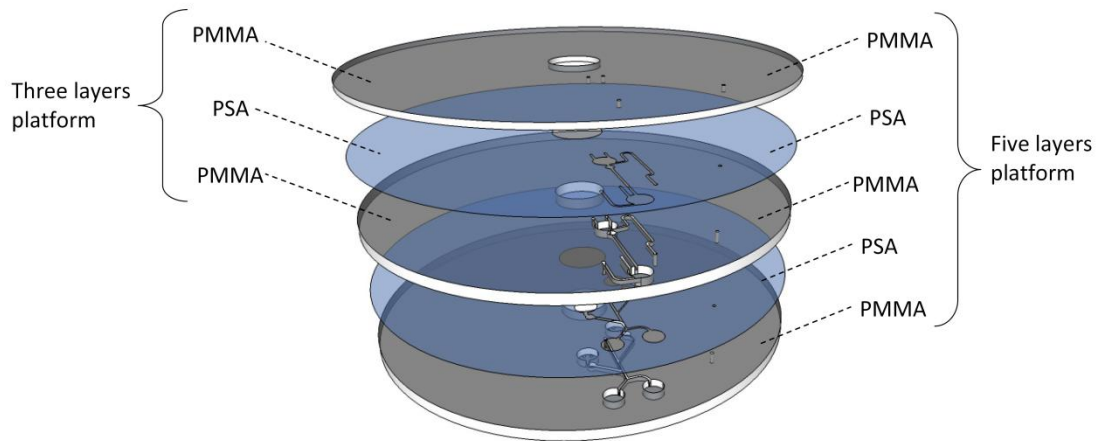
Figure 3.2: Three layers and five layers centrifugal microfluidic platforms
The three layer centrifugal platforms are consist of two PMMA layers (top and bottom) and one PSA layer (middle layer), Fiver layers platforms consist of three PMMA layers (top, middle, and bottom) and two PSA layers (between each two PMMA layers)

The fabrication process starts with designing the microfluidic platform using one of the computer-aided design (CAD) software. Then, the micro-scale features (channels, chambers, and venting/alignment holes) of the platform are micro-machined in the PMMA layers using a computer numerical control (CNC) machine (model VISION 2525, by Vision Engraving and Routing Systems, Phoenix, AZ USA). Meanwhile, the PSA layers are cut using a cutter plotter machine (model PUMA II, by GCC, New Taipei, Taiwan). Channels and chambers, corresponding to the design of the bottom PMMA layer, are cut out from the PSA layers to avoid having the liquid come in contact with the adhesive material of the PSA layer. This ensures a more consistent solid-liquid interface between the liquid and the channel / chamber walls.

Afterwards, the machined PMMA layers pass through different steps of cleaning, washing, sterilization, and drying before the bonding process starts. Finally, the different PMMA layers are aligned and bonded together using the prepared PSA layers. This process is conducted in a clean room with the utilization of custom made alignment jig and press roller machine. After the bonding step, the centrifugal microfluidic platform is ready to be experimentally tested. All the experiments are

conducted using a custom made spin test system that consists of computerized step motor, high speed camera, laser RPM meter, convection heating source (hot-air gun), and computer system as a controlling unit (see Figure 3.3). The hot-air gun is equipped with nozzle of 1 cm diameter to focus the forced convection heat only on the required area. It is proved by Thio *et al.* (2013) that utilizing hot-air gun for heating purpose on the centrifugal platform provides better results than implementing infra-red (IR) or laser. This is because the hot-air gun effect is limited to the upper layer of the platform with less effect on the lower layers. This prevents the unnecessary heating of the other features on the centrifugal platform.
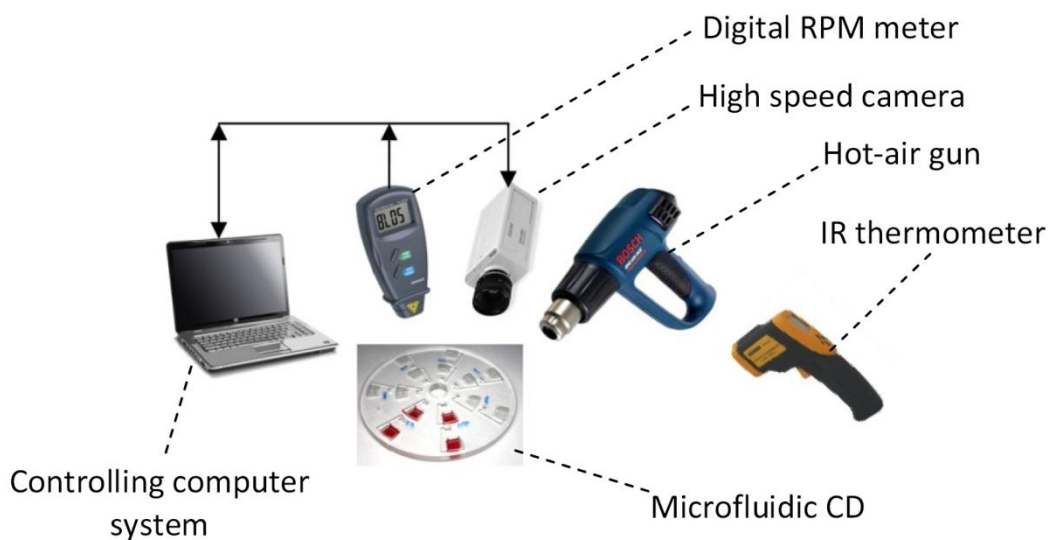
Figure 3.3: Spin test system setup
Custom made spin test system configuration and it consists of computerized step motor, high speed camera, laser RPM meter, heat convection source, controlling computer, and IR thermometer

3.3   Vacuum/Compression Wax Valve

In this part of the study, a novel vacuum/compression valves (VCVs) utilizing paraffin wax is developed. A VCV is implemented by sealing the venting channel/hole with wax plugs (for normally-closed valve), or to be sealed by wax (for normally-open

valve), and is activated by localized heating on the platform surface. Compared with the wax valve presented by Abi-Samra *et al.* (2011), we demonstrate that the VCV provides the advantages of avoiding unnecessary heating of the sample/reagents in the diagnostic process, allowing for vacuum sealing of the centrifugal microfluidic platform, and clear separation of the paraffin wax from the sample/reagents in the microfluidic process. As a proof of concept, the microfluidic processes of liquid flow switching and liquid metering is demonstrated with the VCV.

3.3.1 VCV Design and Principles of Operation

Figure 3.4(a) shows the basic design and implementation of the developed VCV for a simple one step microfluidic process. The design basically consists of two liquid chambers (chamber A and B), each 8 mm diameter and 1 mm height. The two chambers are connected by 0.7 mm width 0.5 mm height liquid channel. In addition, each liquid chamber has one 0.7 mm width 0.5 mm height venting channel (channel A and B). This design is fabricated on three layers platform (two PMMA layers and one PSA layer). All the features in Figure 3.4 are micromilled in the bottom 4 mm PMMA layer. The top 2 mm PMMA layer only contains the venting and alignment holes.

To implement vacuum wax valve, the sample is injected in chamber A then the venting hole A is sealed with wax plug (see Figure 3.4(b)). The sealing process is performed by injecting melted wax in the venting channel of chamber A. This configuration generates trapped air in the area on top the liquid in chamber A and in the venting channel A. During the spinning process, this trapped air creates vacuum state that prevents the liquid in the chamber A from bursting until venting hole A is released.

In contrast, the compression wax valve is implemented by sealing venting channel B with wax plug. This setup traps the air in the destination chamber and creates compression state to prevent the liquid in the chamber A from bursting. Again, the liquid will not burst until venting hole B is released. In other words, the proposed VCV

regulates the liquid flow by controlling the air flow of the source chamber (vacuum valve) or the destination chamber (compression valve).

For better understanding of the developed valve behaviour, two fundamental studies are conducted. The first study is conducted to test the heating profile of the platform during the heating process (during valve actuation). The second study is conducted to investigate the effectiveness of the developed valve (to define the operational limits).
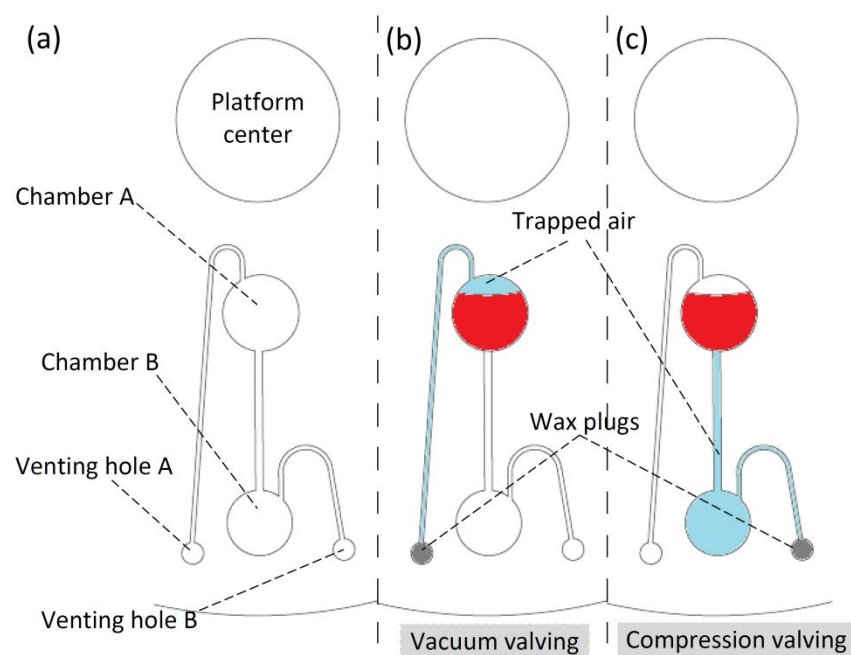
Figure 3.4: VCVs platform design
(a) platform basic design consist of two chambers (A and B) with two venting holes
(A and B) (b) vacuum valving experimental setup, (c) compression valving
experimental setup

3.3.2 Microfluidic Platform Heating Profile

This study is conducted to investigate the heating profile for the centrifugal microfluidic platform for better understanding of its thermal behaviour. This understanding helps during the process of the VCV actuation (wax melting). The same platform design in Figure 3.4 is utilized to perform this study. Forced convection

heating at 130°C is applied to the top surface of the centrifugal platform. The centrifugal platform is spun at different speeds of 0 to 350 rpm (the optimum range to actuate the wax valve), and the platform surface temperature is measured using the digital IR thermometer. This experiment allows for the determination of the surface temperature required to actuate (melt) the wax valves at different rotational speeds.

3.3.3 VCV Effectiveness

As mentioned earlier in *"3.3.1 VCV Design and Principles of Operation"* subsection, the proposed VCV controls the liquid flow on the centrifugal microfluidic platform by controlling the air flow of the source or destination chambers. And because the air is slightly elastic, it can only withstand a limited amount of vacuum (stretching) and compression. In the case of vacuum wax valve, overstretching that air in a high spinning speed can cause the air to break and the liquid to leak or fully burst (Soroori *et al.*, 2013). On the other hand, overcompressing the air in the compression wax valve can creates turbulence (Rayleigh–Taylor instability) in the contact point between the compressed air and the liquid which can cause air-escaping through the liquid in terms of bubbles (Mark *et al.*, 2009).

Therefore, this study is conducted to test the effectiveness (operational range) of the proposed VCV in the two developed configurations: vacuum valve and compression valve. For this study, the same microfluidic platform design shown in Figure 3.4 is employed. To test the effectiveness of the vacuum state, a sample liquid is injected in chamber A, then the venting hole A is sealed with wax. In contrast, by sealing the venting hole B with wax, the effectiveness of the compression state valve can be tested. After the loading and sealing process are performed, the centrifugal platform is spun at a range of spinning speeds to find the resulting burst frequencies. The results of the two experiments will be compared with a control set (set without VCV), and theoretical calculation obtained using equations (2.1) (2.2) and (2.3).

3.3.4   Applications of VCV

Many potential microfluidic processes can be performed using the proposed VCV. In this study, liquid flow switching and liquid metering are implemented by integrating the VCV on the centrifugal microfluidic platform.

Figure 3.5(a) shows the design of the centrifugal microfluidic platform fabricated to perform a liquid flow switching process. The design consists of two source chambers (A and B), two destination chambers (A and B), and the corresponding venting holes with compression wax plugs (venting hole A and B, see Figure 3.5(a)). Two different colored DI water aliquots (red and green) are used to allow for a clearer observation of the switching process. A 40 µl volume of the two colored DI water is injected in each one of the source chambers which are designed to have different burst frequencies. In this process, a VCV incorporating both a normally-closed and a normally-open compression valve (see Figure 3.5(b)) is used to switch the liquid flow direction to the intended destination chamber. Figure 3.5(b, c, d, and e) illustrates how the switching design is expected to work. It can be observed from Figure 3.5(b), that air compression in chamber B (created by the sealing of venting hole B) prevents liquid from flowing into destination chamber B, and forces the liquid to burst into destination chamber A. Afterward, the wax plug is melted and the centrifugal force pushes it towards the U bent junction, effectively blocking the venting channel leading to venting hole A. Air compression now occurs in destination chamber A, and the next bursting of liquid will be forced into destination chamber B. The main advantage of this design is that a single wax plug is used to block the two venting holes in two different steps.

Another microfluidic process implemented in this study using the proposed VCV is liquid metering. The microfluidic centrifugal platform designed to perform this process is presented in Figure 3.6(a). The design consists of three metering chambers that are respectively connected to three destination chambers via 0.4 µm width

channels. The venting holes of the three destination chambers are controlled with the proposed VCV (air compression valve). Figure 3.6(b, c, d, and e) presents the expected sequence of liquid metering process which starts with the pumping of the colored DI water from the source chamber towards the liquid metering chambers. The pumping process is performed by thermo-pneumatic pumping (TPP) method developed by Abi-Samra *et al.* (2011) and Thio *et al.* (2013). The liquid flows and fills the metering chambers, but does not enter the destination chambers because of the air-compression created by the VCV. After the liquid settles and levels in the metering chambers, the venting holes are released by melting the wax plugs and the liquid then flows into the destination chambers.
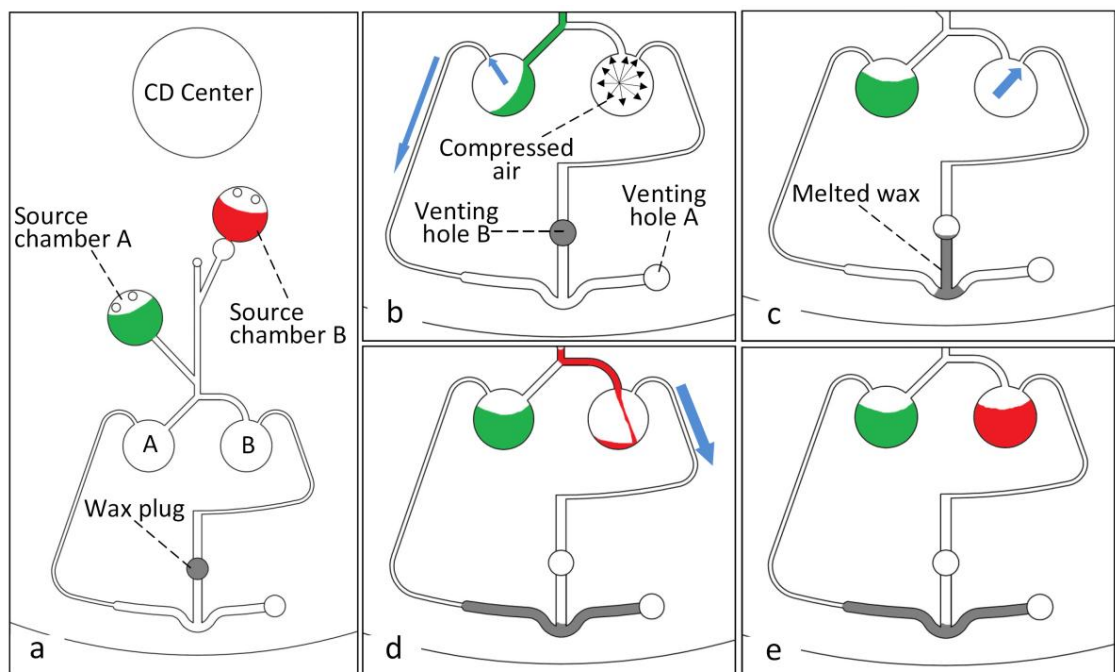
Figure 3.5: Centrifugal microfluidic platform design for liquid switching
(a) position of chambers and wax plug, (b) sealed venting B forces liquid to go to chamber A, (c) melting of wax-plug releases venting hole B and blocks venting hole A, (d) liquid goes to chamber B, (e) final liquid status
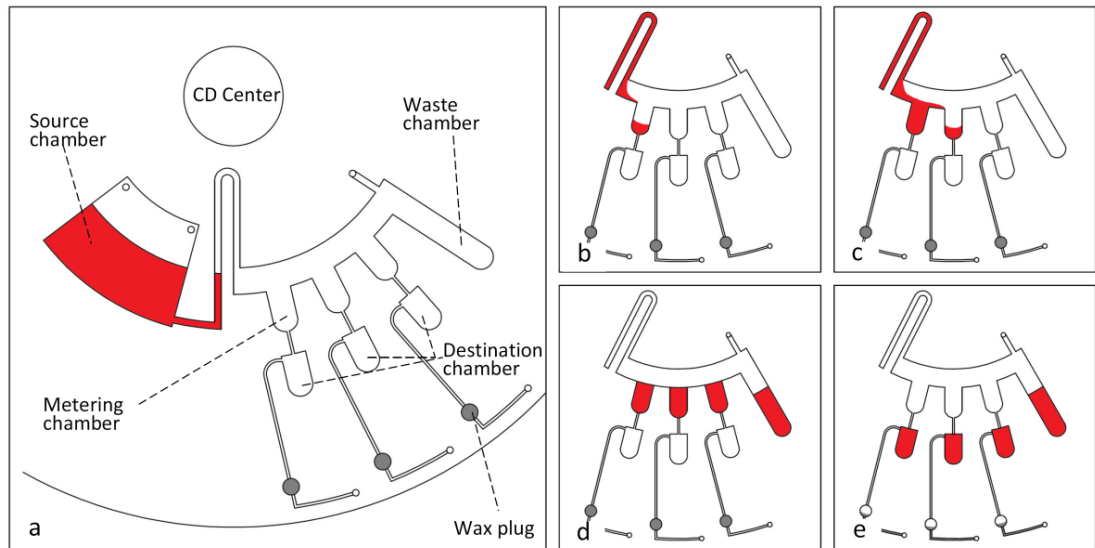
Figure 3.6: Centrifugal microfluidic platform design for liquid metering
(a) position of chambers and wax plugs, (b) liquid fills the first metering chamber,
(c) liquid fills the second metering chamber, (d) liquid filled all metering chambers
and extra liquid flows to the waste chamber, (e) melting of wax-plug allows liquid
to move to the destination chambers

3.4   Passive Liquid Valve (PLV)

In the previous subsection *"3.3 Vacuum/Compression Wax Valve"*, the development of an active valving method that utilizes paraffin wax to control liquid burst frequency was presented. A conventional heating source (hot-air gun) was utilized to actuate the wax valves. Even though the wax valve constitutes an accurate method to control liquid flow, the using of wax and an extra heat source might for some applications be considered a disadvantage.

Therefore, in this part of the work, an easy-to-implement passive liquid valving (PLV) is developed. The PLV employs the same mechanism of the VCV, but instead of using paraffin wax to control the venting holes of the source and destination chambers, the venting holes are controlled by a venting chamber acting as a liquid valve. The PLV mechanism is based on equalizing the main forces acting on the centrifugal microfluidic platform (i.e., the centrifugal and capillary forces) to control the burst frequency of the source chamber liquid. For a better understanding of the physics behind the proposed

PLV, an analytical model is described. Moreover, three parameters that control the effectiveness of the proposed valve, i.e., the liquid height, liquid density, and venting chamber position with respect to the rotational center, are tested experimentally. To demonstrate the ability of the proposed PLV valve, microfluidic liquid switching and liquid metering are performed.

In the following subsections, the microfluidic design and the operational mechanism of the developed PLV is discussed in detail. First, the PLV design and the centrifugal microfluidic platform fabrication method are explored. Then, the operation mechanism is discussed based on the controlled chamber: a passive liquid valve to control the source chamber (S-PLV) and a passive liquid valve to control the destination chamber (D-PLV). An analytical model is described to explain the physical forces involved in the operation of the developed valve. For a better understanding of the different microfluidic designs and the fabricated platform layers, please refer to APPENDIX A.

3.4.1 PLV Design and Fabrication

In this study, two microfluidic designs were fabricated to experimentally test the developed PLV. Figure 3.7 shows the designs of an S-PLV (Figure 3.7(a)) and a D-PLV (Figure 3.7(b)). Both designs consist of three chambers: a source chamber (1 mm deep), a destination chamber (1 mm deep), and a venting chamber (2.5 mm deep). The three chambers are connected together by liquid and venting channels that are 0.7 mm wide and 0.5 mm high. For the S-PLV design (see Figure 3.7(a)), the venting chamber is connected to a ventless source chamber via venting channel A. With this design and the trapped air, the flow of the liquid in the source chamber is controlled by the liquid in the venting chamber. In contrast, in the D-PLV design (see Figure 3.7(b)), the venting chamber is connected to a ventless destination chamber. Therefore, the air flow of the ventless destination chamber is controlled by the liquid in the venting chamber. The proposed valves depend on trapped air, and air compresses and expands easily; thus, the

used of straight channels to connect the source and destination chambers generates fluctuations in the valving performance. This fluctuation is caused by the momentum of the liquid as it bursts from the source chamber, and this momentum can lead to overstretching of the air (in the case of S-PLV) or overcompression of the air (in the case of D-PLV) that prevents proper operation of the valve. To overcome this limitation, a U-shaped bent is introduced in the micro-channel that connects the source and destination chambers to reduce the liquid flow speed and the associated turbulence caused by the liquid momentum (see Figure 3.6(a) and (b)). This U-shaped channel reduces the liquid flow speed and thus, the trapped air produces a more gradual negative pressure (in the case of S-PLV) or gradual positive pressure (in the case of D-PLV).
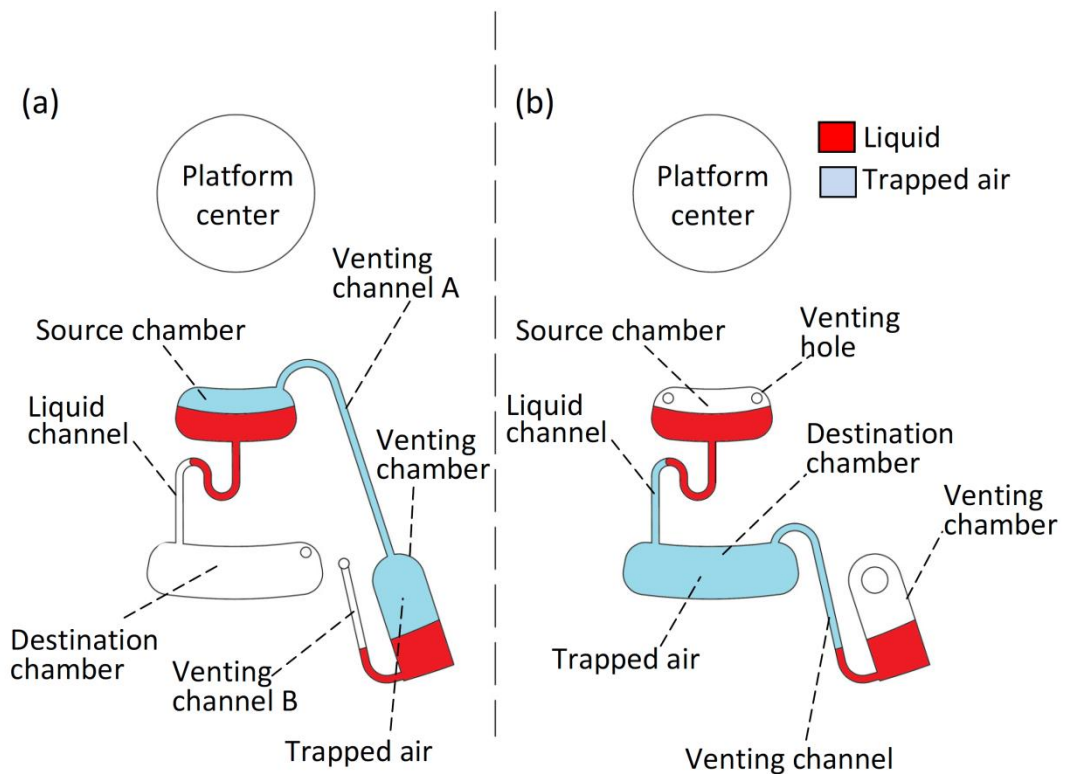

Figure 3.7: Microfluidic design for the developed PLV
(a) S-PLV design where the venting chamber is connected to the source chamber through the venting channel. (b) D-PLV design where the venting chamber is connected to the ventless destination chamber through the venting channel

The centrifugal microfluidic platform fabricated for this study consists of three layers: two PMMA layers and one PSA layer. The bottom 4 mm thick PMMA layer contains all the microfluidic chambers and channels. The top 2 mm thick PMMA layer contains the venting holes which also serve as liquid loading holes and as alignment holes. The adhesive PSA layer bonds the two PMMA layers to each other.

3.4.2 PLV Operation Mechanism

Before we start discussing the operation mechanism of the developed PLV, the reader needs to recall the fundamental forces acting in any centrifugal platform which is described in subsection "*2.3.1.1 Passive Micropumps*". It is very important to remember the $P_{centrifugal}$ and P_{cap} because it will play a key role in the following discussion.

Now, the PLV mechanism can be broken into three main operational stages: air trapping, valve actuation, and liquid bursting. Figure 3.8(a, b, c) shows the liquid in the three different stages for the S-PLV, and Figure 3.8(d, e, f) shows the operational stages for the D-PLV. During the three operational stages, the various pressures involved are the centrifugal pressure acting on the liquid in the source chamber, P_s, the centrifugal pressure acting on the liquid in the venting chamber, P_v, and the capillary pressure against the liquid in the source chamber, P_{cap}. The P_s pressure constantly pushes the source chamber liquid towards the outer edge of the platform, while P_v and P_{cap} both act against liquid flow. Note that P_s and P_v are the result of centrifugal pressure on the centrifugal microfluidic platform. These pressures are calculated using the fundamental centrifugal pressure equation (equation (2.1)). As mentioned before, this is true for any liquid loaded onto the centrifugal microfluidic platform. However, the calculation needs to be made with respect to the parameters related to the source chamber and the venting chamber such as the liquid density and the distance from the center of rotation.

Air trapping stage: the testing of the S-PLV starts with an injection of 40 µl of the colored DI water into the source chamber. Afterward, the required amount of liquid

(for testing the effect of the liquid height on the burst frequency) or the required type of liquid (for testing the effect density on the burst frequency) is injected into the venting chamber. Then, the preloaded platform is mounted on the spin test system, and the spin speed is gradually increased. Initially, the pressures in the system are at equilibrium, and some air is trapped between the source and venting chambers (see Figure 3.8(a)). The critical point just prior to liquid bursting from the source chamber is achieved when the pressures in the system are balanced as follows:

$$P_s = P_v + P_{cap} \tag{3.1}$$

To determine whether the valve holds liquid back in a source chamber or whether the liquid bursts from the source chamber, a balance pressure, $P_{balance}$, which is the difference between the pressures is determined as follows:

$$P_{balance} = P_S - (P_v + P_{cap}) \tag{3.2}$$

A positive $P_{balance}$ indicates that liquid will burst from the source chamber, whereas a negative $P_{balance}$ means that the PLV will hold the liquid back in the source chamber. Figure 3.9 shows the range of $P_{balance}$ for different liquid heights in the venting chamber. The result in Figure 3.9 is valid for both S-PLV and D-PLV as both have the same fundamental principle of operation (based on the centrifugal force VS. capillary pressure and venting chamber pressure). At low frequencies, all venting chamber heights produce a negative balance pressure, indicating that the PLV does hold the liquid back. When the spinning speed is increased, the P_s pressure starts to increase and overcomes the sum of P_v and P_{cap} (giving positive $P_{balance}$ values). However, when the liquid height in the venting chamber is higher than a critical value (such as 3.015 mm

and 3.35 mm) where the combination of the liquid height in the venting chamber and the position in respect the center of the rotation produce P_v value that always higher than P_s, $P_{balance}$ will always be negative. In other words, the valve will hold the liquid in the source chamber indefinitely. Table 3.1 presents all the parameters implemented in the analytical calculations of $P_{balance}$.

Valve actuation stage: when the spinning speed increases, some liquid from the source chamber starts flowing into the microchannel towards the destination chamber (see Figure 3.8(b)). The resulting decrease in liquid level in the source chamber will momentarily expand the volume of trapped air on top of the source and venting chambers. This air expansion creates a state with an instantaneous negative pressure lower than the atmospheric pressure outside the system. This pressure change acts as an actuator that allows the liquid in the venting chamber to flow in the direction of the liquid flow of the source chamber. This negative air pressure tries to suck air through the liquid in the venting chamber. At the same time, the centrifugal pressure acting on the liquid in the venting chamber acts against this air-pulling process. Thus, the valve is actuated, and the burst frequency of the source chamber liquid will increase as long as the venting chamber liquid prevents air from flowing into the system through venting chamber B. Note that the air expansion occurs in this stage is not included in the developed model as it describes the instances of liquid bursting. At the instance of liquid bursting, air expansion and compression is instantaneous, low, and negligible.

Liquid bursting stage: as shown in Figure 3.8(b), as the spinning speed further increases, the increased centrifugal pressure on the source chamber liquid (P_s) tries to suck air through the liquid in the venting chamber by first emptying venting channel B. Further increasing the spinning speed then causes the liquid in the source chamber to approach the top of the U-shaped bent and the pressure acting on the source chamber liquid, P_s, eventually overcomes the combination of the venting chamber pressure (P_v)

and the channel capillary pressure (P_{cap}). At this point, air is forced to enter the system through the venting chamber (bubbles are observed in the venting chamber liquid), and the source chamber liquid is fully transferred to the destination chamber (see Figure 3.8(c)).

The principle of operation of the D-PLV is similar to that of the S-PLV; however, instead of using trapped air on top of the source chamber, the D-PLV works by compressing the air in the destination chamber (see Figure 3.8(d)). Figure 3.8(d) & (e) & (f) show the air-trapping stage, valve actuation stage and liquid bursting stages, respectively, for the D-PLV valve.

In this study, we are also interested in calculating the burst frequency ($Bfreq_{PLV}$) of the liquid in the source chamber when any of the relevant parameters (i.e., venting chamber liquid height, liquid density, and venting chamber position) are changed. Using equation (2.1) to expand P_s and P_v in equation (3.1), we obtain the following expression:

$$\rho_s \omega^2 \Delta r_s \overline{r_s} = \rho_V \omega^2 \Delta r_V \overline{r_V} + P_{cap} \tag{3.3}$$

Further rearranging equation (3.3) then yields:

$$Bfreq_{PLV} = \sqrt{\frac{P_{cap}}{\rho_s \Delta r_s \overline{r_s} - \rho_V \Delta r_V \overline{r_V}}} \left(\frac{30}{\pi}\right) \tag{3.4}$$

Using equation (3.4), the effect of various parameters that control the effectiveness of the proposed valve can be studied theoretically. In this study, three different parameters, (i) the liquid height of the venting chamber, (ii) the density of the liquid in the venting chamber, and (iii) the venting chamber distance from the platform center, are evaluated experimentally.
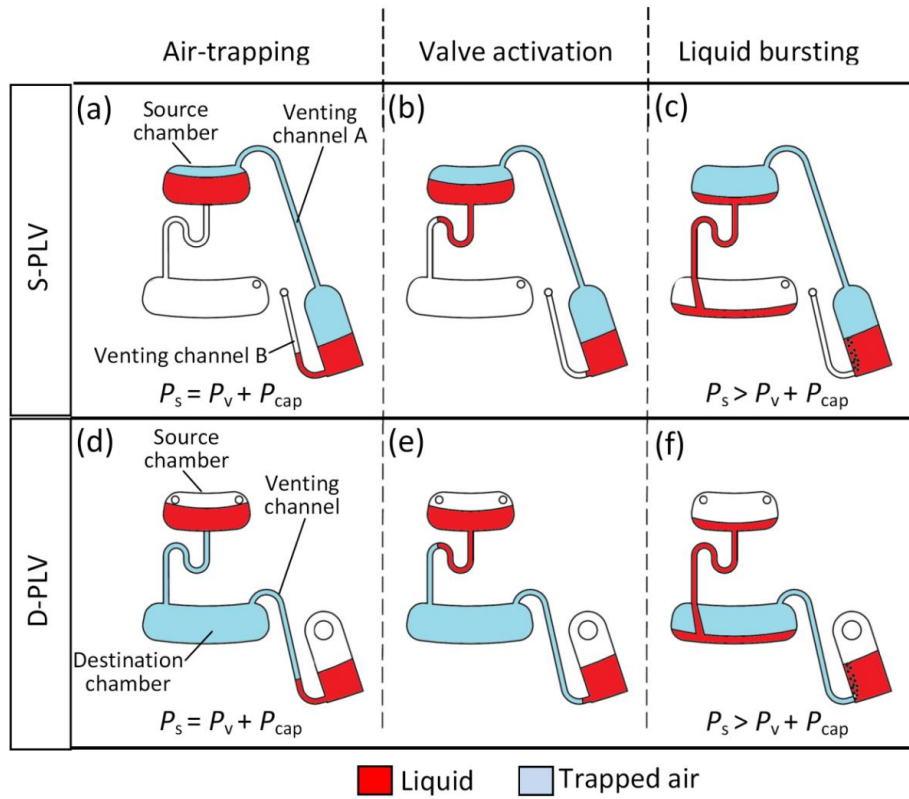
Figure 3.8: PLV Liquid valving stages
(a) S-PLV at low frequency. (b) high spinning speed where the source chamber liquid starts to flow inside the micro-channel, creating a lower pressure effect in the venting chamber. (c) high frequency, the source chamber liquid bursts into the destination chamber. (d) D-PLV at low frequency. (e) high speed, the source chamber liquid starts flowing into the microchannel, creating compression state in the destination chamber. (f) high frequency, the source chamber liquid bursts into the destination chamber

Table 3.1: Values of the parameters implemented in the analytical calculations

Parameters	Values	Parameters	Values	Parameters	Values
Θ_c	68°	r_{s1}	32.3 mm	r_{v2}	60 mm
γ_{la}	71.97 mN/m	r_{s2}	37.5 mm	ρ	1.000 g/cm^3
D_h	3.83e10^{-4} meter	r_{v1}	58.66, 58.32, 58, 57.65, 56.98, and 56.65 mm		
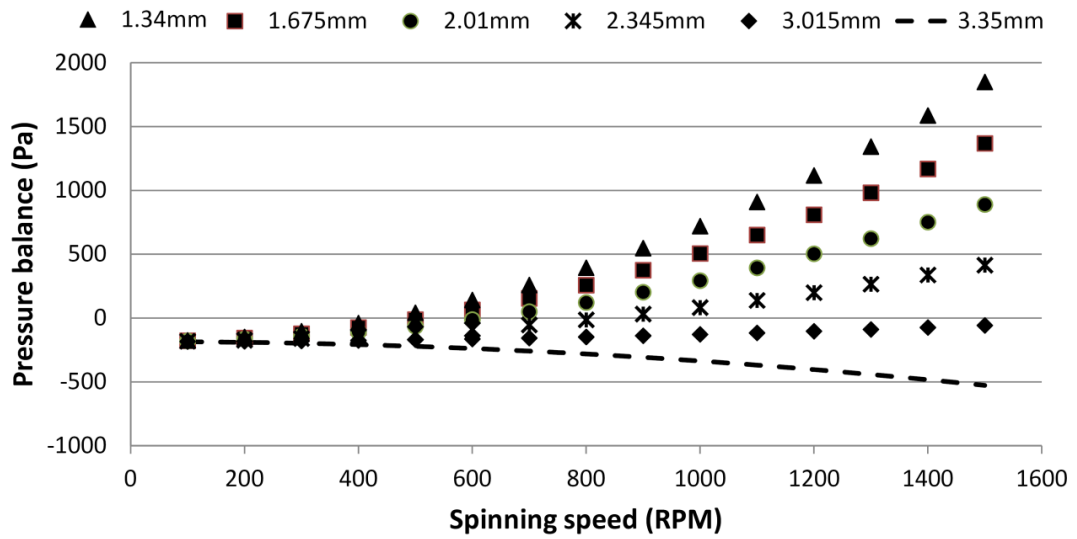
Figure 3.9: Theoretical pressure balance at different venting chamber liquid heights for a range of spinning speeds

3.4.3 Applications of PLV

Various microfluidic processes can be performed utilizing the proposed PLV valves. In this work, microfluidic liquid switching and liquid metering are conducted using the D-PLV valving method. Figure 3.10(a) and (c) shows the centrifugal microfluidic platform designs of the liquid switching and metering processes, respectively.

The liquid switching design consists of two main layers: the switching layer and the venting layer. The switching layer contains two source chambers (A and B) connected to two destination chambers (A and B). The source chambers are placed at different distances from the platform center and thus burst at different rotational speeds (see Figure 3.10(a)). Furthermore, the venting layer consists of two venting chamber (A and B) that are connected to two venting channels (A and B). For liquid switching, the venting channels of the two destination chambers are controlled using two venting

chambers (A and B). For a more practical use of the platform space, the design features are engraved on two different layers that appear to overlap when viewed from the top (3D platform design). This design is fabricated using a five layer platform (please refer to APPENDIX A). To clearly observe the switching process, two solutions of colored DI water (red and green) are utilized in this process.

The liquid switching experiment starts with the injection of 20 µl of green DI water into source chamber A with the injection of the same volume of the red DI water into source chamber B. The second step is the injection of 60 µl of red DI water into venting chamber B. This process will create a normally opened valve for destination chamber A and a normally closed valve for destination chamber B. Afterwards, the platform is mounted on the spinning test system, and the spinning process starts. The switching process can be divided into three main steps. In Step 1, the liquid of source chamber A bursts and is forced to flow towards destination chamber A as the venting channel of destination chamber B is closed by venting chamber B. In Step 2, the liquid in venting chamber B bursts into venting chamber A; this burst opens the venting hole of destination chamber B while sealing venting channel A. In Step 3, liquid bursting from source chamber B will then flow towards destination chamber B without entering destination chamber A.

Figure 3.10(c) shows the design for the liquid metering. The design consists of a main source chamber that contains the liquid that will be metered. The source chamber is connected to four metering chambers (90 µl volume each) and one waste chamber; the excess liquid will overflow into the waste chamber. Finally, the four metering chambers are connected to ventless destination chambers, which are controlled by four separate venting chambers. The metering process starts with the injection of 550 µl of the red DI liquid into the source chamber. Then, 50 µl of the same DI water is injected into each venting chamber. Afterward, the centrifugal microfluidic platform is mounted

on the spin test system, and the centrifugal platform is spun. With this simple design, the 550 µl of DI water can be automatically metered (90 µl) and then transferred into the four destination chambers for use in the next stage in a multistep centrifugal platform.
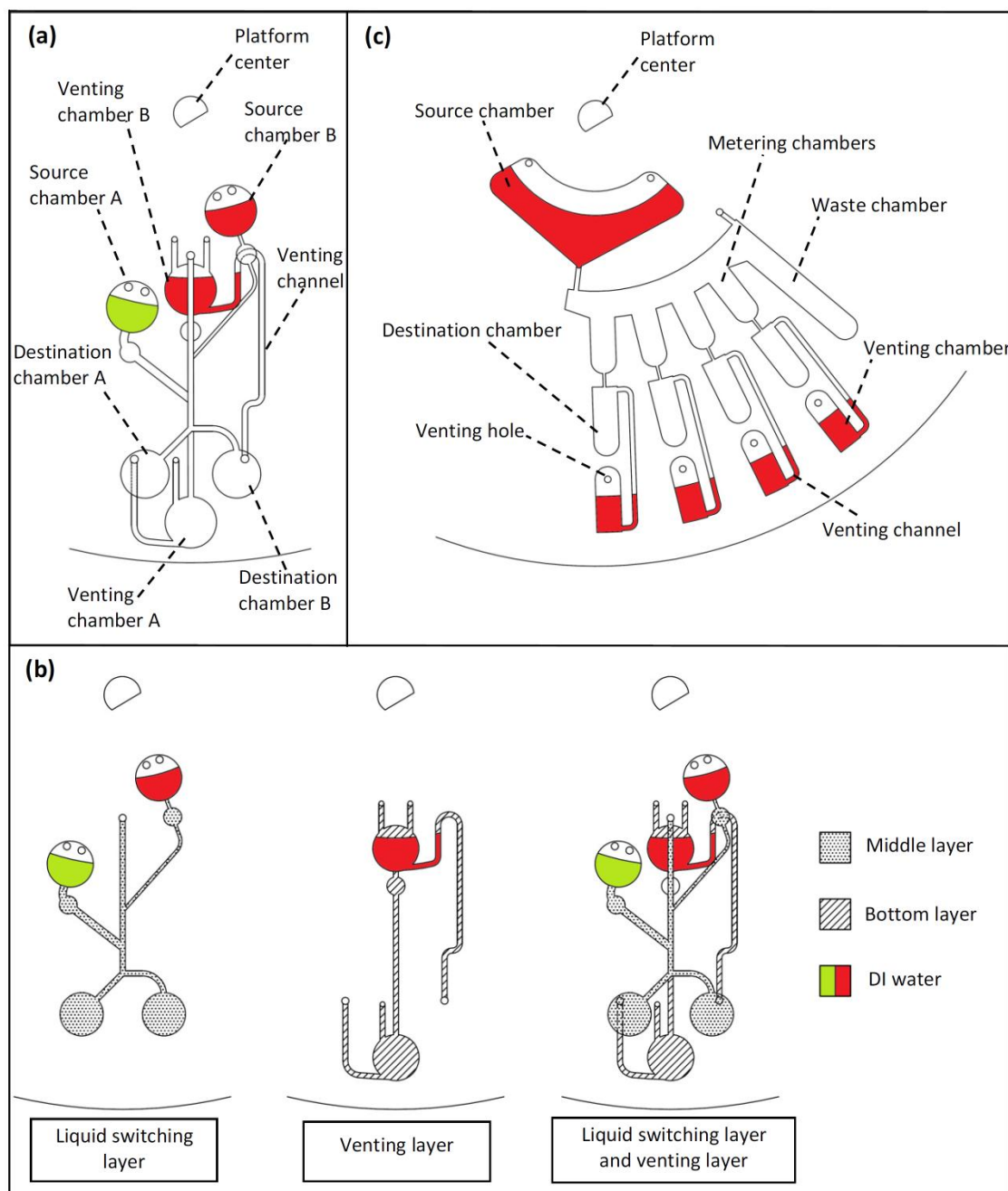

Figure 3.10: Centrifugal Microfluidic platform design for liquid switching and liquid metering
(a) layer-by-layer design of the liquid switching process (b) liquid switching layers (c) design of the liquid metering process

3.5   Check Valve

In this part of the study, simple and easy to fabricate check valves that are modular and easy to implement in any process on a centrifugal microfluidic platform, are developed. The proposed check valves have the ability to restrict liquid and air flow in only one direction. Two types of check valves are developed: a terminal check valve (TCV) and a bridge check valve (BCV). To understand the characteristic of the proposed valves, theoretical and experimental studies are conducted. Moreover, to test the effectiveness of these valves, liquid swapping is demonstrated by integrating TCV and BCV chips with TPP on a centrifugal microfluidic platform.

3.5.1   TCV and BCV

The principle of operation of the TCV and BCV are illustrated in Figure 3.11. Both valves consist of a latex film sandwiched between rigid top and bottom covers. One crucial element of the valves is the air exchange hole: for the TCV chip the hole is cut through the latex film, while for the BCV the hole is cut through the top cover (see Figure 3.11(a1, b1, and c1)). The air exchange hole allows the check valve to operate in one of two modes: *flow* and *blocking* mode.

Figure 3.11(a1-a3) illustrates the operation of the TCV. When positive air pressure is applied to the inlet of the TCV, the latex is deflected upwards towards the open space between the top and bottom covers. Air can then travel through the space created by the deflection, and then via the air exchange hole to escape through the outlet (see Figure 3.11(a2)). However, when a negative pressure is applied on the inlet of the TCV valve, the latex film is pulled slightly into the inlet, thus forming an air tight seal, and air flow through the valve is restricted (see Figure 3.11(a3)). In this configuration, the TCV chip can be installed on the centrifugal microfluidic platform with the inlet facing the platform surface (over a channel opening) to allow only one way air flow from within the platform to the surrounding environment. By flipping the TCV chip

over, and having the top cover placed on the platform surface, it will then allow only one way air flow from the surrounding environment into the platform (see Figure 3.11(b1-b3)).
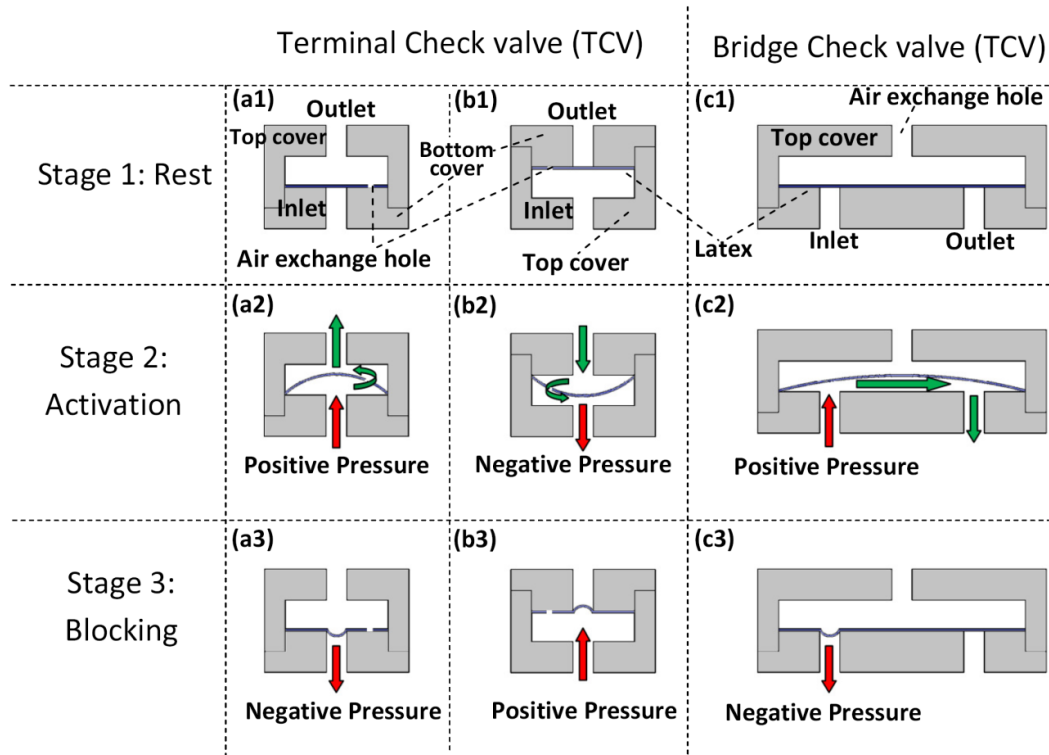
Figure 3.11: Check valve operation principle
(a1, b1, and c1) TCV and BCV valve at rest, (a2) TCV valve activated by applying positive pressure on the inlet, (b2) TCV valve activated by implementing negative pressure on inlet, (c2) BCV valve activated by applying positive pressure on inlet, (a3) TCV valve blocking air-flow due to the negative pressure on inlet, (b3) TCV valve blocking air-flow by implementing positive pressure on inlet, (c3) BCV valve blocking air/liquid flow as negative pressure is applied on inlet

Figure 3.11(c1-c3) demonstrates the principle of operation for the bridge valve. As both the inlet and outlets are in the bottom cover in this case, it is the bottom cover that must be placed on the platform surface. Similar to the TCV chip, when the centrifugal microfluidic platform is at rest, the latex film is flat against the bottom cover (see Figure 3.11(c1)). When a positive pressure is applied on the inlet of the BCV valve, the latex film is deflected upwards, and air / liquid is allowed to flow through the space under the latex to the outlet (see Figure 3.11(c2)). However, when a negative pressure is

applied on the inlet of the BCV valve, the latex forms a tight seal over the inlet, preventing any backward flow of air / liquid (see Figure 3.11(c3)). Note that for the BCV valve, the inlet and outlet positions are interchangeable, and the valve only allows liquid to flow if there is positive pressure on either the inlet or outlet, but blocks fluid flow if there is negative pressure applied instead (i.e., you can push fluid through the valve, but not pull liquid through it).

By implementing this directional flow control on TPP, the capability of this pumping method can be significantly improved. Figure 3.12 presents a microfluidic centrifugal platform design where a detection chamber is connected to a TPP chamber. TPP is a well-established pumping method in the centrifugal microfluidic platform field that employs heat to pump liquid towards the platform center. However, when the detection chamber is connected to two terminals (see Figure 3.12(a)), liquid can only be pumped concurrently from both terminals End 1 and End 2 (or pumped concurrently to both End 1 and End 2). This is an impractical process as there is no way to control the liquid volume pumped, and the flow of liquid to only a particular terminal. By installing a TCV valve on terminal End 1, and a BCV valve on terminal End 2, the direction of liquid/air flow is restricted to be on way: from terminal End 1 towards the detection chamber, and subsequently towards terminal End 2 (see Figure 3.12(b)). This enhancement greatly extends the ability to perform multi-stepped complex process on the centrifugal microfluidic platform.
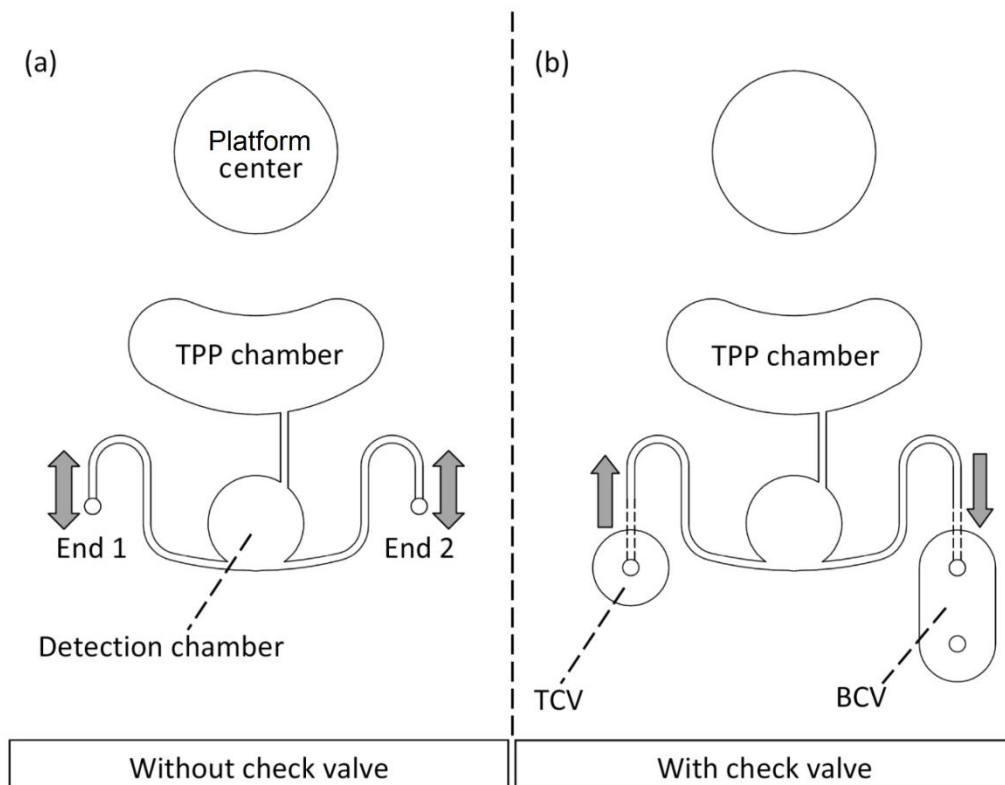
**Figure 3.12: Thermo-pneumatic pumping with and without the check valve
(a) without check valve where the direction of air/liquid from End 1 and End 2 is
incontrollable (b) with the proposed TCV check valve and BCV check valve
installed on End 1 and End 2 respectively**

3.5.2   Check Valve Design and Fabrication

In this part of the work, the presented check valves are simple to fabricate. Each valve consists of three layers (2 PMMA layers, and one latex layer). The fabrication process for the top and bottom covers of the TCV and the BCV are described separately in the following two subsections. The final subsection discusses how the latex film is prepared and how the check valves are assembled.

3.5.2.1   Terminal Check Valve (TCV)

The TCV chip is in the form of a flat cylindrical chip that is approximately 7mm in diameter, and 5mm in height dimensions. Figure 3.13 shows the detailed specification of the top and bottom covers of the chip, while Figure 3.14 shows the 3D

model of the chip. The two covers are made of rigid PMMA plastics, and when precisely machined, the fit is tight.
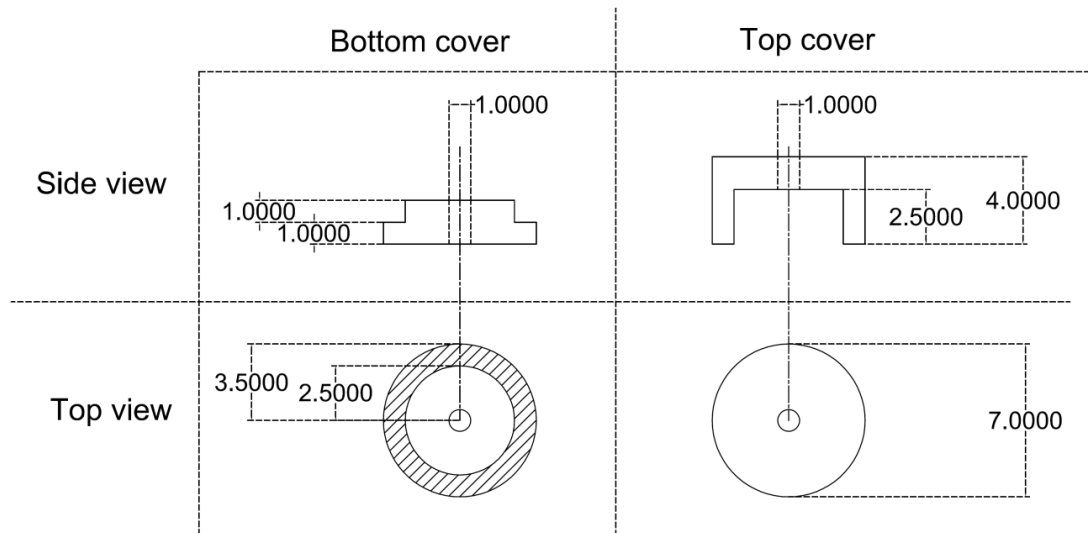
Figure 3.13: Terminal check valve (TCV) design
Full design dimensions from top and side view (all mesurements are in millimeter)

The bottom cover is fabricated from a 2mm PMMA, with an outer track of width 1 mm near the edge of the chip engraved down to 1 mm in thickness with the CNC machine (see Figure 3.13 & Figure 3.14). This leaves only a circle area of radius 5 mm in the middle of the chip with 2 mm thickness. A through hole of 1 mm in diameter is then drilled in the center of the chip for air flow. Similarly, the top cover is fabricated from a 4 mm PMMA plastic, but with the inner area of diameter 5 mm engraved down to 2.5 mm in thickness using the CNC machine. This engraved inner area leaves a 1.5 mm spacer area that limits the latex material from over extension when the valve is in operation. A through hole is then drilled in the center of the chip for air flow. Once cut, the top and bottom covers then can be snapped together with the latex film in between without the need for any adhesive material.
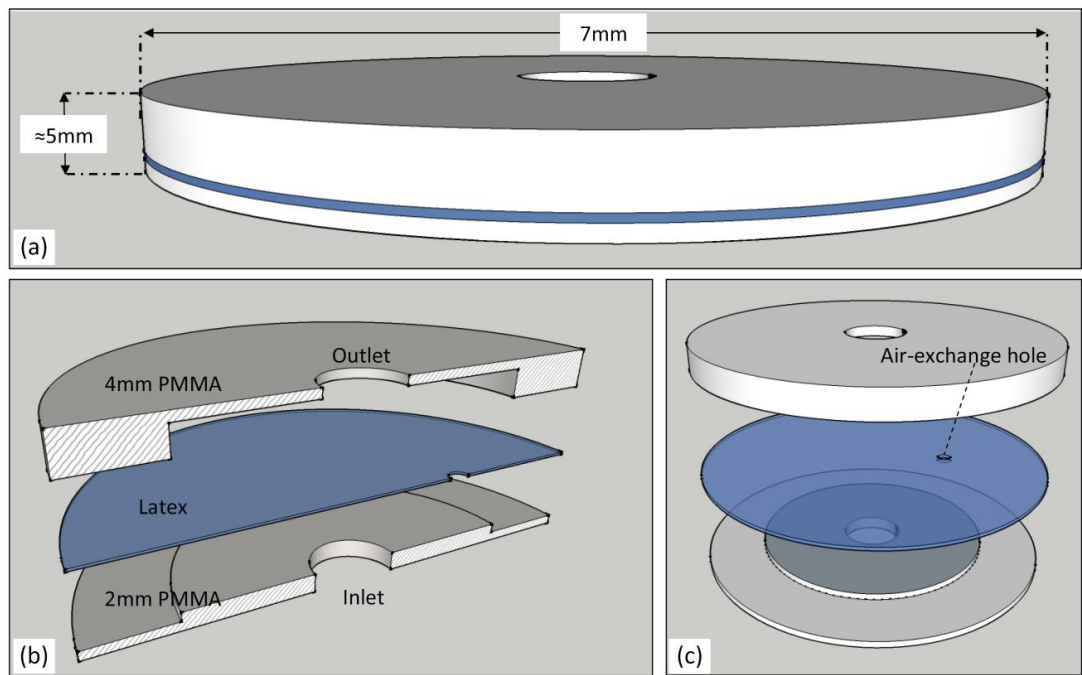
**Figure 3.14: Terminal Check Valve (TCV) 3D layers arrangement
(a) TCV final fabricated chip, (b) TCV layers arrangement, (c) TCV full layers
and air-exchange hole position**

The core of the TCV is the middle layer which is made of a thin commercially available latex sheet. When placed between the top and bottom covers, the deflection of the latex is limited by the height of the spacer area (1.5 mm). The latex material is chosen for its high transparency (>89.9%) (Pekcan & Arda, 1999), vapor impermeability (Arda & Pekcan, 2001), and hydrophilicity properties (Ho & Khew, 2000). More importantly is the latex's elastic characteristic that allows it to form an air tight seal when the valve is blocking air flow (see Figure 3.11(a3, b3)) (Zheng *et al.*, 2013). More details of the latex preparation will be discussed in subsection "*3.5.2.3 Latex Fabrication, Valve Assembly and Installation*".

3.5.2.2 Bridge Check Valve (BCV)

The BCV chip is a variation of the TCV chip which can be used to connect two points on the centrifugal microfluidic platform to control the liquid and air flow direction between the two points. The BCV chip is fabricated in the form of a flat

capsule with a set of inlet and outlet holes at the bottom of the chip, and an air exchange hole on the top. Figure 3.15 and Figure 3.16 respectively show the detailed specification, and the 3D model of the chip. The chip has dimensions of 14 mm x 7 mm x 5 mm (Length x Width x Height). Similar to the TCV chip, the BCV chip is fabricated with a top cover and a bottom cover that snaps together sandwiching the latex film in between. To achieve this, the bottom cover has an outer track of width 1 mm engraved along the edge of the chip, while the top cover has an engraved inner area. The inlet and outlet holes are then drilled through the bottom cover, and the air exchange hole is drilled through the top cover. The hole on the top cover ensures that there is no air compression in the spacer area when the latex deflects upward during operation.
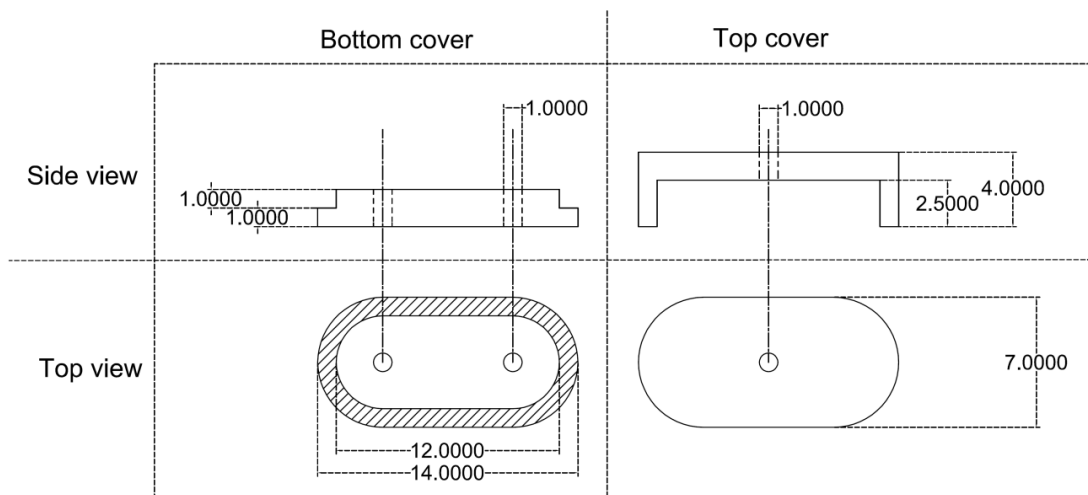
Figure 3.15: Bridge check valve (BCV) design
Full design details from top and side view (all mesurements are in millimeter)
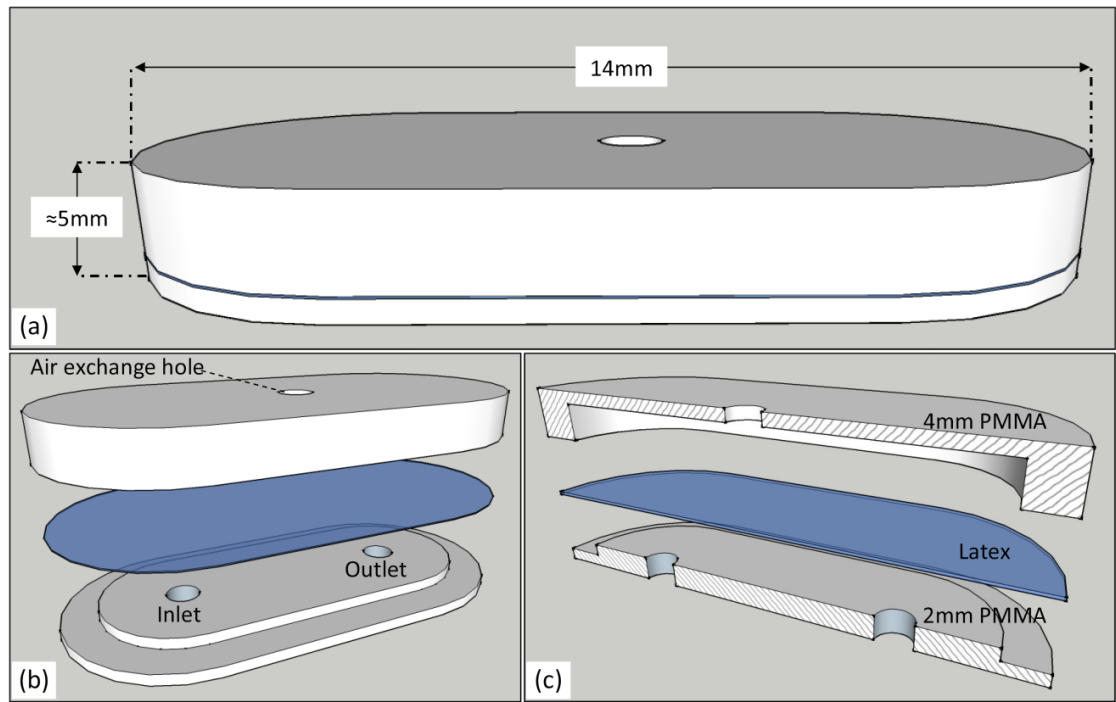
Figure 3.16: Bridge check valve (BCV)
(a) final fabricated chip, (b) BCV layers arrangement and the position of the inlet, outlet, and air-exchange hole, (c) side view for BCV layers

3.5.2.3 Latex Fabrication, Valve Assembly and Installation

For consistent preparation of the latex layer in the fabrication of the check valves, a latex fabrication base was prepared. Figure 3.17(a) shows the top and bottom frames of the latex fabrication base, and Figure 3.17(b) illustrates how the frames are snapped together with the latex in between. The latex is stretched ten percent in both the length and width dimensions to make it taut. The size of the frame provides enough stretched latex to fabricate nice check valve chips simultaneously. This method ensures that the check valves fabricated have latex layers that are consistent in terms of elasticity. Once the latex is stretched on the base, holes are manually introduced in the latex by a small needle (one hole for each TCV valve to be fabricated). The holes are measured to be approximately 0.5 mm in diameter. Finally, the top and bottom covers of the check valves are snapped together from the top and bottom of the latex layer. The fabricated check valves are then cut out one by one from the latex sheet. The final

produced check valves are then installed as needed onto the surface of the centrifugal platform using adhesive material.

3.5.3 Applications of Check Valve

To evaluate the effectiveness of the TCV and BCV chips on a centrifugal microfluidic platform, a design that performs liquid swapping was fabricated and tested. In Figure 3.18(a) we show a centrifugal microfluidic platform design consisting of three chambers (chamber A, chamber B and the waste chamber), and with connecting micro channels with widths and depths given by 0.7 mm and 0.5 mm respectively. A TCV chip was installed in conjunction with chamber B, and a BCV chip was installed in the channel between chamber A and the waste chamber. The TCV chip is configured to only allow air flow from the outside of the platform into chamber B (and not from chamber B to the outside), while the BCV chip only allows the liquid to flow from chamber A to the waste chamber. For controlled one-way liquid pumping, a TPP chamber is placed near the centrifugal platform center and connected directly to chamber A to allow for push/pull pumping. For TPP chamber heating, a customized industrial hot-air gun is fixed 1 cm on top of radial track of the TPP chamber. A 1 cm diameter focusing nozzle is installed on the hot-air gun focuses the heat and prevents heating other parts of the centrifugal microfluidic platform. The platform surface temperature during spinning is measured using a digital infrared (IR) thermometer. Push pumping creates positive pressure in chamber A during heating of the TPP chamber, while pull pumping creates negative pressure in the chamber during cooling of the TPP chamber. Further details of push/pull pumping can be found in Thio *et al.* (2013). Although the purpose of the platform design shown in Figure 3.18 is to demonstrate the effectiveness of the check valves, the design can be easily modified to incorporate check valves in a wide variety of complex biomedical diagnostic assays.
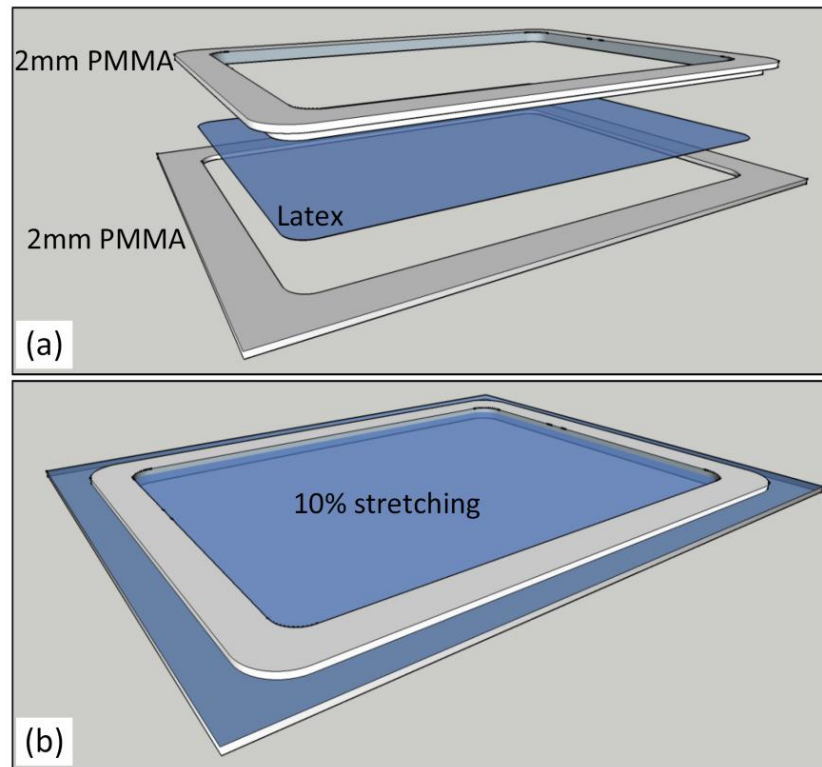
Figure 3.17: Latex fabrication bases
(a) fabrication base layers arrangement, (b) fabrication base after stretch and fix the latex

The experiment starts with the filling of chamber A with 45 μl of red colored deionized (DI) water, and the filling of chamber B with the same amount of blue colored DI water (see Figure 3.18(a)). Two different colored DI water are implemented in this test to make the liquid swapping process more visible. First, the loaded centrifugal microfluidic platform is spun up to 300 rpm, and the heat source is powered on to activate push pumping. The positive pressure created this way pushes on the liquid in chamber A, and the liquid flows through the BCV chip towards the waste chamber (see Figure 3.18(b)). The heat source is then turned off, and pull pumping is activated. The negative pressure generated pulls the liquid from chamber B into chamber A (Figure 3.18(c) and (d)). The heat source is then turned on again to repeat pushing the liquid from chamber A to the waste chamber (Figure 3.18(e) and (f)).

3.6   Biomedical Applications

Different biomedical and chemical applications can be performed using the proposed three valves. In this work, Bradford assay and ELISA assay are demonstrated as potential biomedical applications using the PLV and the check valve, respectively. Both assays were selected as example of well known benchtop procedures that widely utilized in healthcare centers to detect various diseases and/or reflect medical information from patients' biological samples. Moreover, Bradford assay is selected as an example for simple assays and ELISA is selected as an example of multistep complex assays. Therefore, the ability of the developed valves to perform different application with different complexity will be highlighted.

3.6.1   Bradford Assay for Measuring Protein Concentrations

The Bradford procedure is a well-known colorimetric assay that utilizes the color shift of the utilized reagent (Coomassie Brilliant Blue G-250) to calculate the protein concentration in a specific sample (Bradford, 1976). When the Bradford reagent, which is originally brown, is mixed with a specific sample, the mixture will become blue. The intensity of the blue corresponds to the protein concentration in that specific sample.

To perform the Bradford assay, the liquid metering design using the developed PLV is utilized to test various samples in parallel (see Figure 3.10(b)). A bovine serum albumin (BSA) sample with a known protein concentration of 10 mg/ml is used in this assay. The BSA is serially diluted five times to obtain samples with protein concentrations of 1 mg/ml, 0.5 mg/ml, 0.25 mg/ml, 0.125 mg/ml, and 0.0625 mg/ml.

The experiment starts with the injection of 550 µl of the Bradford reagent into the source chamber and the injection of 10 µl of each prepared concentration into the destination chambers. Then, the inlet and venting holes of the preloaded destination chambers are tightly sealed using a PSA product. Afterward, 50 µl of red DI water is

injected into each venting chamber. Next, the centrifugal microfluidic platform is mounted on the spin test system, and the rotation process is started. When the spinning reaches specific speed, the Bradford reagent will burst and fill the metering chambers while the rest will overflow to the waste chamber. Then, the spinning speed further increased for the metered Bradford reagent to burst into the destination chambers and mix with the BSA samples. Finally, the mixture will be transferred to 96 microplate and the final results will be read using micro-plate colorimetric reader.
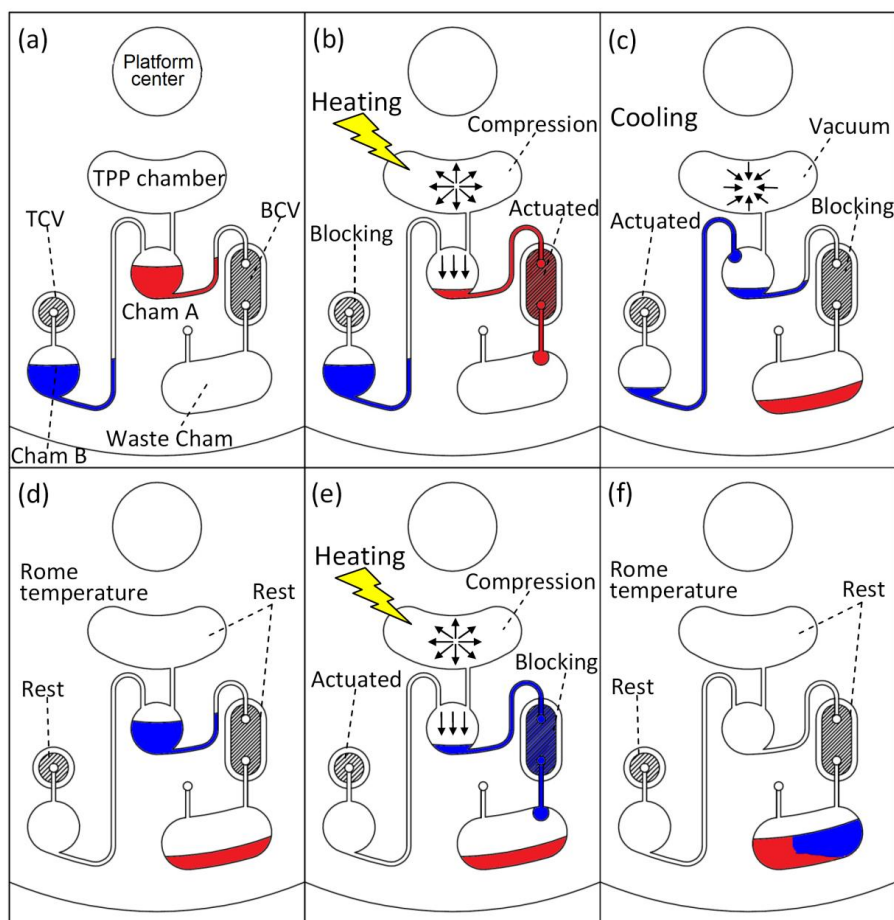
Figure 3.18: Liquid swapping sequence
(a) liquid status before start the process, (b) heating the TPP chamber where the TCV valve is blocked while the BCV chip is activated, (c) cooling the TPP chamber actuates pull pumping where the TCV valve is activated and the BCV chip is blocking reverse airflow from the waste chamber, (d) liquid position after the cooling process stops, (e) heating the TPP chamber pushes the liquid from chamber A towards the waste chamber, (f) final liquid status

3.6.2 ELISA Assay for Dengue Detection

To demonstrate the ability of the proposed check valves to perform multistep processes, a sandwich ELISA assay is performed by integrating the BCV and TCV with TPP method. ELISA is a biochemistry assay utilized to detect the antigen and/or antibody of specific infectious diseases in patient serum. Figure 3.19 shows the microfluidic design developed for the ELISA assay. In this design, we utilize one continuous spiral micro-channel to store the reagents (such as conjugate antigen, TMB, and stopping solution) and washing buffer in a sequence following the steps of the ELISA process. Essentially, this ELISA design is similar to the liquid swapping process discussed previously (see Figure 3.18) but we replaced chamber B with the continuous spiral micro-channel, and let chamber A as the ELISA detection chamber that is coated with a specific antigen such as Dengue antigen. For clearer process observation, the ELISA assay is demonstrated with colored DI water representing each liquid involved in the process (most of the liquid involve in the ELISA process are clear transparent fluids). As can be seen from Figure 3.19, A TCV valve is installed at the end of the spiralled channel to ensure one-way flow of the reagents and washing solutions towards the detection chamber and not the other way. On the other hand, a BCV valve is positioned between the detection chamber and the waste chamber to control the flow in a similar manner for the design in the "Liquid Swapping process". In this design, the reagent and washing solutions are injected in the spiral channel though the inlet holes separated by a specific predefined volume of "air-plug" to ensure that no mixing happens between two consecutive liquids. Similar to the "liquid swapping process", repeated TPP (activated through sequential heating and cooling) pulls the different reagents and washing solution in to the detection chamber, then subsequently flushes out the liquid into the waste chamber.
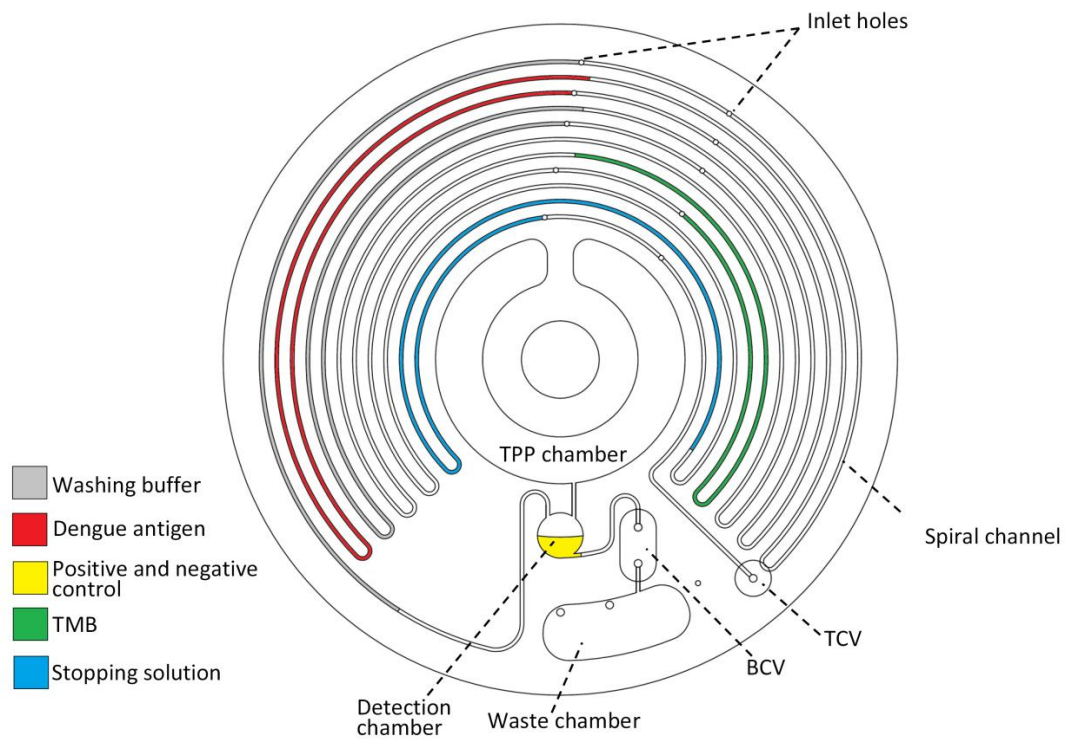
Figure 3.19: Centrifugal microfluidic platform design for ELISA assay
Centrifugal microfluidic platform design to perform ELISA assay by integrating the developed TCV and BCV check valves with TPP

CHAPTER 4: RESULTS AND DISCUSSION

4.1 Introduction

In this chapter, the experimental results of the three developed valves are presented and discussed. The results are divided into three main subsections following the developed micro-valves: wax vacuum/compression valve, liquid passive valve (PLV), and check valve. Then, the results of the demonstrated biomedical applications (i.e., Bradford assay, and ELISA assay) are illustrated.

4.2 Vacuum/Compression Wax Valve Results

In this section, the experimental results of the developed VCV valve are presented. This section is divided into three parts according to the conducted experiments: microfluidic platform heat profile, VCV effectiveness, and applications of VCV.

4.2.1 Microfluidic Platform Heat Profile

Figure 4.1 shows the heating profile for the centrifugal microfluidic platform during the heating process. The x-axis represents the experiment time and the platform spinning speed, while the y-axis represents the temperature of the platform surface. The forced convection heating is fixed at 130°C for this experiment.

The graph can be divided up into two main parts: the first part represents the heating profile of the centrifugal platform (heater is ON), while the second part represents the cooling profile of the centrifugal platform (heater is OFF). The platform surface temperature increases dramatically in the first 2 minutes from room temperature at 27°C to approximately 48°C, then continues to rise somewhat slower to the minimum wax melting temperature of 57.2°C (135°F), and peaks out around 60°C at around the 8th minute mark. The temperature is observed to remain around 60°C for the next 4 minutes. The forced convection heating is then shut off, and the centrifugal platform

spinning is also stopped temporarily before the start of the cooling process. Next, the centrifugal platform is left to cool at increasing rpm speeds and the temperature reaches room temperature in 12 minutes. The result provides an understanding of how the centrifugal platform surface responds to forced convection heating. It is clear that with the forced convection heating set at 130°C, the platform would require 8 minutes to melt the wax to operate the VCV.
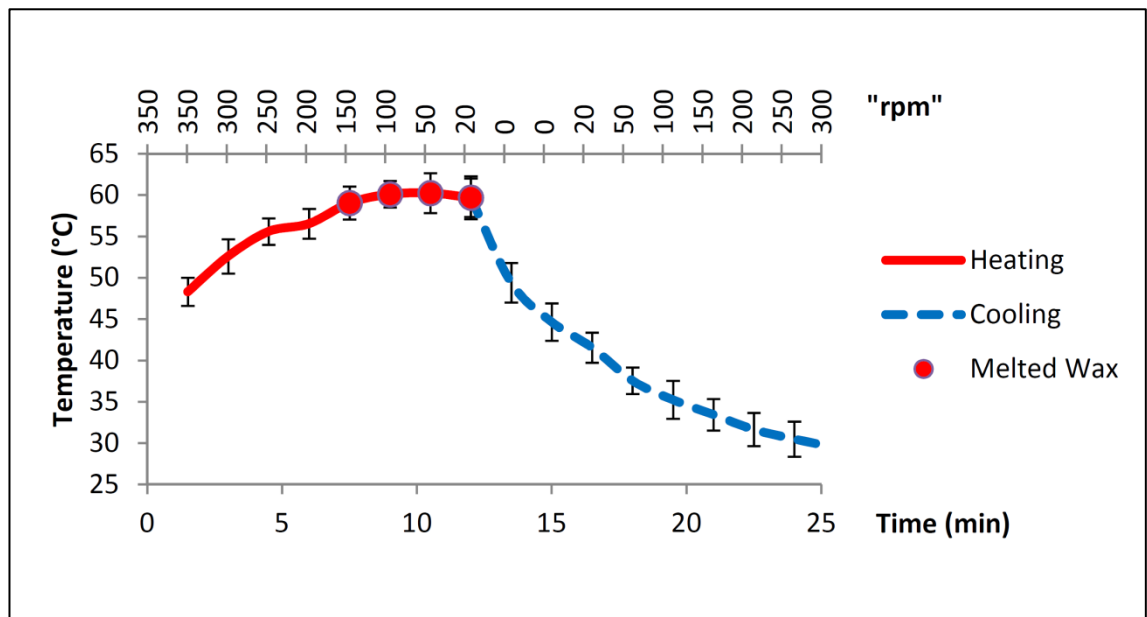
Figure 4.1: **Heating profile for the centrifugal microfluidic platform and wax melting points**

4.2.2 VCV Effectiveness

The second part of this study focuses on testing the effectiveness of the proposed valve and its response towards increasing pressure produced by an incremental spinning speed. Figure 4.2 presents the liquid behaviour at three different points of the experimental test for the air-vacuum state (venting hole A is sealed). Figure 4.2(a) shows the initial status of the liquid before and during the early stages of spinning, Figure 4.2(b) illustrates liquid spilling into the micro-channel due to the high spinning speed (more than 900 rpm) that leads to air compression inside the destination chamber. Figure 4.2(c) shows the final result at 1500 rpm where a minor leakage of one droplet

occurs when the liquid/compressed-air interface destabilizes and some air escapes in the form of bubbles up the micro-channel. This result shows that the proposed VCV is able to prevent liquid from bursting into the destination chamber up to speeds of 1000 rpm. However, at spinning speeds above 1000 rpm, although the fluid still does not flow into Chamber B, some leakage is observed.
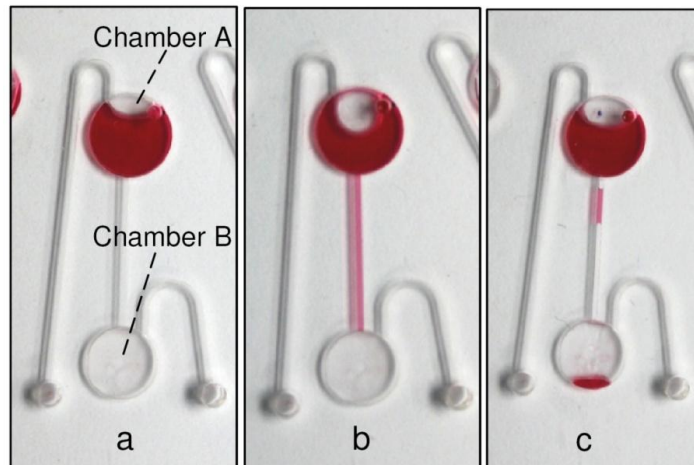
Figure 4.2: Liquid state during the testing of VCV valving effectiveness
(a) initial liquid postion during low spinning speed, (b) liquid goes into the channel at spinning frequency > 900 rpm, (c) final position of liquid at 1500 rpm

Experimental data for compression and vacuum valving is presented separately in Figure 4.3. Moreover, the experimental results are compared to the control (experimental results without valving) and theoretical results calculated using equations (2.1) and (2.2). From our results it is clear that vacuum valving (source chamber venting hole sealed) is more dynamic than compression valving (destination chamber venting hole sealed). There are two reasons for this; the first is the smaller volume of air in vacuum valving (air that is trapped in the source chamber on top of the liquid and inside the venting channel), is hard to expand. The second is the effect of the lower centrifugal force experienced by the liquid in the source chamber with a vacuum valve. In comparison to the liquid in the micro-channel in the configuration with a compression valve, the liquid in a configuration with a vacuum valve is closer to the center of the centrifugal platform.
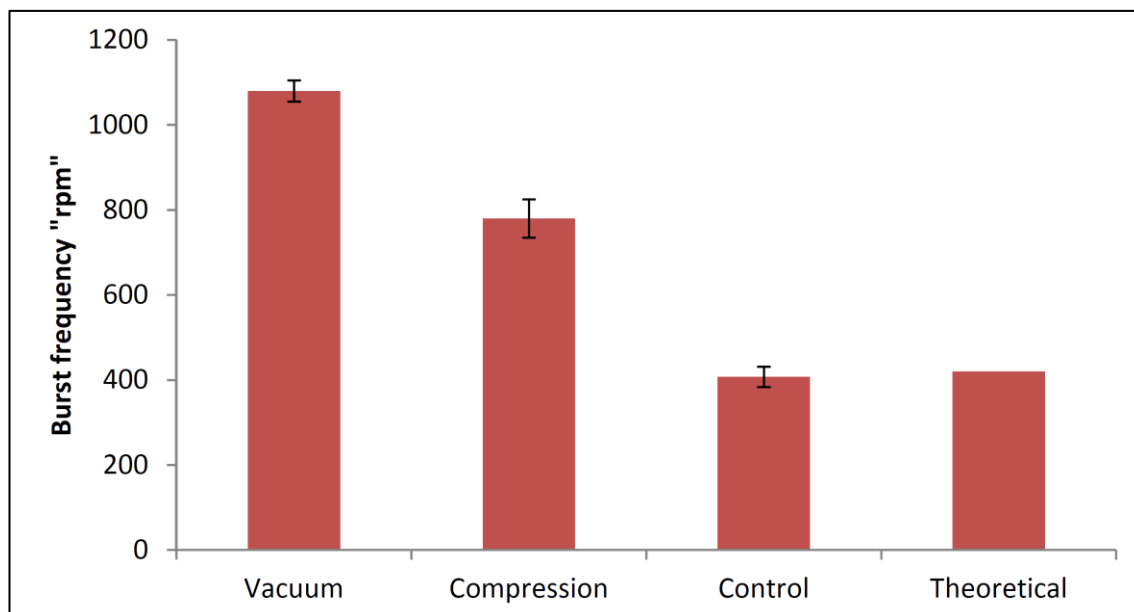
Figure 4.3: Liquid burst frequency using the VCV
Burst frequency for liquid using the proposed Vacuum/Compression valaving,
and burst frequency for Control & Theoretical calculation

In comparison to the wax valving proposed by Abi-Samra *et al.* (2011), the proposed VCV prevents any mixing between the sealing material and the test samples. This design improvement gives way to the possibility of different types of material for valving which may be more easily managed. Moreover, the layout of the VCV on the centrifugal microfluidic platform can be easily relocated to be further away from the test samples. This is an advantage when compared to the valving method by Abi-Samra *et al.* (2011) where the heating source is directly focused on the micro-channels, concurrently heating the wax and the liquid in the channel.

4.2.3 Applications of VCV

In Figure 4.4 and Figure 4.5 we show photos from two types of applications at various stages during the tests. Figure 4.4(b) shows the liquid bursting out of source chamber A at 360 rpm. The liquid is forced towards destination chamber A due to the air compression created in destination chamber B (see Figure 4.4(b)). When the liquid from source chamber A completely enters destination chamber A, the forced convection

heating is turned ON to melt the wax plug and to release venting hole A (see Figure 4.4(c)). The centrifugal force pushes the molten wax towards venting hole B and seals it. The heating source is then turned OFF and the spinning speed is increased gradually. At 650 rpm, the liquid from source chamber B bursts and flows toward destination chamber B, and does not enter destination chamber A due to the air-compression in destination chamber A (see Figure 4.4(d)).

The result shows that switching with a VCV can be controlled accurately, cleanly, and at low spinning speed. This is advantageous when compared to switching processes applying external air pressure by M C R Kong and E D Salin (2011), and Coriolis force by Kim *et al.* (2008). Moreover, by applying more VCVs, liquid flow switching into more than two destination chambers can be accomplished.

Figure 4.5 presents the experimental sequence for the microfluidic metering process. As shown, the liquid is pumped from the source chamber to the metering chambers (see Figure 4.5(b)). Then, liquid starts to flow and fill the three metering chambers without entering the destination chamber because of the compressed air (see Figure 4.5(b and c)). After all metering chambers are filled; the extra liquid flows into the waste chamber (see Figure 4.5(d)). The heating source is turned ON to heat the platform surface to 60°C (which is the melting temperature for the wax plugs). Once the wax-plug has been melted away, the venting hole is opened and the liquid bursts from the metering chambers into the destination chambers (see Figure 4.5(e)).

The presented microfluidic metering process has many advantages in comparison to published metering method introduced by Mark (Mark *et al.*, 2009; Mark *et al.*, 2011). Mark *et al.* (2009) method requires high spinning frequency to generate the turbulence at the air-liquid contact point for the liquid to burst into the destination chambers. In contrast, our proposed metering process can be performed at low spinning speeds (less than 400 rpm). Furthermore, the destination chamber for our proposed

method can be connected to other microfluidic networks on the centrifugal microfluidic platform (where other processes can be performed) by implementing the VCV at appropriate points.
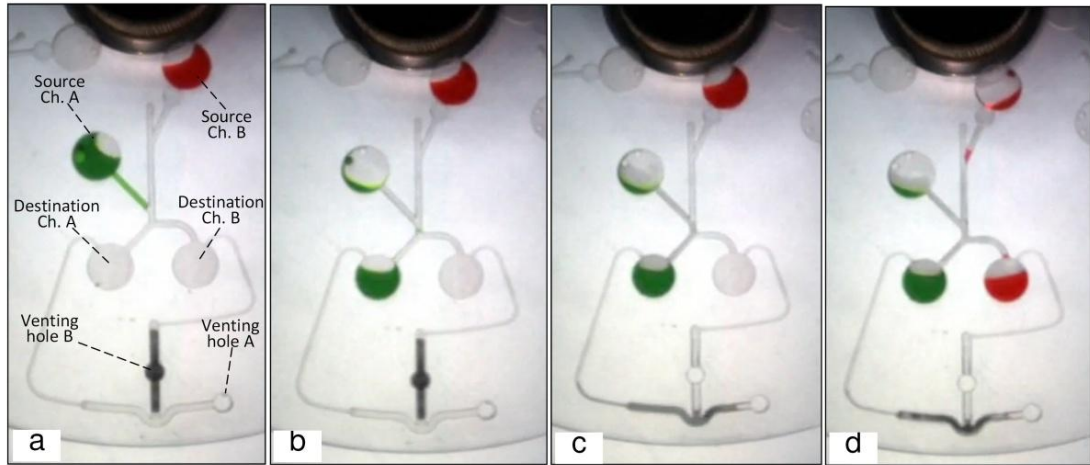
Figure 4.4: Experiment sequence for liquid switching using VCV valving method (a) green colored liquid flows out from source chamber A, (b) green liquid switched to chamber A due to the compressed air in chamber B, (c) venting hole B released by melting wax plug, and wax moves to block venting hole A, (d) red liquid switched to chamber B due to the air compression in chamber A
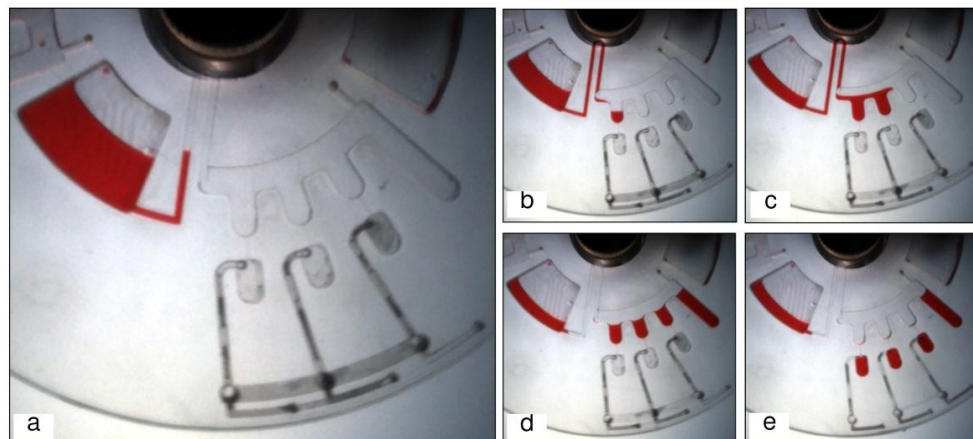
Figure 4.5: Experiment sequence for liquid metering using VCV valving method (a) liquid pumped from source chamber to the metering chambers, (b) liquid filling the first metering chamber, (c) liquid filled the second metering chamber and moving to the third, (d) liquid filled all metering chambers and overflowed to the waste chamber, (e) wax-plug melted and liquid moved to the destination chambers

4.3 Passive Liquid Valve (PLV) Results

In this section, the experimental results of the proposed PLV are presented. Moreover, the experimental results are compared with the theoretical calculations to

assess the analytical model we described earlier. For both the S-PLV and D-PLV designs, the control burst frequency (when there is no liquid in the venting chamber) was tested to be 275 RPM. The U-shaped bent channel increases the burst frequency by 10 RPM because the control burst frequency in the case of a straight microchannel was tested to be 265 RPM. This 10 RPM difference results from the short distance of the reverse flow in the second leg of the U-shaped bent. Each experiment in this section was repeated 10 times for validation of the results.

4.3.1   Effect of the Liquid Height on the Burst Frequency

To test the effect of the venting chamber liquid height on the burst frequency, a range of liquid heights from 1.34 to 3.35 mm of deionized colored water (corresponding to 20 to 50 µl) was loaded into a venting chamber. Figure 4.6(a) shows the experimental results demonstrating the effect of liquid height on the burst frequency for both the S-PLV and D-PLV valves. Moreover, the theoretical result using equation (3.4) is included in the figure for comparison purposes.

From equation (2.1), it is obvious that the height of the liquid in the venting chamber will affect the centrifugal pressure acting on the liquid in the venting chamber, and this effect in turn will affect the burst pressure (frequency). From the design of the venting chamber in this study, each additional 1 µl of liquid is equivalent to a 0.067 mm increase in the liquid height in the venting chamber. As an example, 50 µl of liquid in the venting chamber produces an effective liquid height of approximately 3.35 mm.

The theoretical result in Figure 4.6(a) shows that initially the burst frequency gradually increases as the venting chamber liquid height increases. Then, a sudden steep increase in the burst frequency for liquid heights greater than 2.68 mm is followed by a rapid drop in the burst frequency (after 3.015 mm). The experimental results show good agreement with the theoretical result for chamber liquid heights in the range between 1.34 mm to 2.68 mm. For both S-PLV and D-PLV, it is clear that the burst frequency is

almost doubled from 275 RPM (for the control without liquid in the venting chamber) to 405 RPM by an increase of only 1.34 mm in the liquid height in the venting chamber.

For a chamber liquid height of 3.015 mm (exceeding 2.68 mm), the liquid height in the venting chamber starts to be close or equal to the liquid height in the source chamber. Therefore, the theoretical result curve peaks at the highest burst frequency and then drops to zero (no bursting) when the liquid pressure of the venting chamber is always higher than the pressure of the source chamber (see Figure 4.6(a)). However, the experimental result does not follow the theoretical result because air, which is slightly elastic, can only withstand a limited amount of stretching/compression. If a high pressure is suddenly applied on the trapped air (such as when venting chamber liquid height is more than 3.015), it will be overstretched/overcompressed and the valve will not work or will not follow the theoretical calculations. This air effect and elasticity limitation is well described by Soroori *et al.* (2013). Therefore, in Figure 4.6, when the spinning speed exceeds the specific threshold, the source chamber will burst although the theoretical calculation says otherwise.

4.3.2   Effect of Liquid Density on the Burst Frequency

In this experiment, the effect of the density of the liquid in the venting chamber on the burst frequency is investigated. The experimental and theoretical results for five different liquids with five different densities are presented in Figure 4.6(b). The following five liquids were used: distilled water (1.000 g/cm^3), soy milk (1.103 g/cm^3), glycerol (1.290 g/cm^3), purified juice (1.335 g/cm^3), and honey (1.415 g/cm^3). The liquid densities were measured using an Anton Paar DMA 4100 Density Meter (U-Tube). In each experiment, 30 µl of each liquid was injected into the venting chamber while the source chamber was loaded with 40 µl of distilled water.

Figure 4.6(b) shows that an increase in the liquid density in the venting chamber from 1.000 g/cm^3 to 1.450 g/cm^3 increases the burst frequency from approximately 500

RPM to 1200 RPM. In this range, the experimental result shows good agreement with the theoretical calculation. In a manner similar to the effect of the chamber liquid height, when the venting chamber density exceeded 1.450 g/cm^3, the theoretical result shows a sharp increase where the burst frequency exceeds 2100 RPM. Then, the burst frequency dropped to zero, which corresponds to the valve holding the liquid in the source chamber indefinitely.

4.3.3 Effect of the Venting Chamber Position on the Burst Frequency

In this part of the study, the effect of changing the position of the venting chamber relative to the centrifugal platform center is investigated. The position of the venting chamber was varied from 40 mm to 60 mm from the platform center in steps of 5 mm. In each experiment, the venting chamber was loaded with 30 µl of distilled water while the source chamber was loaded with 40 µl.

Figure 4.6(c) shows the experimental and theoretical results of this study. Increasing the relative distance between the venting chamber and the platform center steadily increases the burst frequency of the source chamber liquid. When the distance from the platform center is increased from 40 mm to 60 mm, the burst frequency increases by approximately 100 RPM (from 520 to 620 RPM). Although the S-PLV valve yielded experimental results that were closer to the theoretical calculations, the D-PLV valve was more effective in increasing burst frequency.
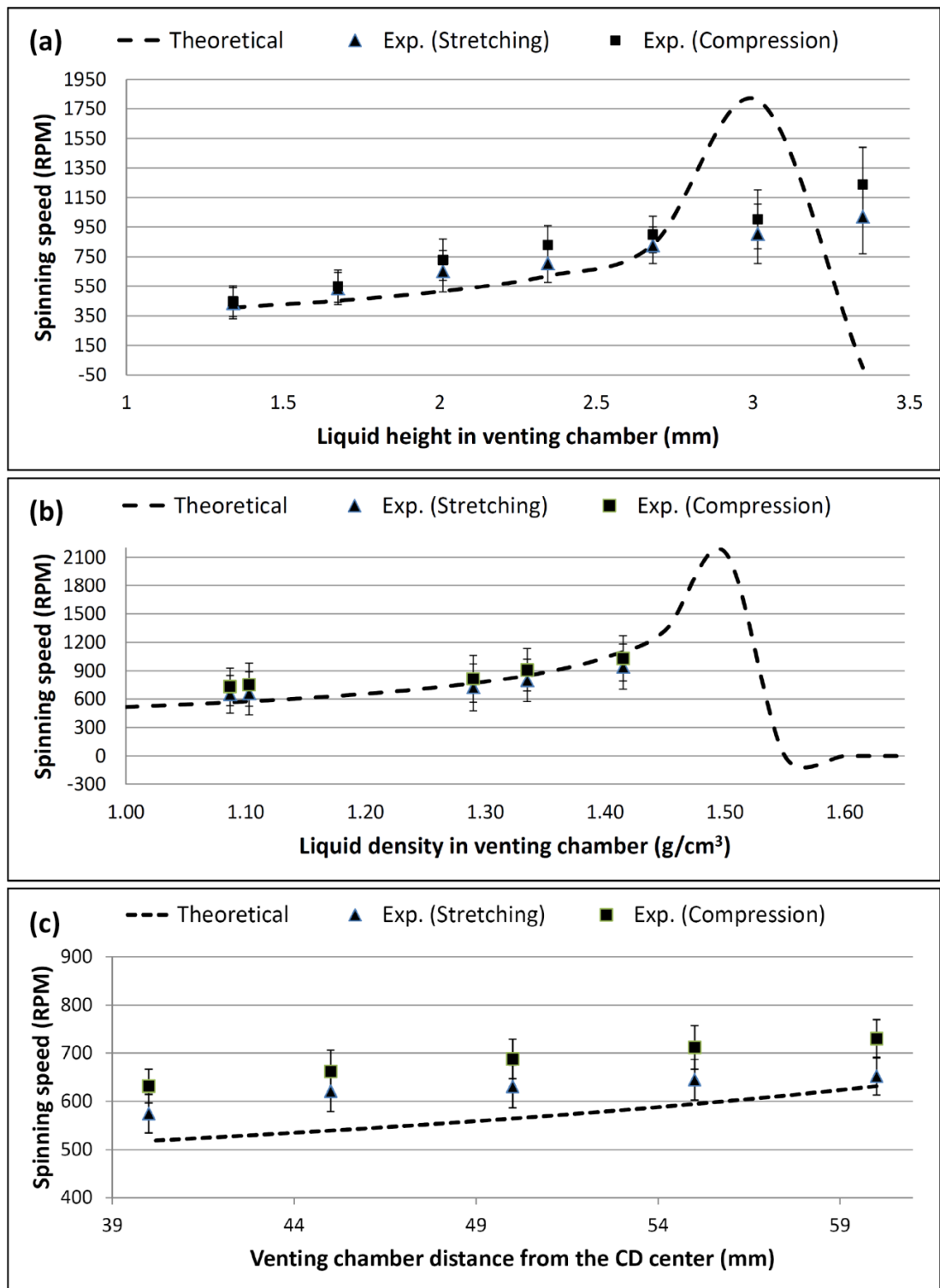
Figure 4.6: Theoretical and experimental results of the PLV (a) the effect of different venting chamber liquid heights on burst frequency, (b) the effect of different venting chamber liquid densities on burst frequency, and (c) effect of different venting chamber positions on burst frequency (theoretical result calculated using equation (3.4))

4.3.4 Liquid Switching and Liquid Metering Results

Photos of the microfluidic liquid switching and liquid metering processes at various stages of the experiment are presented in Figure 4.7 and Figure 4.8, respectively. Figure 4.7(a) shows the centrifugal microfluidic platform at the preliminary stage with a spinning speed lower than 250 RPM where all liquids are in their original positions. When the platform spinning speed is increased to 260 RPM, the green liquid in source chamber A bursts (see Figure 4.7(b)). The liquid flow is forced towards destination chamber A by the effect of the PLV valve on venting chamber B. Then, the spinning speed is increased to 300 RPM, and the liquid in venting chamber B to burst towards venting chamber A (see Figure 4.7(c)). This step will release the venting channel of destination chamber B while sealing the venting channel of destination chamber A. Therefore, when the liquid in source chamber B bursts at 370 RPM, the flow is forced towards destination chamber B (see Figure 4.7(d)).

Two observations were made during our experiments: (1) Some residual liquid can stay in venting channel B after the liquid burst from venting chamber B (see Figure 4.7(c)). This liquid will not affect the switching process because the liquid volume is very low (low pressure), and this liquid will be pushed back as soon as the liquid in the source chamber B bursts towards destination chamber B. (2) Often, a drop of the liquid in source chamber B will flow towards destination chamber A due to the high speed bursting, which overcompresses the trapped air in destination chamber A.

Compared with the switching process that were proposed previously by Kazemzadeh *et al.* (2014), the present liquid switching process shows two main advantages: first, the process can be performed at a lower spinning speed (less than 400 RPM), and this speed is adjustable depending on the utilized venting chamber specifications. Moreover, compared to the earlier performed switching process using the wax valve, the PLV valve can be easily and passively perform liquid switching without

any need for an external force or trigger. Finally, the valve state of the proposed PLV can be reversed from normally opened to normally closed and vice versa. This capability is a very important feature for some applications where the valve must be switched ON and OFF at different stages of the process.

Figure 4.8(a) shows the metering process at a low spinning speed. When the spinning speed is increased to 370 RPM, the source chamber liquid bursts and fills the metering chambers (90 µl each), whereas the extra liquid overflows to the waste chamber (see Figure 4.8(b) and (c)). Finally, the spinning speed increased steadily to 500 RPM, when the liquid in the metering chambers starts to burst to the destination chambers. However, the spinning speed must be steadily increased to 2000 RPM for all the liquid to be transferred to the destination chambers. The reason for the speed increase is as follows: as liquid flows away from the metering chamber, the decreasing liquid height results in a reduction in liquid pressure. Therefore, the spinning speed is increased to increase the pressure on the metering chamber liquid to maintain the bursting of liquid.

This experiment shows that the proposed PLV valve is capable of controlling liquid that flows at a high speed. In addition, multistep process can be performed on the centrifugal microfluidic platform utilizing the developed valve. Compared with the pneumatic metering process proposed by Mark *et al.* (2009), the process that is controlled using PLV liquid is more controllable/adjustable because the spinning speed can be increased or decreased depending on user requirements. Finally, compared to the metering process performed earlier using the wax valve, this valve is easier to implement and will extend the flexibility of centrifugal microfluidic platforms by allowing for passive control of fluid flow without the need for active valving.
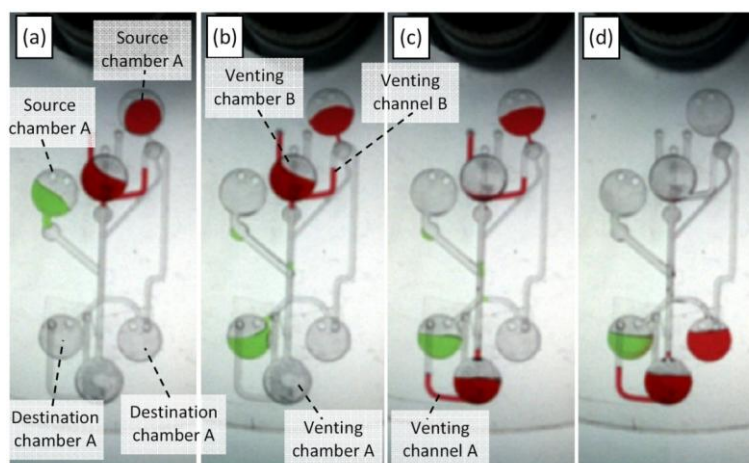
Figure 4.7: Photos of the microfluidic switching process at various stages (a) spinning speed less than 250 RPM where all liquids at its original positions, (b) source chamber A liquid bursts towards destination chamber A at 260 RPM, (c) venting chamber B liquid bursts towards venting chamber A at 300 RPM, and (d) source chamber B liquid bursts towards destination chamber B at 370 RPM
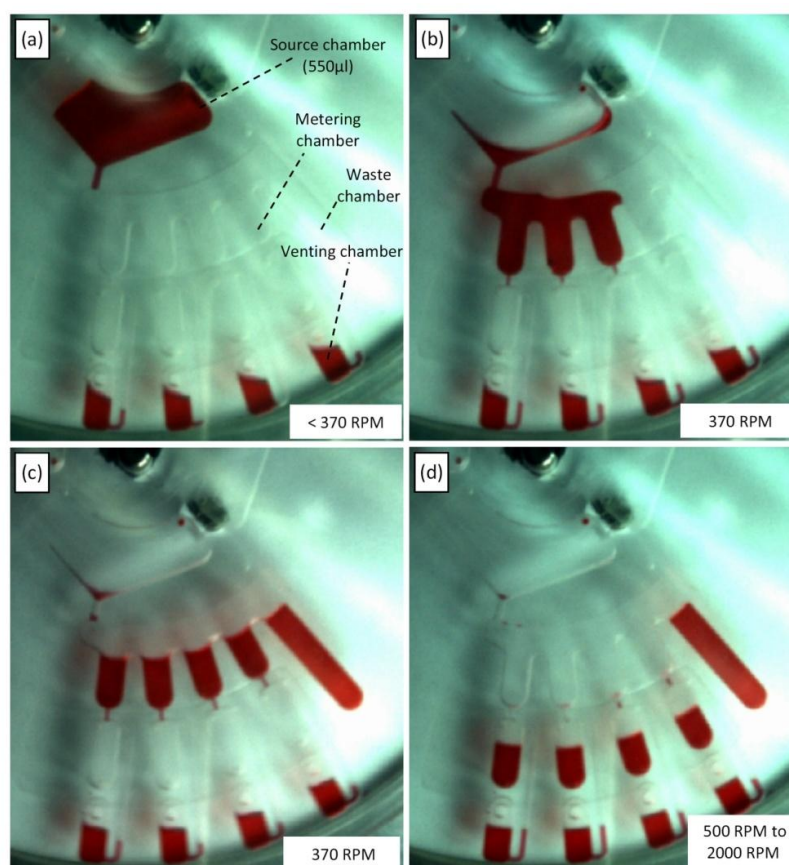
Figure 4.8: Photos of liquid metering at various stages of the process (a) spinning speed less that 370 RPM, (b) & (c) the metering chambers are filled whereas the extra liquid overflowed to the waste chamber at 370 RPM, and (d) liquid transferred from the metering chamber towards the destination chambers (500 RPM to 2000 RPM)

4.4 Check Valve Results

This section is split into two subsections, an analysis section that theoretically evaluates the check valve, and an experimental results section that discusses the implementation of the liquid swapping process.

4.4.1 Analytical Model and Results

In this section, the operation of the developed TCV and BCV chips are evaluated both theoretically and experimentally. The theoretical study is conducted to confirm that very little pressure is needed to actuate the chips (to allow air/liquid flow) and that this required pressure is negligible, and does not affect the burst frequencies of liquids on the centrifugal microfluidic platform. Subsequently, experimental work is conducted to investigate the actuation points of the two check valves, and the flow rate of air/liquid under different pressure.

To evaluate the operation of valves on the centrifugal microfluidic platform, the centrifugal pressure resulting from the spinning of the platform must first be evaluated. The centrifugal pressure acting on a volume of liquid, $P_{centrifugal}$ can be calculated using equation (2.1). The pressure on a spinning centrifugal platform varies in the range of kilo- to mega-pascals depending on the spinning speed, liquid density and the relative position of the liquid from the platform center. To experimentally determine both the activation pressure, and achievable flow rate, channels of dimensions 150 mm length by 1 mm width and 1mm depth are fabricated in a vertically standing PMMA plastic (please refer to APPENDIX B). The TCV or BCV valve is installed at the bottom end of the channel, and the channel is then loaded with liquid of different heights (to achieve a range of pressure) to test the operation of the valve. By positioning the channels vertically, the resulting pressure can be calculated as follows:

$$P_{centrifugd} = \rho g h \qquad\qquad (4.1)$$

where ρ is the liquid density, g is the acceleration of gravity, and h is liquid height. In our experiment, the height of the liquid in the channel was varied from 24 mm to 58 mm (with an incremental step of 2 mm) to give a range of pressure from 220 Pa to 580 Pa (for more information about the developed flow rate test platform, please refer to APPENDIX B). Figure 4.9 shows the experimental flow results for the TCV and BCV valve under different pressures. It is observed that both valves are actuated under the same pressure which is 220 Pa. However, it can be seen that the flow rate of TCV valve is much higher compared to the BCV valve especially under high pressure. This is because the longer pathway between within the BCV (from the inlet to the outlet of the valve) which is constantly constricted by the deflected latex film (i.e., this decreases the flow rate). It is also observed that at the actuation pressure, liquid flow rate is intermittent as the latex deflection fluctuates.

On a typical centrifugal microfluidic platform with a liquid column of 5 mm height, the check valve actuation pressure of 220 Pa can be achieved with a spin speed as low as 270 rpm to 480 rpm for relative liquid distance of 17 mm to 67 mm from the platform center (refer to equation (2.1)). Centrifugal microfluidic platforms are typically designed to operate at frequencies of 300 rpm and above, (up to thousands of rpm). This range of operation allows for the easy integration and actuation of the check valves in microfluidic processes on the platform. In other words, the developed valves can be implemented for controlling fluid flow direction during both passive pumping of liquid (which depends only on the centrifugal pressure), and active pumping of liquid (for example using TPP).

Once the actuation pressure is experimentally determined above (as 220 Pa), the deflection of the latex film in the TCV chip can be calculated using the following equation (Brask *et al.*, 2006):

$$u = \frac{3pa^4}{16t^3E}\left(1-v^2\right)$$ (4.2)

where u is the deflection of the latex layer, p is the pressure applied across the latex layer, a is the radius of the TCV chip, v is Poisson's ratio (0.5 for latex), E is Young's modulus (0.1 Gpa for latex), and t is the thickness of the latex layer (220 μm). The same equation can be applied to approximate the deflection for the BCV chip as the maximum deflection is limited by the smallest dimension of the chip (where the smallest dimension of the BCV chip is identical to the TCV chip). However, there is some variation in the amount of deflection between the TCV and BCV chips due to the difference in path length and the air / fluid flow direction within the two chips.

Using equation (4.2), the effect of the pressure on the deflection of the latex layer is shown in Figure 4.10, while the effect of the chip size on the deflection of the latex is shown in Figure 4.11.
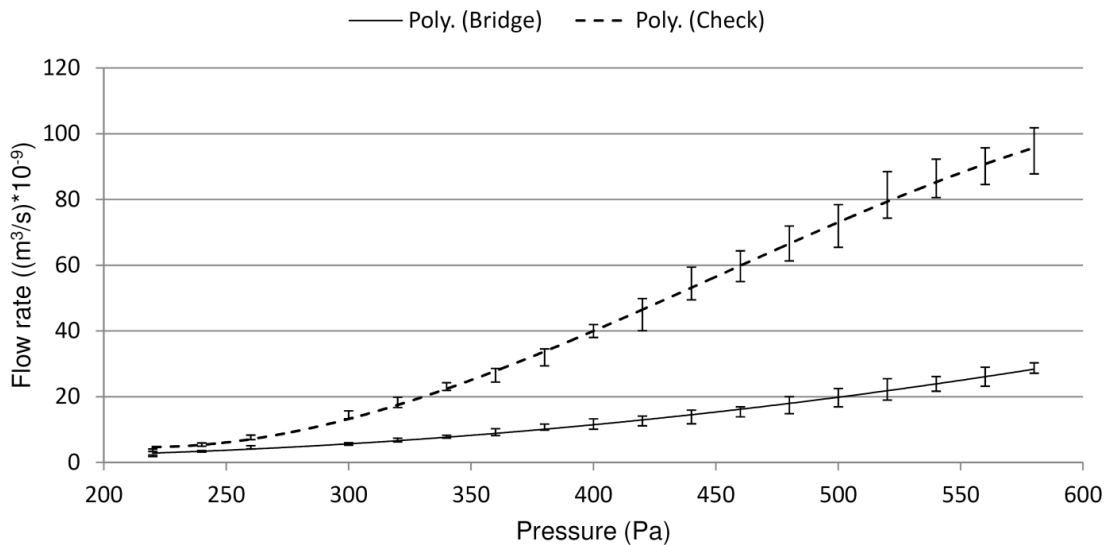

Figure 4.9: TCV and BCV flow rate at different pressure

The result in Figure 4.10 shows that the deflection of the latex film increases linearly with the increase of the pressure applied on the chip. Also, the results indicate that latex film deflection is approximately 100 µm at the valve activation pressure (for air and liquid to flow at a minimum pressure of 220 Pa). On the other hand, the result in Figure 4.11 shows that at the actuation pressure of 220 Pa, the maximum latex film deflection theoretically increases exponentially with increasing chip diameter. It can be seen that increasing the chip diameter by 2 mm approximately increases the deflection threefold. This indicates that a larger chip is easier to operate under low pressure. However, the exponential increase in latex deflection is true as long it does not exceed the elasticity limit of the latex film. To protect the latex film from overstretching, the spacer area is limited to a height of 1.5 mm in our chips.
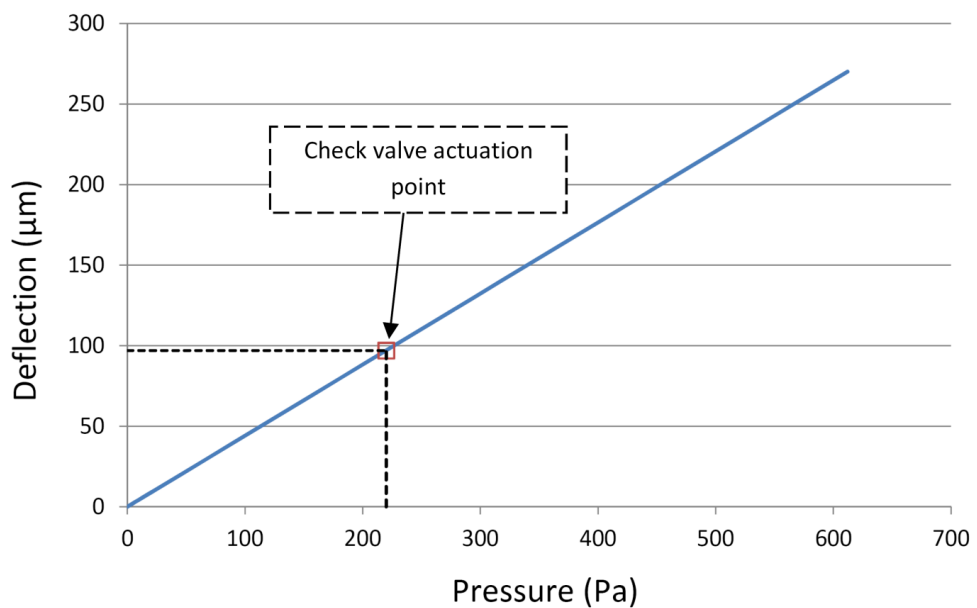

Figure 4.10: Latex deflection for different pressure during valve activation
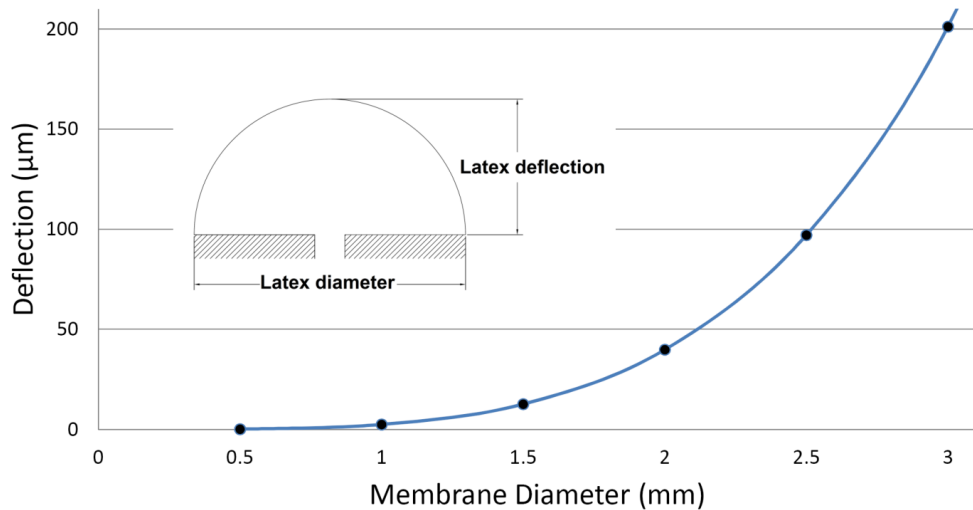
Figure 4.11: Latex deflection for different valve diameter

4.4.2 Liquid Swapping Results

The steps of the experimental demonstration mentioned in the methodology section are shown in Figure 4.12 while actual images recorded are shown in Figure 4.13. The process starts with the loading of both chambers A and B each with 45 µl of differently colored DI water (see Figure 4.13(a)). After loading the chambers, the venting holes on both chambers are sealed with a special thermal transparent tape. The holes are sealed to trap the air inside the microfluidic system to allow the TPP to work (Thio *et al.*, 2013). At the same time, the TCV and BCV chips are installed in designated positions on the bottom surface of the centrifugal microfluidic platform using PSA material. Then, the microfluidic platform is mounted on the spin test system to start the spinning process. The experimental step for the microfluidic process can be broken into three steps (see Figure 4.12): step 1: first heating process (push the liquid from chamber A to waste chamber), step 2: cooling process (sucks the liquid from chamber B into chamber A), step 3: second heating process (to push the liquid from chamber A into the waste chamber). The three steps are discussed in details afterwards.

Step 1 First Heating Process:

This step starts with the spin up of the centrifugal microfluidic platform to 300 rpm (pretested spinning speed for optimum push/pull pumping performance (Thio *et al.*, 2013)) and the focusing of the heat source on the TPP air chamber. Next, the heat source is set to 150˚C and turned ON (see Figure 4.12). The heating process gradually raises the temperature in the TPP air chamber from room temperature (25˚C) to reach a temperature sufficient for the air to start expanding significantly. This air expansion exerts pressure on the liquid in chamber A and B. However, the blue liquid from chamber B cannot be pushed from the adjoining channel because of the TCV chip preventing any air from escaping from chamber B. Therefore, the pressure generated by the TPP air expansion will only force the red liquid in chamber A to move towards the waste chamber through the BCV chip. It is observed that the red liquid from chamber A is completely transferred to the waste chamber in 85 seconds when the temperature reaches 64˚C (Figure 4.13(b) and (c)). After the red liquid is fully transferred, the heating process is stopped and the cooling process then starts.
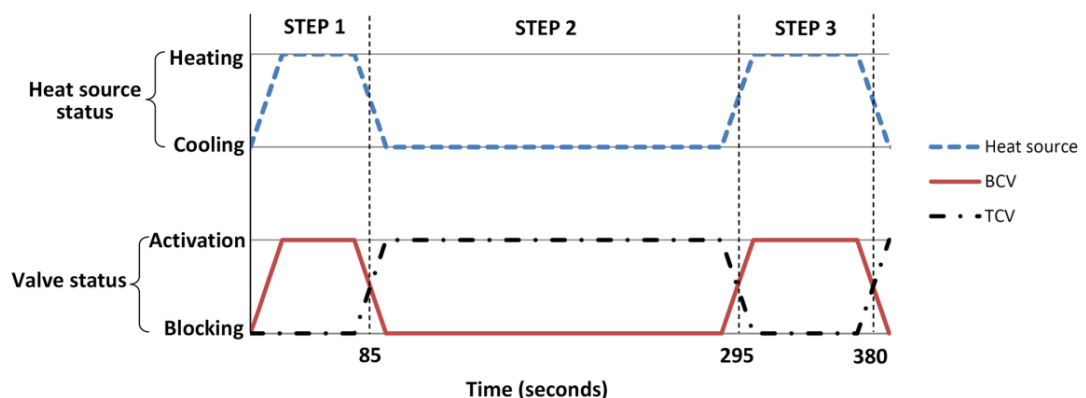
Figure 4.12: Check valve experimental steps
(Step1) heating source is turned ON, BCV valve is activated, and TCV valve is in blocking mode: liquid is pumped from chamber A to the waste chamber, (Step2) heating source is turned OFF, BCV valve is in blocking mode, and TCV valve is activated: liquid pulled from chamber B into chamber A, (Step3) heating source is turned ON, BCV valve is activated, TCV valve is in blocking mode: liquid pumped from chamber A to the waste chamber. The experiment performed at 300 RPM

Step 2 Cooling Process:

After step 1 is completed, the cooling process starts. During this process, the centrifugal microfluidic platform is kept spinning at 300 rpm to cool the platform. The cooling process causes the trapped air volume in the TPP air chamber to contract. As the platform temperature drops towards room temperature, the air volume shrinking process creates a vacuum-like state in chambers connected to the TPP chamber. As the BCV chip does not operate under negative pressure conditions, this vacuum-like state closes the BCV chip and prevents any transfer of air from the waste chamber (see Figure 4.12). At the same time, the vacuum-like state in the TPP chamber sucks the blue liquid from chamber B into chamber A (see Figure 4.13(d)). From the experimental test, it is observed that the suction process takes 210 seconds to fully transfer the liquid from chamber B to chamber A. This is longer compared to the transfer of liquid from chamber A to the waster chamber in Step 1. The reason for this is that in this design the suction of liquid from chamber B to chamber A is working against the centrifugal force, while the pushing of liquid from chamber A to the waste chamber is amplifying the centrifugal force. Another factor is that the cooling process is passive, relying only on the spinning process to air cool the centrifugal microfluidic platform.

Step 3 Second Heating Process:

This step is similar to Step 1, but now the blue liquid that was transferred from chamber B to chamber A in Step 2 is pushed into the waste chamber. As in step 1, the heat source is set at 150˚C to heat the TPP chamber, and the heating process causes the trapped air in the TPP chamber to expand. The expanding air then pushes the blue liquid in chamber A into the waste chamber through the BCV chip (see Figure 4.13(e) and (f)). The check valve experiments demonstrate the effective application and the usefulness of these simple structures on microfluidic platforms. The process demonstrates the ability

of check valve chips to control the flow direction of fluid in biological processes under

pneumatic and centrifugal pumping.
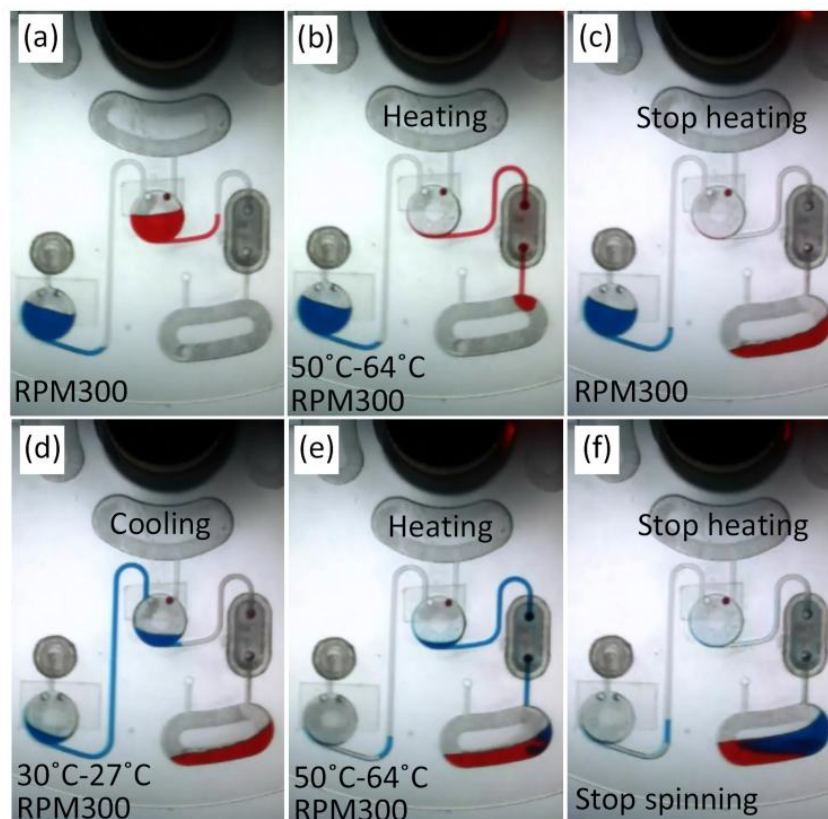
Figure 4.13: Liquid swapping experimental results
(a) liquid status before the start of the heating process, (b) heating the TPP chamber pushes the red DI liquid towards the waste chamber, (c) the heating process is stopped, (d) cooling the TPP chamber pulls the blue DI liquid from chamber B into chamber A, (e) heating the TPP chamber pushes the blue liquid from chamber A into the waste chamber, (f) final liquid status after completion of the experiment

4.5   Biomedical Applications Results

4.5.1   Bradford Assay Results

As mention before in subsection "*3.6 Bradford Assay*", the experiments starts

with serially diluted the BSA sample five times to obtain samples with protein

concentrations of 1 mg/ml, 0.5 mg/ml, 0.25 mg/ml, 0.125 mg/ml, and 0.0625 mg/ml.

Then, 550 µl of the Bradford reagent is injected into the source chamber and inject 10

µl of each prepared concentration into the destination chambers (see Figure 4.14). Afterwards, the inlet and venting holes of the preloaded destination chambers are tightly sealed using a PSA product. To implement the PLV, 50 µl of red DI water is injected into each venting chamber. Next, the preloaded centrifugal microfluidic platform is mounted on the spin test system, and the rotation process is started. Via the same steps as those described for the previous metering experiment, the source chamber liquid (with Bradford reagent) is burst at 370 rpm to fill each of the metering chambers with 90 µl of Bradford reagent (see Figure 4.14(b)). Then, at increasing speeds of 500 to 2000 rpm, the metered Bradford reagent bursts to the destination chambers to be mixed with the preloaded BSA samples. To ensure good mixing between the reagent and the BSA, a multistep process comprising a batch mode (stop flow) mixing method and manual pipette mixing is performed (Grumann *et al.*, 2005). Figure 4.14(c) shows that the resulting mixture has different intensities in the blue color region depending on the protein concentration in the sample. Finally, after the mixtures are incubated for 5 minutes at room temperature, the mixtures are pipetted into a 96 micro-well plate and read at 450 nm. To evaluate the present method, the centrifugal microfluidic platform result is compared with the result of a Bradford assay that was performed traditionally using microwell plate and the same samples.

Figure 4.14(d) presents the micro-plate reader results for the Bradford assay on the microplate and the centrifugal microfluidic platform. The results show that the intensity at the wavelength corresponding to the blue color increases when the protein concentration increases. The results also prove that the assay can be performed on the microfluidic platform with an accuracy very close to that of the traditional method. Therefore, multiple samples can be processed together in parallel by designing a multi-metering centrifugal platform (up to 30 samples per platform). Moreover, using the resulting curve as a standard reference for the assay on the platform and a simple first

order equation, the centrifugal platform can be used to test the protein concentration of any unknown sample via the same procedure. Therefore, the centrifugal microfluidic platform can be utilized as a platform for detecting different diseases; for example, a liver functionality test can be performed by measuring the albumin concentration in the urine. This capability can be important for handling samples from patients with infectious diseases, such as HIV. Finally, the experiment shows that the proposed valve provides control of the burst frequency when a liquid other than water (different in terms of biochemical properties) is injected into the source chamber.
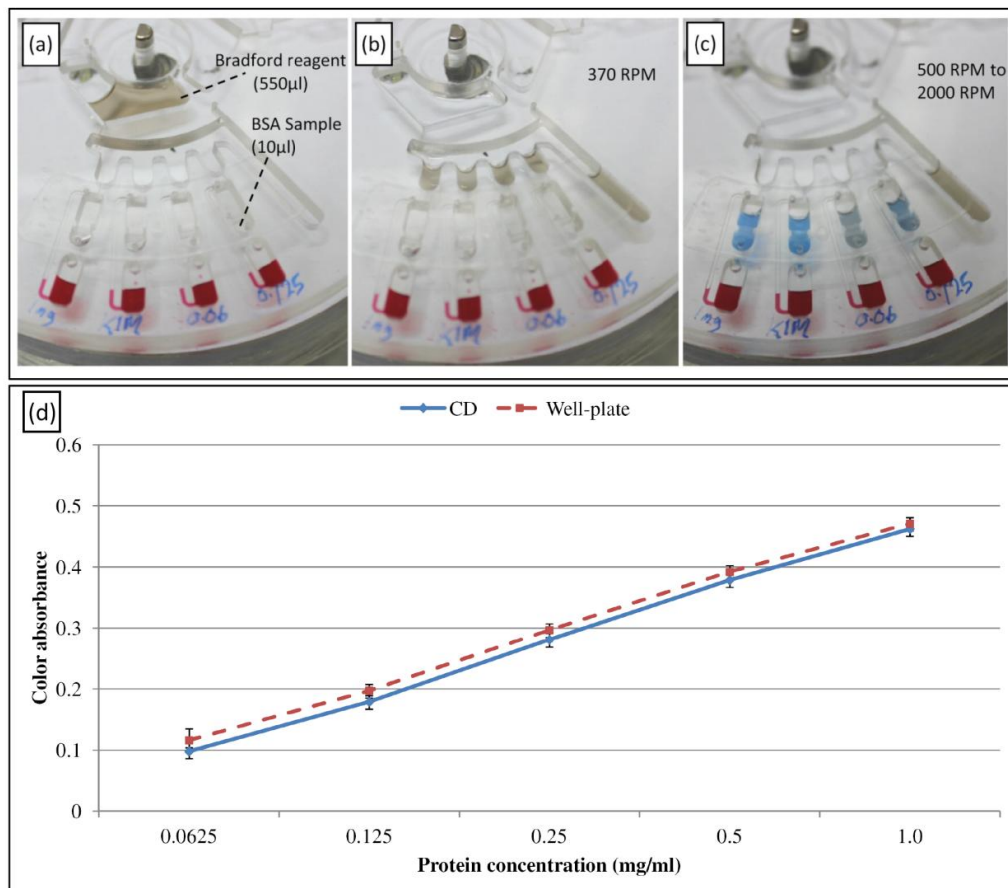
Figure 4.14: Experimental result of a Bradford assay
(a) spinning speed less than 370 RPM, with the Bradford reagent in the source chamber and the samples in the destination chambers, (b) The Bradford reagent bursts and fill the metering chambers at 370 RPM, (c) the Bradford reagent bursts from the metering chamber to the destination chambers to mix with the BSA samples (500 RPM to 2000 RPM), and (d) results for different BSA samples with different concentrations using the centrifugal microfluidic platform and the micro-well plate as assay platform

4.5.2 ELISA Assay Results

Figure 4.15 presents various pictures of the experimental test at different stages of the process. The preparation process starts with injecting 100 μl of the positive or negative control sample in the detection chamber. Afterwards, 100 μl of the following fluids are respectively injected in the spiral channel in sequence: washing buffer, Dengue conjugated antigen, washing buffer, TMB and stopping solution. Then, the venting holes of the detection chamber and spiral channel are sealed.

Table 4.1: Step-by-step the ELISA on the centrifugal platform

	ELISA Steps on centrifugal microfluidic platform	Starting time (seconds)	Starting temperature (˚C)	Ending time (seconds)	Ending temperature (˚C)
Step 1	Flush out the serum	0	24	38	47
Step 2	Pull in the washing buffer	39	47	200	24
Step 3	Flush out the washing buffer	201	24	241	46
Step 4	Pull in the Dengue antigen	242	46	447	24
Step 5	Flush out the Dengue antigen	448	24	485	45
Step 6	Pull in the washing buffer	486	45	696	24
Step 7	Flush out the washing buffer	697	24	733	48
Step 8	Pull in the TMB buffer	734	48	954	25
Step 9	Balance the temperature	955	25	1555	29-31
Step 10	Pull in the stopping solution	1556	31	1916	24
	Total time		≈ 32min		
	Total time for ELISA with 2 hours of incubation	2 hour 32min			

As shown in Table 4.1, the experiment can be divided into 10 main steps: *step 1*: incubating the preloaded centrifugal microfluidic platform for 60 minutes at 37˚C to allow the Dengue IgM antibodies from the positive sample in the detection chamber to bind with the antigen coating (see Figure 4.15(a)). *Step 2*: heating the TPP chamber to flush out the unbinded positive sample from the detection chamber (see Figure 4.15(b)). *Step 3*: cooling the TPP chamber to pull the washing buffer into the detection chamber (see Figure 4.15(c)). *Step 4*: heating the TPP chamber to flush out the washing buffer from the detection chamber to the waste chamber (see Figure 4.15(d)). *Step 5*: cooling the TPP chamber to pull in the Dengue conjugated antigen into the detection chamber (see Figure 4.15(e)). In this step, the centrifugal platform is incubated for 60 minutes at 37˚C for the antigen to conjugate with the Dengue IgM antibody bound to the antigen coating (sandwich ELISA). *Step 6*: heating the TPP chamber to flush out the detection chamber (see Figure 4.15(f)). *Step 7*: cooling the TPP chamber to pull the washing buffer into the detection chamber (see Figure 4.15(g)). *Step 8*: heating the TPP chamber to flush out the washing buffer from the detection chamber (see Figure 4.15(h)). *Step 9*: cooling the TPP chamber to pull in the TMB into the detection chamber. Then, the platform is incubated for 10 minutes at room temperature for the TMB to react and release blue color. *Step 10*: cooling the detection chamber to pull the stopping solution in the detection chamber to be mixed with the TMB solution and release the yellow color. The final resulted liquid should then transferred to a 96 mico-well plate to be read by a BIO RAD microplate reader. For better understanding of the process different stages, please refer to the illustration video in Al-Faqheri *et al.* (2015).

The result shows the ability to perform the ELISA assay with reliable result and fully automated fashion. Moreover, two of the main advantages behind this design are: (1) the simplicity in design and implementation where all the reagents are injected in

one continuous micro-channel, and (2) the ability to utilize this method to inject and store the platform as all venting holes are covered with check valves to reduce liquid contamination and evaporation over time. The full design and process details will be presented in a future paper.
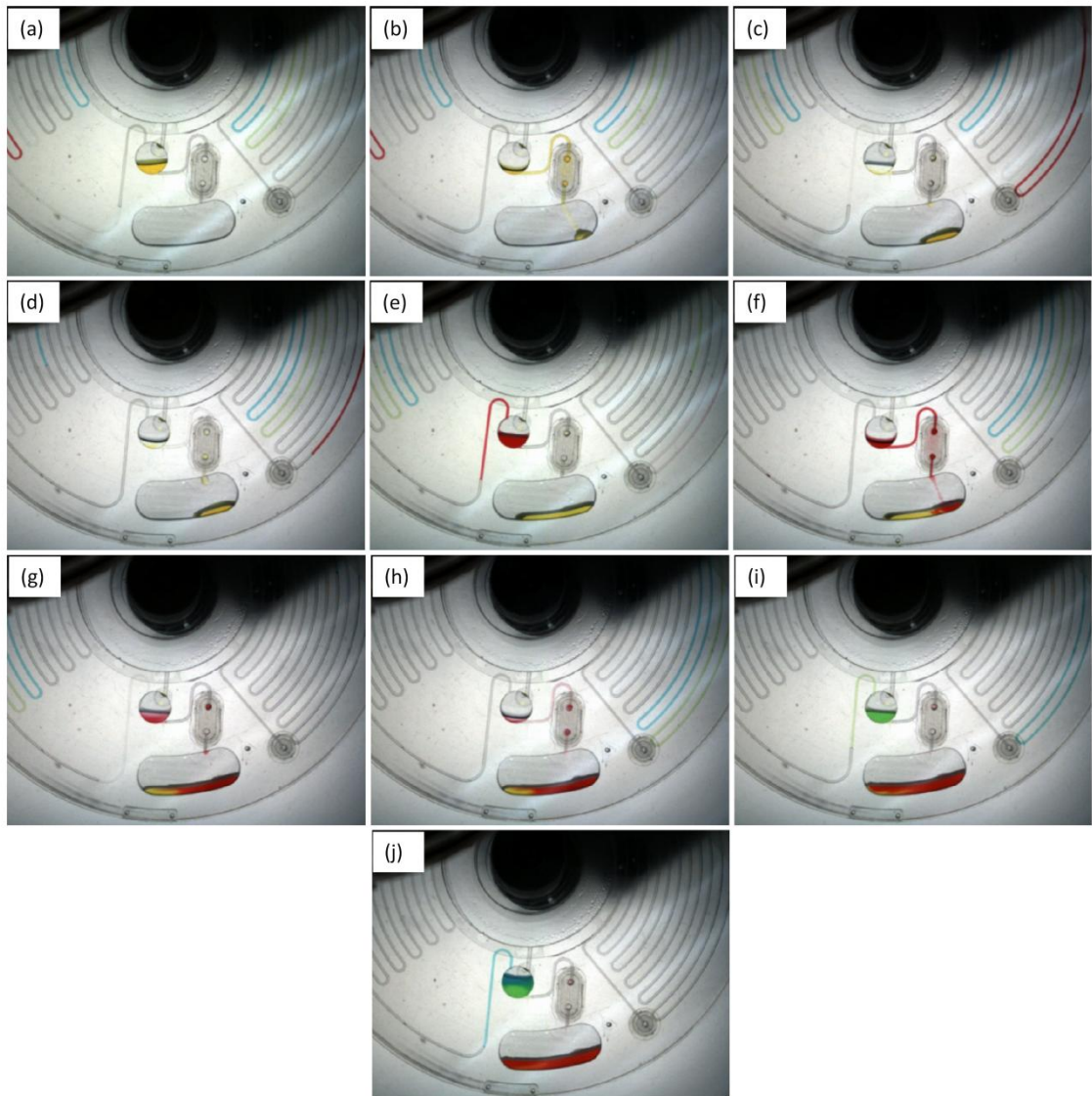

Figure 4.15: ELISA assay experimental results
(a) incubate the serum in the detection chamber for 60 minutes in 37˚C (b) flush out the detection chamber (c) inject the washing buffer in the detection chamber (d) flush out the detection chamber (e) inject the conjugated Dengue antigen in the detection chamber and incubate for 60 minutes in 37˚C (f) flush out the detection chamber (g) inject the washing buffer in the detection chamber (h) flush out the detection chamber (i) inject the TMB in the detection chamber and incubate for 10 minutes in room temperature (j) inject the stopping solution in the detection chamber

4.6 Summary

In this chapter, the experimental results of the developed microvalves are presented and evaluated. In general, the results show the ability of the developed valves to accurately control the burst frequency of the liquid on the centrifugal microfluidic platform. Moreover, the results illustrate that presented valves can be implemented in biomedical applications where the compatibility of valves are required.

The results of the wax vacuum/compression valve show the ability to accurately control the burst frequency of the source chamber. Moreover, the presented valving method prevents any direct contact (contamination) between the sample and the valving material (wax). On the other hand, the proposed PLV valve can be controlled by different parameters (i.e., liquid height in the venting chamber, liquid density, and the position of the venting chamber in respect with platform center). Finally, the result of the Bradford assay shows the ability of integrating the PLV valve to perform biomedical applications on the centrifugal microfluidic platform. For the proposed check valve, the experimental results shows the ability of this valving method to control flow direction of the fluid (air/liquid) on the centrifugal microfluidic platform. The results indicate that the valve chip requires very low pressure to be actuated. The developed valving methods can widen the range of the biomedical process that can be performed on the centrifugal microfluidic platform such as ELISA assay.

Table 4.2 shows a summary of the developed valves characteristics in different aspects (i.e., valve category, valving mechanism, physical barrier, compatibility, isolation, actuation time, reusability, and fabrication complexity). As can be seen, all the developed valves have good compatibility with biomedical application, good vapour isolation, reusability, and easy fabrication.

Table 4.2: Characteristic summery of the developed valves

Valve	Category	Mechanism	Physical barrier	Compatible with biomedical applications/ contamination	Isolation / vapor	Actuation time	Multi-actuation	Fabrication complexity / system setup
Wax valve	Active	Implementing wax plug to control the burst frequency of the source and destination chambers	YES	YES	Good	Slow	YES*	Easy
PLV	Passive	Implementing venting chamber to control the burst frequency of the source and destination chambers	YES	YES	Depend on the valving liquid**	Fast	YES	Easy
Check valve	Passive	Implementing latex material to control the flow direction of air and liquid	YES	YES	Good	Fast	YES	Easy

* Can be used multitimes in the same process as shown in the switching process using the wax valve.

** The PLV valve can be good vapor isolator when high dense non-evaporating materials are applied in the venting chamber such as silicone oil.

CHAPTER 5: CONCLUSION AND RECONMMENDATION

5.1   Conclusion

In this work, three liquid sequencing micro-valves are developed for the centrifugal microfluidic platform. The three valves are: vacuum/compression wax valve (VCV), passive liquid valve (PLV), and passive check valve. Different microfluidic processes were conducted using the proposed valves such as liquid flow switching, liquid metering, and liquid swapping. Moreover, to show the capability of the proposed valves, Bradford assay and ELISA assay were demonstrated on the centrifugal microfluidic platform.

The VCV is developed on the centrifugal microfluidic platform by implementing paraffin wax to seal venting chambers/holes. The results indicate high flexibility and accuracy in controlling the liquid burst frequency. It is noticed that a vacuum valve on the source chamber is more resilient against bursting at high spinning frequencies compared to compression valves. Furthermore, the presented VCV method can reduce the direct heating of samples and reagents in the microfluidic process. Two microfluidic processes (i.e., liquid flow switching and liquid metering) have been implemented with by utilizing the VCV. The experimental results show that by using the VCV valving, the required spinning frequency to perform the process is reduced greatly, and the VCV valving allows for multiple path switching. Furthermore, the demonstration showed a novel way of implementing two valves using a single VCV wax plug. This is done by positioning the valves such that melted wax from a normally-closed valve (which releases it when the wax is melted) is later transferred to a normally-opened valve (which seals it when the wax solidifies) by centrifugal force (reversibility).

In the second part of the study, an easy-to-implement passive liquid valve (PLV) for the centrifugal microfluidic platform is presented. The main advantage of the proposed valve is that the valve can be actuated without an external force or trigger.

Compared with the VCV, the PLV can easily be introduced into any microfluidic process by simply injecting liquid into the venting chamber. Moreover, the lack of contact between the sample and valving material allows for the use of a variety of valving liquids without affecting the microfluidic process. Different parameters, such as the liquid height, liquid density, and venting chamber distance from the platform center, can be adjusted to control the effectiveness of the PLV valve. In addition, the ability to reverse the valve status from normally opened to normally closed and vice versa is a very important feature for the use of the PLV valve in multistep processes. The experimental and theoretical results show that the developed valve can be utilized to control the liquid burst frequency within a specific range of spinning speeds and liquid volumes. This range is defined by the ability of the utilized trapped air to withstand a specific amount of compression or expansion. Within this range, the burst frequency can be easily controlled by adjusting the height and/or density of the liquid in the venting chamber and by adjusting the position of the venting chamber with respect to the rotational center. The results show that using the proposed valve, the burst frequency of the source chamber liquid can be increased from 275 rpm to 1000 rpm. As a proof of concept, the presented new valve is successfully utilized to demonstrate two microfluidic processes: liquid switching and liquid metering.

In the last part of the study, two easy to fabricate check valve chips (i.e., TCV and BCV) for the centrifugal microfluidic platform are developed. The two check valves can control air/liquid flow within the platform, and also between the platform and the surrounding environment. To determine the effect of the check valve chips on liquid burst frequency on the centrifugal microfluidic platform, fundamental experimental work has been carried out. The findings indicate that the valve chips can be consistently activated at a low pressure of 220 Pa, which is achievable on a typical microfluidic process on the centrifugal platform. In this study, we also conclude that

under constant pressure, increasing the chip diameter increases the amount of deflection in the latex layer. This allows adjustment of the required pressure to operate the check valves by changing the chip size. As a demonstration of the effectiveness of the developed valve chips, the TCV and BCV chips are utilized in a liquid swapping microfluidic process. The designed liquid swapping process is developed to demonstrate the ability of the chips in expanding the usability of TPP on the centrifugal microfluidic platform. The results show that the developed TCV and BCV chips are able to accurately control the direction of the air/liquid flow.

Various biomedical applications can be performed on the centrifugal microfluidic platform by utilizing the developed valving mechanisms. As a proof of concept, Bradford assay and ELISA assay were demonstrated using the developed PLV and check valve, respectively. The results show that the developed valves can be successfully integrated to perform biomedical applications on the centrifugal microfluidic platform. The results also show that the centrifugal microfluidic platform can be utilized as a platform for detecting different diseases; for example, a liver functionality test can be performed by measuring the albumin concentration in the urine. This capability can be important for handling samples from patients with infectious diseases, such as HIV. It is also demonstrated that with the developed valves, multistep assays, such as ELISA, can be performed in fully automatic fashion and that will reduce the need for tedious labour work and procedures.

In conclusion, the developed valves proof to be reliable mechanism with physical barrier, vapor-tight for long term storage (VCV and check valve), reduce contact between sample and valving material, reactuatable in multistep assay, and easy to fabricate and implement. These specifications make the developed valves integratable in most biomedical and chemical applications on the centrifugal platform.

5.2 Recommendation

Some recommendations for future work are listed below based on the output of this work:

- Extend the study on the developed VCV valve, and in particular miniaturizing the actuation heating source to improve the portability of the whole system.

- Improve the injection process of the wax plug for easier valve implementation.

- Extend the study of the developed PLV valve in 3D configuration to miniaturize the centrifugal platform.

- Develop mass production method for the proposed TCV and BCV check valves for more fabrication accuracy, and easier implementation.

- Continue the study to utilize the developed check valves to perform different chemical and biomedical assays.

REFERENCES

Abi-Samra K. (2012). Electrochemical and Thermal Techniques for Detection and Fluidic Handling on Centrifugal Microfluidic Platforms. Doctor of Philosophy Dissertation, University of California, Irvine. Retrieved from http://search.proquest.com/pqdtglobal/docview/1112846910/CCDDA0B996C94 375PQ/4?accountid=28930 (3540471)

Abi-Samra K, Clime L, Kong L, Gorkin III R, Kim T-H, Cho Y-K, and Madou M. (2011). Thermo-pneumatic pumping in centrifugal microfluidic platforms. Microfluid Nanofluid, 11(5) 643–652.

Abi-Samra K, Hanson R, Madou M, and Gorkin III R. (2011). Infrared controlled waxes for liquid handling and storage on a CD-microfluidic platform. Lab on Chip, 11(4), 723-726.

Accoto D, Carrozza M, and Dario P. (2000). Modelling of micropumps using unimorph piezoelectric actuator and ball valves. Journal of Micromechanics and Microengineering, 10(2), 277.

Aeinehvand M M, Ibrahim F, Harun S W, Al-Faqheri W, Thio T H G, Kazemzadeh A, and Madou M J. (2013). Latex Micro-balloon Pumping in Centrifugal Microfluidic Platforms. Lab on a Chip, 14(5), 988-997.

Al-Faqheri W, Ibrahim F, Thio T H G, Aeinehvand M M, Arof H, and Madou M. (2015). Development of Novel Passive Check Valves for the Microfluidic CD Platform. Sensors and Actuators A: Physical, 222, 245-254.

Al-Faqheri W, Ibrahim F, Thio T H G, Moebius J, Joseph K, Arof H, and Madou M. (2013). Vacuum/Compression Valving (VCV) Using Parrafin-Wax on a Centrifugal Microfluidic CD Platform. PLOS ONE, 8(3), e58523.

Amasia M, Cozzens M, and Madou M J. (2012). Centrifugal microfluidic platform for rapid PCR amplification using integrated thermoelectric heating and ice-valving. Sensors and Actuators, B: Chemical, 161 (1), 1191-1197.

Anderson N G. (1969). Computer interfaced fast analyzers. Science, 166(3903), 317-324.

Arda E, and Pekcan Ö. (2001). Time and temperature dependence of void closure, healing and interdiffusion during latex film formation. Polymer, 42(17), 7419-7428.

Au A K, Lai H, Utela B R, and Folch A. (2011). Microvalves and micropumps for biomems. Micromachines, 2(2), 179-220.

Auroux P-A, Iossifidis D, Reyes D R, and Manz A. (2002). Micro total analysis systems. 2. Analytical standard operations and applications. Analytical Chemistry, 74(12), 2637-2652.

Bae B, Kim N, Kee H, Kim S-H, Lee Y, Lee S, and Park K. (2002). Feasibility test of an electromagnetically driven valve actuator for glaucoma treatment. Microelectromechanical Systems, Journal of, 11(4), 344-354.

Bradford M M. (1976). A rapid and sensitive method for the quantitation of microgram quantities of protein utilizing the principle of protein-dye binding. Analytical Biochemistry, 72(1), 248-254.

Brask A, Snakenborg D, Kutter J P, and Bruus H. (2006). AC electroosmotic pump with bubble-free palladium electrodes and rectifying polymer membrane valves. Lab on Chip, 6(2), 280-288.

Burger R, Reith P, Kijanka G, Akujobi V, Abgrall P, and Ducrée J. (2012). Array-based capture, distribution, counting and multiplexed assaying of beads on a centrifugal microfluidic platform. Lab on Chip, 12, 1289-1295. doi: 10.1039/C2LC21170J

Burtis C, Mailen J, Johnson W, Scott C, Tiffany T, and Anderson N. (1972). Development of a miniature fast analyzer. Clinical Chemistry, 18(8), 753-761.

Carrozza M, Croce N, Magnani B, and Dario P. (1995). A piezoelectric-driven stereolithography-fabricated micropump. Journal of micromechanics and microengineering, 5(2), 177.

Czugala M, Gorkin III R, Phelan T, Gaughran J, Curto V F, Ducrée J, Diamond D, and Benito-Lopez F. (2012). Optical sensing system based on wireless paired emitter detector diode device and ionogels for lab-on-a-disc water quality analysis. Lab on a Chip, 12(23), 5069-5078.

Ducr´ee J, Haeberle S, Lutz S, Pausch S, Von Stetten F, and Zengerle R. (2007). The centrifugal microfluidic Bio-Disk platform. Journal of Micromechanics and Microengineering, 17(7), S103-S115.

Feng G-H, and Kim E S. (2004). Micropump based on PZT unimorph and one-way parylene valves. Journal of micromechanics and microengineering, 14(4), 429.

Focke M, Stumpf F, Faltin B, Reith P, Bamarni D, Wadle S, Müller C, Reinecke H, Schrenzel J, and Francois P. (2010). Microstructuring of polymer films for sensitive genotyping by real-time PCR on a centrifugal microfluidic platform. Lab on Chip, 10(19), 2519-2526.

Fu C, Rummler Z, and Schomburg W. (2003). Magnetically driven micro ball valves fabricated by multilayer adhesive film bonding. Journal of micromechanics and microengineering, 13(4), S96.

Garcia-Cordero J L, Basabe-Desmonts L, Ducrée J, and Ricco A J. (2010). Liquid recirculation in microfluidic channels by the interplay of capillary and centrifugal forces. Microfluidics and Nanofluidics, 9(4-5), 695-703.

Gorkin R, Clime L, Madou M, and Kido H. (2010). Pneumatic pumping in centrifugal microfluidic paltform. Microfluidics and Nanofluidics, 9(2-3), 541-549.

Gorkin R, Nwankire C E, Gaughran J, Zhang X, Donohoe G G, Rook M, O'Kennedy R, and Ducrée J. (2012). Centrifugo-pneumatic valving utilizing dissolvable films. Lab on a Chip, 12(16), 2894-2902.

Gorkin R, Park J, Siegrist J, Amasia M, Lee B S, Park J M, Kim J, Kim H, Madou M, and Cho Y K. (2010). Centrifugal microfluidics for biomedical applications. Lab Chip, 10(14), 1758-1773.

Grumann M, Geipel A, Riegger L, Zengerle R, and Ducrée J. (2005). Batch-mode mixing on centrifugal microfluidic platforms. Lab on a Chip, 5(5), 560-565.

Haeberle S, Mark D, von Stetten F, and Zengerle R. (2012). Microfluidic Platforms for Lab-On-A-Chip Applications. Microsystems and Nanotechnology, 853-895.

Haeberle S, Schmitt N, Zengerle R, and Ducrée J. (2007). Centrifugo-magnetic pump for gas-to-liquid sampling. Sensors and Actuators A: Physical, 135(1), 28-33.

Ho C, and Khew M. (2000). Surface free energy analysis of natural and modified natural rubber latex films by contact angle method. Langmuir, 16(3), 1407-1414.

Ibrahim F, Jahanshahi P, Abd Rahman N, Kahar M K B A, Madou M, Nozari A A, Soin N, Dawal S Z M, and Abi Samra K. (2010). Analysis and experiment of centrifugal force for microfluidic ELISA CD platform. Paper presented at the Biomedical Engineering and Sciences (IECBES), 2010 IEEE EMBS Conference, Kuala Lumpur.

Imaad S M, Lord N, Kulsharova G, and Liu G L. (2011). Microparticle and cell counting with digital microfluidic compact disc using standard CD drive. Lab on Chip, 11(8), 1448-1456.

Ishizawa M, Azeta T, Nose H, Ukita Y, and Utsumi Y. (2012). Three-dimensional lab-on-a-CD with enzyme-linked immunosorbent assay. Paper presented at the Nano/Micro Engineered and Molecular Systems (NEMS), 2012 7th IEEE International Conference, Kyoto.

Kazemzadeh A, Ganesan P, Ibrahim F, Aeinehvand M M, Kulinsky L, and Madou M J. (2014). Gating vales on spinning microfluidic platforms: a flow switch/control concept. Sensors and actuators B: Chemical, 204, 149–158.

Kim J, Kido H, Rangel R H, and Madou M J. (2008). Passive flow switching valves on a centrifugal microfluidic platform. Sensors and Actuators B: Chemical, 128(2), 613-621.

Kim N, Dempsey C M, Zoval J V, Sze J-Y, and Madou M J. (2007). Automated microfluidic compact disc (CD) cultivation system of Caenorhabditis elegans. Sensors and actuators B: Chemical, 122(2), 511-518.

Kirby D, Siegrist J, Kijanka G, Zavattoni L, Sheils O, O'Leary J, Burger R, and Ducrée J. (2012). Centrifugo-magnetophoretic particle separation. Microfluidics and Nanofluidics, 13(6), 899-908.

Kitsara M, Nwankire C, O'Reilly A, Siegrist J, Donohoe G G, Zhang X, O'Kennedy R, and Ducrée J. (2012). Hydrophilic polymeric coatings for enhanced, serial-siphon based flow control on centrifugal lab-on-disc platforms. Paper presented at the The 16th International Conference on Miniaturized Systems for Chemistry and Life Sciences, Okinawa.

Kong L X, Parate K, Abi-Samra K, and Madou M. (2014). Multifunctional wax valves for liquid handling and incubation on a microfluidic CD. Microfluidics and Nanofluidics, 1-7.

Kong M C, Bouchard A P, and Salin E D. (2011). Displacement pumping of liquids radially inward on centrifugal microfluidic platforms in motion. Micromachines, 3(1), 1-9.

Kong M C R, and Salin E. (2011). A Valveless Pneumatic Fluid Transfer Technique Applied To Standard Additions on a Centrifugal Microfluidic Platform. Analytical Chemistry, 83(23), 9186–9190.

Kong M C R, and Salin E D. (2011). Pneumatic flow switching on centrifugal microfluidic platforms in motion. Analytical Chemistry, 83(3), 1148-1151.

Lai S, Wang S, Luo J, Lee L J, Yang S-T, and Madou M J. (2004). Design of a Compact Disk-like Microfluidic Platform for Enzyme-Linked Immunosorbent Assay. Analytical Chemistry, 76(7), 1832-1837.

Lee B S, Lee J N, Park J M, Lee J G, Kim S, Cho Y K, and Ko C. (2009). A fully automated immunoassay from whole blood on a disc. Lab Chip, 9(11), 1548-1555.

Li B, Chen Q, Lee D-G, Woolman J, and Carman G P. (2005). Development of large flow rate, robust, passive micro check valves for compact piezoelectrically actuated pumps. Sensors and Actuators A: Physical, 117(2), 325-330.

Li H, Roberts D, Steyn J, Turner K, Yaglioglu O, Hagood N, Spearing S, and Schmidt M. (2004). Fabrication of a high frequency piezoelectric microvalve. Sensors and Actuators A: Physical, 111(1), 51-56.

Liu R H, Bonanno J, Yang J, Lenigk R, and Grodzinski P. (2004). Single-use, thermally actuated paraffin valves for microfluidic applications. Sensors and Actuators B: Chemical, 98(2), 328-336.

Madou M, Lee J, Daunert S, Lai S, and Shih C-H. (2001). Design and Fabrication of CD-like Microfluidic Platform for Diagnostic Functions. Biomedical Microdevices, 3(3), 245-254.

Madou M, Zoval J, Jia G, Kido H, Kim J, and Kim N. (2006). Lab on a CD. Annual Review of Biomedical Engineering 8, 8, 601-628.

Madou M J, Lee L J, Daunert S, Lai S, and Shih C-H. (2001). Design and fabrication of CD-like microfluidic platforms for diagnostic: Mircofluidic functions. Biomedical Microdevices, 3(3), 245-254.

Manz A, Graber N, and Widmer H. (1990). Miniaturized total chemical analysis systems: a novel concept for chemical sensing. Sensors and actuators B: Chemical, 1(1), 244-248.

Mark D, Metz T, Haeberle S, Lutz S, Ducrée J, Zengerle R, and von Stetten F. (2009). Centrifugo-pneumatic valve for metering of highly wetting liquids on centrifugal microfluidic platforms. Lab Chip, 9(24), 3599-3603.

Mark D, Weber P, Lutz S, Focke M, Zengerle R, and von Stetten F. (2011). Aliquoting on the centrifugal microfluidic platform based on centrifugo-pneumatic valves. Microfluidics and Nanofluidics, 10(6), 1279-1288.

Meckes A, Behrens J, Kayser O, Benecke W, Becker T, and Müller G. (1999). Microfluidic system for the integration and cyclic operation of gas sensors. Sensors and Actuators A: Physical, 76(1), 478-483.

Morijiri T, Hikida T, Yamada M, and Seki M. (2010). Microfluidic counterflow centrifugal elutriation for cell separation using density-gradient media.

Morijiri T, Hikida T, Yamada M, and Seki M. (2010). Microfluidic counterflow centrifugal elutriation for cell separation using densitygradient media. Paper presented at the 14th International Conference on Miniaturized Systems for Chemistry and Life Sciences (uTAS). Groningen, The Netherlands.

Neagu C, Gardeniers J, Elwenspoek M, and Kelly J. (1997). An electrochemical active valve. Electrochimica Acta, 42(20), 3367-3373.

Nguyen N-T, and Truong T-Q. (2004). A fully polymeric micropump with piezoelectric actuator. Sensors and actuators B: Chemical, 97(1), 137-143.

Ni J, Huang F, Wang B, Li B, and Lin Q. (2010). A planar PDMS micropump using in-contact minimized-leakage check valves. Journal of micromechanics and microengineering, 20(9), 095033.

Noroozi Z, Kido H, Peytavi R, Nakajima-Sasaki R, Jasinskas A, Micic M, Felgner P L, and Madou M J. (2011). A multiplexed immunoassay system based upon reciprocating centrifugal microfluidics. Review of Scientific Instruments, 82(6), 064303.

Oh K W, and Ahn C H. (2006). A review of microvalves. Journal of Micromechanics and Microengineering, 16(5), R13.

Pan T, McDonald S J, Kai E M, and Ziaie B. (2005). A magnetically driven PDMS micropump with ball check-valves. Journal of micromechanics and microengineering, 15(5), 1021.

Pandolfi A, and Ortiz M. (2007). Improved design of low-pressure fluidic microvalves. Journal of micromechanics and microengineering, 17(8), 1487.

Park J, Sunkara V, Kim T-H, Hwang H, and Cho Y-K. (2012). Lab-on-a-disc for fully integrated multiplex immunoassays. Analytical chemistry, 84(5), 2133-2140.

Pekcan Ö, and Arda E. (1999). Void closure and interdiffusion in latex film formation by photon transmission and fluorescence methods. Colloids and Surfaces A: Physicochemical and Engineering Aspects, 153(1), 537-549.

Reyes D R, Iossifidis D, Auroux P-A, and Manz A. (2002). Micro total analysis systems. 1. Introduction, theory, and technology. Analytical chemistry, 74(12), 2623-2636.

Rich C A, and Wise K D. (2003). A high-flow thermopneumatic microvalve with improved efficiency and integrated state sensing. Microelectromechanical Systems, 12(2), 201-208.

Shao P, Rummler Z, and Schomburg W K. (2004). Polymer micro piezo valve with a small dead volume. Journal of micromechanics and microengineering, 14(2), 305.

Siegrist J, Gorkin R, Clime L, Roy E, Peytavi R, Kido H, Bergeron M, Veres T, and Madou M. (2010). Serial siphon valving for centrifugal microfluidic platforms. Microfluidics and Nanofluidics, 9(1), 55-63.

Soroori S. (2013). Novel Flow Control Schemes Utilizing Intrinsic Forces on Centrifugal Microfluidic Platforms. Doctor of Philosophy Dissertation, University of California, Irvine. Retrieved from http://gradworks.umi.com/35/56/3556960.html (3556960)

Soroori S, Kulinsky L, Kido H, and Madou M. (2013). Design and implementation of fluidic micro-pulleys for flow control on centrifugal microfluidic platforms. Microfluidics and Nanofluidics, 16(6), 1117-1129.

Strohmeier O, Emperle A, Roth G, Mark D, Zengerle R, and von Stetten F. (2013). Centrifugal gas-phase transition magnetophoresis (GTM)–a generic method for automation of magnetic bead based assays on the centrifugal microfluidic platform and application to DNA purification. Lab on a Chip, 13(1), 146-155.

Strohmeier O, Marquart N, Mark D, Roth G, Zengerle R, and von Stetten F. (2014). Real-time PCR based detection of a panel of food-borne pathogens on a centrifugal microfluidic "LabDisk" with on-disk quality controls and standards for quantification. Analytical Methods, 6(7), 2038-2046.

Studer V, Hang G, Pandolfi A, Ortiz M, Anderson W F, and Quake S R. (2004). Scaling properties of a low-actuation pressure microfluidic valve. Journal of Applied Physics, 95(1), 393-398.

Suzuki H, and Yoneyama R. (2003). Integrated microfluidic system with electrochemically actuated on-chip pumps and valves. Sensors and actuators B: Chemical, 96(1), 38-45.

Takao H, Miyamura K, Ebi H, Ashiki M, Sawada K, and Ishida M. (2005). A MEMS microvalve with PDMS diaphragm and two-chamber configuration of thermo-pneumatic actuator for integrated blood test system on silicon. Sensors and Actuators A: Physical, 119(2), 468-475.

Terry S C, Jerman J H, and Angell J B. (1979). A gas chromatographic air analyzer fabricated on a silicon wafer. Electron Devices, IEEE Transactions on, 26(12), 1880-1886.

Teymoori M M, and Abbaspour-Sani E. (2005). Design and simulation of a novel electrostatic peristaltic micromachined pump for drug delivery applications. Sensors and Actuators A: Physical, 117(2), 222-229.

Thio T, Nozari A A, Soin N, Kahar M K B A, Dawal S Z M, Samra K A, Madou M, and Ibrahim F. (2011, 2011/01/01). Hybrid Capillary-Flap Valve for Vapor Control in Point-of-Care Microfluidic CD. Paper presented at the 5th Kuala Lumpur International Conference on Biomedical Engineering, Kuala Lumpur.

Thio T H G, Ibrahim F, Al-Faqheri W, Moebius J, Khalid N S, Soin N, Abdul Kahar M K B, and Madou M. (2013). Push pull microfluidics on a multi-level 3D CD. Lab on a Chip, 13, 3199-3209.

Thio T H G, Soroori S, Ibrahim F, Al-Faqheri W, Soin N, Kulinsky L, and Madou M. (2013). Theoretical development and critical analysis of burst frequency equations for passive valves on centrifugal microfluidic platforms. Medical & Biological Engineering & Computing, 51(5), 525-535.

van der Wijngaart W, Ask H, Enoksson P, and Stemme G. (2002). A high-stroke, high-pressure electrostatic actuator for valve applications. Sensors and Actuators A: Physical, 100(2), 264-271.

van Oordt T, Barb Y, Smetana J, Zengerle R, and von Stetten F. (2013). Miniature stick-packaging–an industrial technology for pre-storage and release of reagents in lab-on-a-chip systems. Lab on a Chip, 13(15), 2888-2892.

Voigt P, Schrag G, and Wachutka G. (1998). Electrofluidic full-system modelling of a flap valve micropump based on Kirchhoffian network theory. Sensors and Actuators A: Physical, 66(1), 9-14.

Voldman J, Gray M L, and Schmidt M A. (2000). An integrated liquid mixer/valve. Microelectromechanical Systems, 9(3), 295-302.

Yamahata C, Lacharme F, Burri Y, and Gijs M A. (2005). A ball valve micropump in glass fabricated by powder blasting. Sensors and actuators B: Chemical, 110(1), 1-7.

Yang B, and Lin Q. (2007). A latchable microvalve using phase change of paraffin wax. Sensors and Actuators A: Physical, 134(1), 194-200.

Yang E-H, Lee C, Mueller J, and George T. (2004). Leak-tight piezoelectric microvalve for high-pressure gas micropropulsion. Microelectromechanical Systems, Journal of, 13(5), 799-807.

Yobas L, Durand D M, Skebe G G, Lisy F J, and Huff M A. (2003). A novel integrable microvalve for refreshable braille display system. Microelectromechanical Systems, Journal of, 12(3), 252-263.

Yobas L, Huff M A, Lisy F J, and Durand D M. (2001). A novel bulk micromachined electrostatic microvalve with a curved-compliant structure applicable for a pneumatic tactile display. Microelectromechanical Systems, Journal of, 10(2), 187-196.

Yoo J-C, Choi Y, Kang C, and Kim Y-S. (2007). A novel polydimethylsiloxane microfluidic system including thermopneumatic-actuated micropump and paraffin-actuated microvalve. Sensors and Actuators A: Physical, 139(1), 216-220.

Yusoff N A, Soin N, and Ibrahim F. (2009). Lab-on-a-disk as a Potential Microfluidic Platform for Dengue NS1-ELISA. Paper presented at the Industrial Electronics & Applications, ISIEA, Kuala Lumpur.

Zehnle S, Schwemmer F, Roth G, von Stetten F, Zengerle R, and Paust N. (2012). Centrifugo-dynamic inward pumping of liquids on a centrifugal microfluidic platform. Lab on a Chip, 12(24), 5142-5145.

Zhang C. X D, Li Y. (2007). Micropumps, microvalves and mocromixers within PCR microfluidic chips:Advances and trends. Biotehnology Advances, 483-514.

Zheng W, Alici G, Clingan P R, Munro B J, Spinks G M, Steele J R, and Wallace G G. (2013). Polypyrrole stretchable actuators. Journal of Polymer Science Part B: Polymer Physics, 51(1), 57-63.

LIST OF PUBLICATIONS AND PAPERS PRESENTED

Articles in Academic Journals (Published)

1. **W. Al-Faqheri**, F. lbrahim, T. H. G. Thio, K. Joseph, H' Arof, and M. Madou. 2013."Vacuum/Compression Valving (VCV) Using Parrafin-Wax on a Centrifugal Microfluidic CD Platform". PLOS One. PLoS ONE 8(3) pp. 1-7 (Q1, IF 3.534).

2. **W. Al-Faqheri**, F. lbrahim, T. H. G. Thio, M. M. Aeinehvand, H' Arof, and M. Madou. 2015. "Development of Novel Passive Check Valves for the Microfluidic CD Platform". Sensors and Actuators A, (222) pp. 245-254 (Q1, IF 1.943).

3. **W. Al-Faqheri**, F. Ibrahim, T. H. G. Thio, H. Arof, H. A. Rothan, R. Yusof, M. Madou. "Development of Passive Liquid Valve (PLV) Utilizing a Pressure Equilibrium Phenomenon on the Centrifugal Microfluidic Platform". (2015). Sensors (Q1, IF 2.048).

4. T. H. G. Thio, F. Ibrahim, **W. Al- Faqheri**, J. Moebius, N. S. Khalid, N. Soin, M. K. B. Abdul Kahar, M. Madou. (2013), "Push pull microfluidics on a multi-level 3D CD", Lab on Chip Journal, 51(5), pp. 525-535 (Q1, IF 5.748).

5. T. H. G. Thio, S. Soroori, F. Ibrahim, **W. Al-Faqheri**, N. Soin, M. Madou. (2013). "Theoretical Development and Critical Analysis of Burst Frequency Equations for Passive Valves on Centrifugal Microfluidic Platforms". Journal of Medical & Biological Engineering & Computing (51) pp. 525-535, (Q2, IF 1.97).

6. M. Ainehvand, F. Ibrahim, S. W. Harun, **W. Al-Faqheri**, T. H. G. Thio, A. Kzemzadeh, M. Madou. (2013). "Latex Micro-balloon pumping in Centrifugal Microfluidic Platforms". Lab on a Chip (5) pp. 988-997 (Q1, IF 5.748).

7. T. H. G. Thio, F. Ibrahim, **W. Al-Faqheri**, N. Soin, M. K. Bador, M. Madou. "Sequential push-pull pumping mechanism for washing and evacuation of an immunoassay reaction chamber on a microfluidic CD platform". PLOS One, DOI: 10.1371/journal.pone.0121836.

8. K. Joseph, F. Ibrahima, J. Cho, T. H. G. Thio, **W. Al-Faqheri**, M. Madou. "Design and Development of Micro-Power Generating Device for Biomedical Applications of Lab-on-a-Disc". PLOS One, DOI: 10.1371/journal.pone.0136519.

Proceeding

1. **W. Al-Faqheri**, F. Ibrahim, T. H G. Thio, H. Arof, M. Madou. "Novel Liquid Equilibrium Valving on Centrifugal Microfluidic CD Platform". IEEE EMBC 2013, Osaka Japan. (ISI-Cited Publication).

2. **W. Al-Faqheri**, F. Ibrahim, T. H G. Thio, K. Joseph, M. S. Mokhtar, M. Madou. "Liquid Density Effect on Burst Frequency in Centrifugal Microfluidic Platforms ". IEEE EMBC 2015, Milan Italy. (ISI-Cited Publication)

3. T. H. G. Thio, F. Ibrahim, **W. Al-Faqheri**, N. Soin, M. K. B. Abdul Kahar, M. Madou. "Multi-Level 3D Implementation of Thermo- Pneumatic Pumping on Centrifugal Microfluidic CD Platforms ". IEEE EMBC 2013, Osaka Japan. (ISI-Cited Publication).

4. T. H. G. Thio, F. Ibrahim, **W. Al-Faqheri**, N. Soin, M. K. B. Abdul Kahar, M. Madou. "Sequential Biosensor Chamber Evacuation Using Thermo-Pneumatic (TP) Pull Pumping on the Microfluidic CD Platform". Biosensors 2014, Melbourne, Australia.

PLOS ONE

Vacuum/Compression Valving (VCV) Using Parrafin-Wax on a Centrifugal Microfluidic CD Platform

Wisam Al-Faqheri[1], Fatimah Ibrahim[1]*, Tzer Hwai Gilbert Thio[1], Jacob Moebius[1,3], Karunan Joseph[1], Hamzah Arof[2], Marc Madou[1,3,4,5]

1 Medical Informatics and Biological Micro-electro-mechanical Systems Specialized Laboratory, Department of Biomedical Engineering, Faculty of Engineering, University of Malaya, Kuala Lumpur, Malaysia, 2 Department of Electrical Engineering, Faculty of Engineering, University of Malaya, Kuala Lumpur, Malaysia, 3 Department of Biomedical Engineering, University of California Irvine, Irvine, United States of America, 4 Department of Mechanical and Aerospace Engineering, University of California Irvine, Irvine, United States of America, 5 Ulsan National Institute of Science and Technology, World Class University, Ulsan, South Korea

Abstract

This paper introduces novel vacuum/compression valves (VCVs) utilizing paraffin wax. A VCV is implemented by sealing the venting channel/hole with wax plugs (for normally-closed valve), or to be sealed by wax (for normally-open valve), and is activated by localized heating on the CD surface. We demonstrate that the VCV provides the advantages of avoiding unnecessary heating of the sample/reagents in the diagnostic process, allowing for vacuum sealing of the CD, and clear separation of the paraffin wax from the sample/reagents in the microfluidic process. As a proof of concept, the microfluidic processes of liquid flow switching and liquid metering is demonstrated with the VCV. Results show that the VCV lowers the required spinning frequency to perform the microfluidic processes with high accuracy and ease of control.

Introduction

Centrifugal microfluidic CD platforms offer many advantages over larger traditional fluidic platforms such as a reduction of the required sample/reagent volumes, portability, low fabrication cost, and full automation. In one of its simplest embodiments, a microfluidic CD platform controls fluid sequencing based on the balancing of the centrifugal force and the capillary force [1]. Examples of applications developed on the centrifugal microfluidic CD platform include enzyme linked immunosorbent assays (ELISA) [2,3], real time polymerase chain reaction (PCR) [4,5], and particle separation [6–8].

The most essential of mechanisms on a microfluidic CD is a valve that allows for fluid flow sequencing. A valve is a component that stops (normally-open valve), starts (normally-closed valve) or controls (proportional valve) fluid flow through a specialized passage or channel [1,9,10]. According to Oh et al [9], microfluidic valves fall under two main categories: passive (dependent on centrifugal forces) and active (independent of centrifugal forces) valves. Many kinds of valves fall under these two categories such as mechanical, non-mechanical, and externally actuated valves. These valves were categorized according to the mechanism of operation and/or actuation methods. For a valve to function effectively in a diagnostic process, several requirements must be met. First, it must be able to operate with relevant clinical samples and reagents of widely varying physicochemical properties typically used in diagnostic processes [1,10,11]. The valves must be unaffected by these substances to prevent the degradation of the valve before its actuation. Second, for all the steps of a traditional clinical diagnostic process to be replicated identically on a microfluidic CD platform [12] may require a multitude of valves including passive and active valves, proportional valve, normally-closed valves, and normally-open valves. Third, fluid manipulation for any diagnostic process must be tightly controlled. Failure to adhere to any of these requirements will result in rejection by the FDA and misdiagnosis of a disease or error in clinical test results, especially when biomarkers are present in very low concentrations. In general, the main criteria for a successful microvalve includes the prevention of evaporation or leakage sample, reduction of the dead volume, short time to actuation, and reduced power consumption [9].

While there are a wide variety of passive valves available, such as hydrophobic, hydrophilic, siphon, Coriolis, flap valves [1,10,12–16] etc, in most cases, these valving techniques lack a physical barrier to prevent evaporation of liquids during test storage and operation [16]. Furthermore, there are serious challenges involved in making passive valves repeatable and manufacturable. To meet the requirements for a diagnosis process, active valves are often required alone or in addition to passive valves.

109

Article

Development of a Passive Liquid Valve (PLV) Utilizing a Pressure Equilibrium Phenomenon on the Centrifugal Microfluidic Platform

Wisam Al-Faqheri [1,2], **Fatimah Ibrahim** [1,2,*], **Tzer Hwai Gilbert Thio** [1,2,3], **Norulain Bahari** [1,2], **Hamzah Arof** [1,2,4], **Hussin A. Rothan** [7], **Rohana Yusof** [7] **and Marc Madou** [1,2,5,6]

[1] Centre for Innovation in Medical Engineering (CIME), Faculty of Engineering, University of Malaya, 50603 Kuala Lumpur, Malaysia; E-Mails: wisamfakhri83@yahoo.com (W.A.-F.); ainbahari@yahoo.com (N.B.)

[2] Department of Biomedical Engineering, Faculty of Engineering, University of Malaya, 50603 Kuala Lumpur, Malaysia

[3] Faculty of Science, Technology, Engineering and Mathematics, INTI International University, Persiaran Perdana BBN, Putra Nilai, 71800 Nilai, Negeri Sembilan, Malaysia; E-Mail: gilbert_thio@hotmail.com

[4] Department of Electrical Engineering, Faculty of Engineering, University of Malaya, 50603 Kuala Lumpur, Malaysia; E-Mail: ahamzah@um.edu.my

[5] Department of Biomedical Engineering, University of California, Irvine, 92697 CA, USA; E-Mail: mmadou@uci.edu

[6] Department of Mechanical and Aerospace Engineering, University of California, Irvine, 92697 CA, USA

[7] Department of Molecular Medicine, Faculty of Medicine, University of Malaya, 50603 Kuala Lumpur, Malaysia; E-Mails: rothan@um.edu.my (H.A.R.); rohana@um.edu.my (R.Y.)

* Author to whom correspondence should be addressed; E-Mail: fatimah@um.edu.my; Tel.: + 603-7967-6818; Fax: +603-7967-6878.

Academic Editor: Kwang W. Oh

Abstract: In this paper, we propose an easy-to-implement passive liquid valve (PLV) for the microfluidic compact-disc (CD). This valve can be implemented by introducing venting chambers to control the air flow of the source and destination chambers. The PLV mechanism is based on equalizing the main forces acting on the microfluidic CD (*i.e.*, the

Development of novel passive check valves for the microfluidic CD platform

Wisam Al-Faqheri[a], Fatimah Ibrahim[a,*], Tzer Hwai Gilbert Thio[a],
Mohammad Mahdi Aeinehvand[a], Hamzah Arof[b], Marc Madou[a,c,d]

[a] Centre for Innovation in Medical Engineering(CIME), Department of Biomedical Engineering, Faculty of Engineering, University of Malaya, 50603 Kuala Lumpur, Malaysia
[b] Department of Electrical Engineering, Faculty of Engineering, University of Malaya, 50603 Kuala Lumpur, Malaysia
[c] Department of Biomedical Engineering, University of California, Irvine, Irvine 92697, United States
[d] Department of Mechanical and Aerospace Engineering, University of California, Irvine, Irvine 92697, United States

ARTICLE INFO

ABSTRACT

Microfluidic CD platforms are utilized to perform different biological processes and chemical analyses. In general, a microfluidic CD implements the centrifugal force that is created by the spinning of the platform to pump liquid through the microfluidic network of chambers and channels. Over the last few decades, a wide range of active and passive valving methods were proposed and tested on various microfluidic platforms. Most of the presented valves are too complex to design and involve lengthy fabrication processes. In this paper, easy to fabricate air and liquid check valves for centrifugal microfluidic platforms are presented: a Terminal Check Valve (TCV) and a Bridge Check Valve (BCV). To understand the characteristic of the proposed valves, theoretical and experimental studies are conducted. Moreover, to test the effectiveness of these valves, liquid swapping is demonstrated by integrating TCV and BCV chips with thermo-pneumatic (TP) pumping on a CD. The valves are shown to accurately control flow direction which makes them an excellent choice for a variety of complex microfluidic processes. The experimental and theoretical results also indicate that these valves require low pressure for actuation. Furthermore, the theoretical results confirm the ability to adjust the required actuation pressure by changing the valve chip size. Finally, as a proof of concept for implementing the check valves on a biological application, an enzyme linked immunosorbent assays (ELISA) is performed. The result shows that the TCV and BCV valving chips enhance the operating range of the processes that can be performed on the microfluidic CD.

© 2014 Elsevier B.V. All rights reserved.

1. Introduction

Since the introduction of the miniaturized total analysis system by Manz et al. [1], the miniaturization of commercial bio-analytical systems became the focus of many researchers in this field. As a result of these efforts, several microfluidic biomedical and chemical processes were successfully performed on two main types of microfluidic platforms: the Lab-on-Chip (LOC) and the Lab-on-Disc (LOD)/microfluidic compact disc (CD) [1–3]. Although both platforms aim to reduce the amount of liquid and time consumed in any process, the LOC is a stationary platform mostly dependent on external forces for liquid flow, while the microfluidic CD

platform relies on the centrifugal force (which is derived from the spinning of the disc) to pump liquid on the platform. In addition to not needing any external pumping source, the microfluidic CD platform also has the benefit of utilizing capillary valves for fluid flow sequencing [3]. Some examples of the implementation of the microfluidic CD platform for biomedical processes include enzyme linked immunosorbent assays (ELISA) [4,5], plasma and particles separation [6–8], and real time polymerase chain reaction (PCR) [9,10].

Liquid flow control on both microfluidic platforms present a serious challenge for the researchers in this field. In the last few decades, the field of micro-valves has been heavily investigated and various types of valves have been presented. According to Madou et al. and Oh et al. [3,11], most of the developed micro-valves belong to one of two main categories: active valves or passive valves. An active valve can be defined as a valve that requires an external force to actuate (open or close). Examples of active valves that have been

* Corresponding author. Tel.: +60 3 7967 6818; fax: +60 3 7967 6878/4579; mobile: +60 123352921.
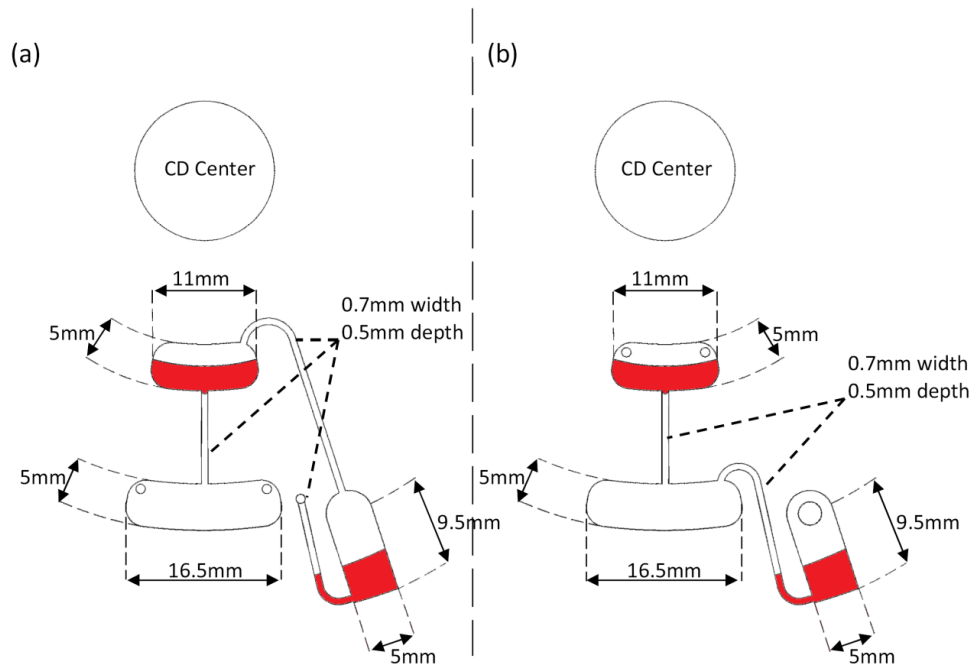E-mail address: fatimah@um.edu.my (F. Ibrahim).

Figure A 1: S-PLV and D-PLV designs dimensions
(a) and (b) respectively shows the designs specification of S-PLV and D-PLV. As mentioned in the main manuscript, both designs are consists of three main chambers: source chamber, destination chamber and venting chamber. The three chambers are connected together with liquid channels and venting channels.
Source chamber is 5mm height, 11mm width and 1mm depth.
Destination chamber is 5mm height, 16.5mm width, and 1mm depth.
Venting chamber is 9.5mm height, 5mm width and 2.5mm depth.
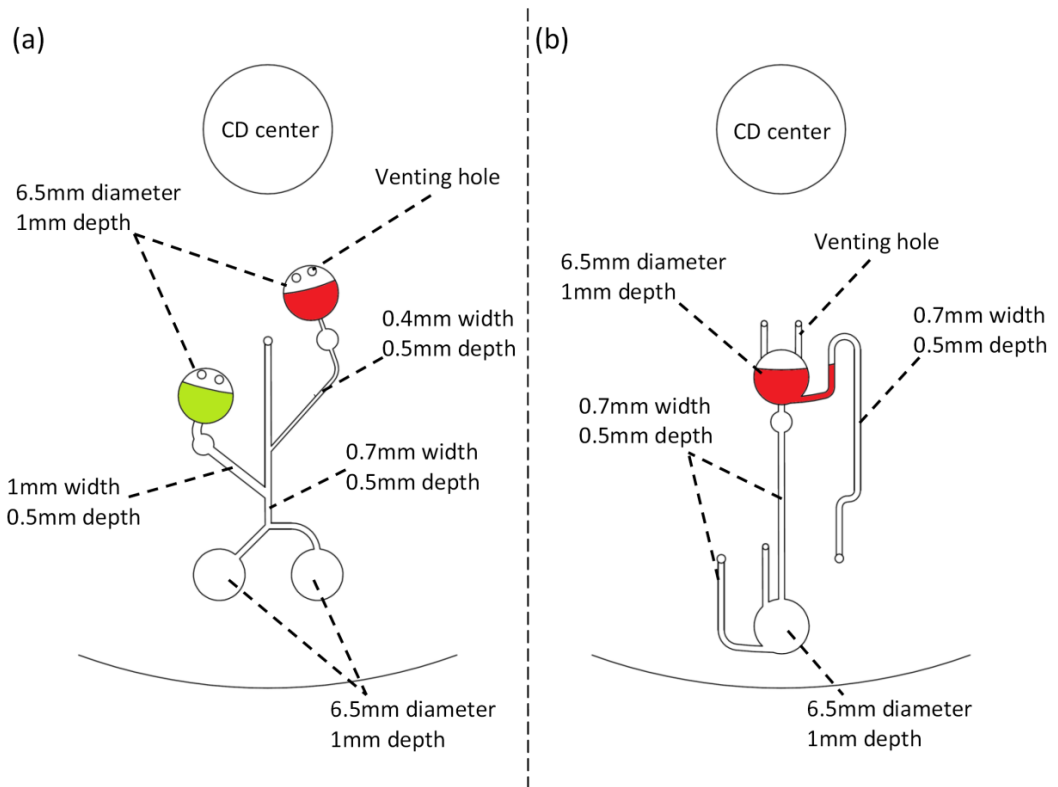**_Venting and liquid channels_ are all 0.7mm width and 0.5mm depth.**

Figure A 2: PLV liquid switching design dimensions

(a) *switching layer*: source chambers and destination chambers are 6.5mm diameter and 1mm depth. Source chamber A liquid channel is 1mm width and 0.5mm depth. Source chamber B liquid channel is 0.4mm width by 0.5mm depth. All the other channels are 0.7mm width by 0.5mm depth.

(b) *Venting layer:* Venting chamber A and B are 6.5mm diameter and 1mm depth. All the liquid and venting channels are 0.7mm width and 0.5mm depth.
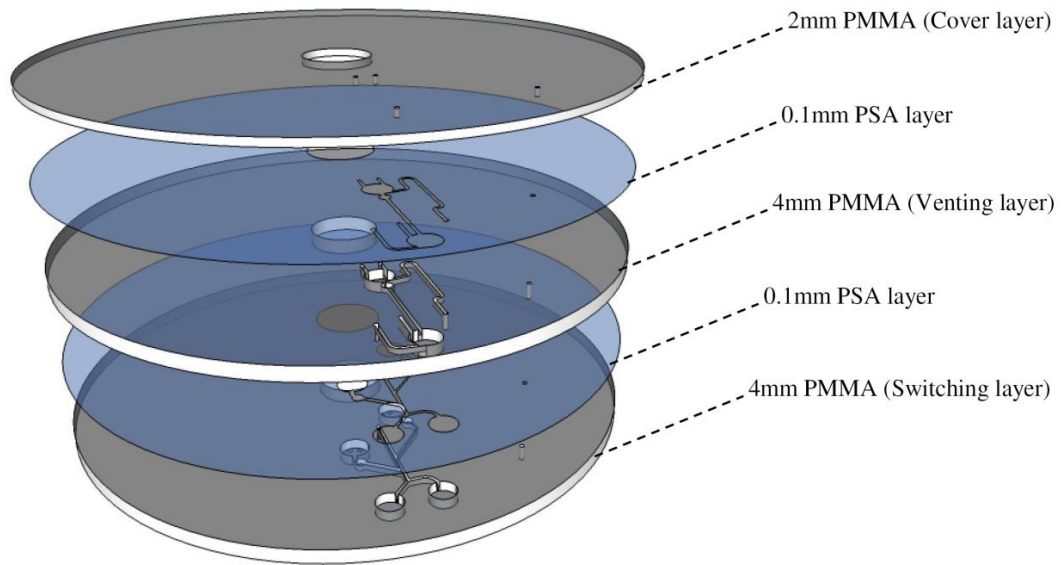
2mm PMMA (Cover layer)

0.1mm PSA layer

4mm PMMA (Venting layer)

0.1mm PSA layer

4mm PMMA (Switching layer)

Figure A 3: Microfluidic platform layers for Liquid switching

Top layer: **2mm PMMA with only venting holes cut-through (cover layer).**

Second layer: **0.1 PSA with the venting layer design cut-through.**

Third layer: **4mm PMMA where the venting design in Figure A 3(b) engraved-in (venting layer).**

Fourth layer: **0.1 PSA adhesive layer with the switching design cut-through.**

Fifth layer: **4mm PMMA layer where the switching design in Figure A 3(a) engraved-in.**
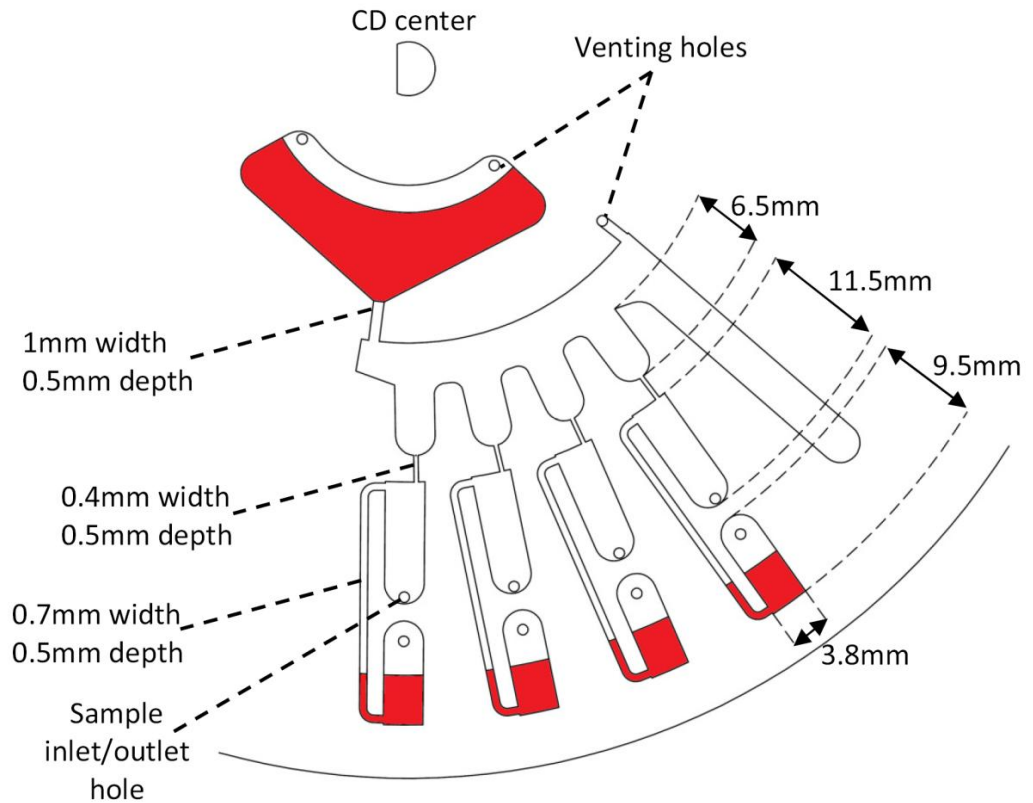
Figure A 4: Microfluidic design of liquid metering
Chambers:
Metering chambers: 3.8mm width, 6.5mm length, and 4mm depth.
Destination chambers: 3.8mm width, 11.5mm length, and 4mm depth.
Venting chambers: 3.8mm width, 9.5mm length, and 2.5mm depth.

Channels:
Source chamber liquid channel: 1mm width and 0.5mm depth.
Metering chambers channel to the destination chambers: 0.4mm width and 0.5mm depth.
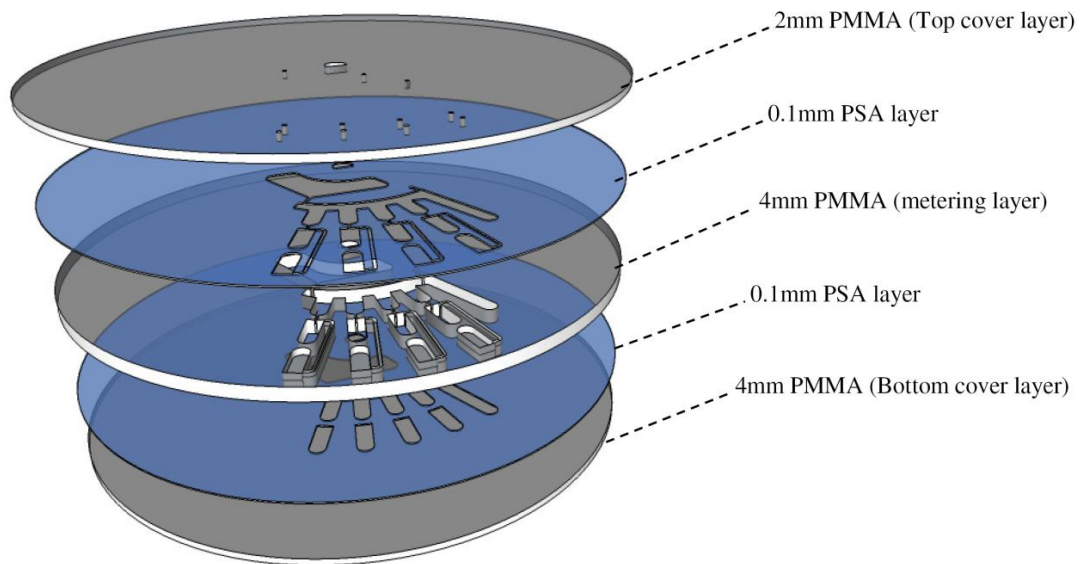*Venting channels:* 0.7mm width and 0.5mm depth.

Figure A 5: Microfluidic platform layer for liquid metering
Top layer: **2mm PMMA with only venting holes cut-through (cover layer).**
Second layer: **0.1 PSA with the metering design cut-through.**
Third layer: **4mm PMMA where the venting design in Figure A5 engraved-in (venting layer).**
Fourth layer: **0.1 PSA adhesive layer with the metering design cut-through.**
Fifth layer: **2mm PMMA layer (bottom cover layer).**

APPENDIX B

Test Platform Dimensions:

Channel length=15cm, Channel width=1mm

Channel depth=1mm

Experimental steps:

1- Install the check valve.
2- Inject a specific height of the testing liquid from the inlet hole.
3- Reposition the platform standing vertically such that the inlet hole is on top and the check valve is at the bottom.
4- The minimum pressure (based on the liquid height) where the liquid starts flowing is considered the actuation point of the check valve.
5- The time it takes for the liquid to travel between two different points in the channel is recorded to calculate the flow rate at that specific pressure.
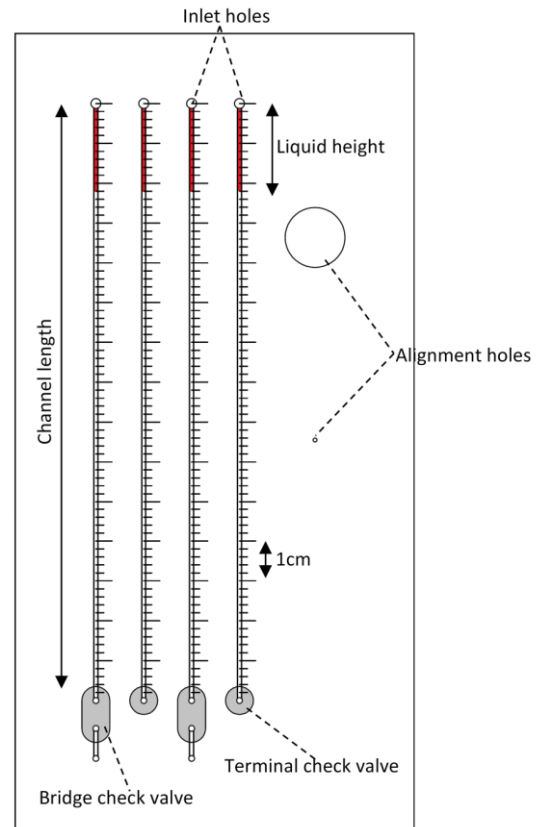

Figure A 6: Actuation pressure and flow rate test platform